

U. AYBARÇ

IZMIR KATIP CELEBI UNIVERSITY

2019

**IZMIR KATIP CELEBI UNIVERSITY
GRADUATE SCHOOL OF NATURAL AND APPLIED SCIENCES**

**DEVELOPMENT OF CAST ALUMINUM METAL MATRIX
COMPOSITES BY ADDITIONAL PROCESSES**



**PhD THESIS
Uğur AYBARÇ**

Department of Materials Science and Engineering

MARCH 2019

**IZMIR KATIP CELEBI UNIVERSITY
GRADUATE SCHOOL OF NATURAL AND APPLIED SCIENCES**

**DEVELOPMENT OF CAST ALUMINUM METAL MATRIX
COMPOSITES BY ADDITIONAL PROCESSES**



PhD THESIS

**Uğur AYBARÇ
D140111001**

Department of Materials Science of Engineering

Thesis Advisor: Assoc. Prof. Mehmet Özgür Seydibeyođlu

MARCH 2019

İZMİR KATİP ÇELEBİ ÜNİVERSİTESİ
FEN BİLİMLERİ ENSTİTÜSÜ

DÖKÜM ALÜMİNYUM METAL MATRİKS KOMPOZİTLERİNİN
İLAVE PROSESLERLE GELİŞTİRİLMESİ



DOKTORA TEZİ

Uğur AYBARÇ
D140111001

Malzeme Bilimi ve Mühendisliği Ana Bilim Dalı

Tez Danışmanı: Doç Dr. Mehmet Özgür SEYDİBEYOĞLU

MART 2019



Uğur AYBARÇ, a PhD student of IKCU Graduate School Of Natural And Applied Sciences, successfully defended the thesis entitled “DEVELOPMENT OF CAST ALUMINUM METAL MATRIX COMPOSITES BY ADDITIONAL PROCESSES”, which he prepared after fulfilling the requirements specified in the associated legislations, before the jury whose signatures are below.

Thesis Advisor :

Assoc. Prof. Dr. M. Özgür SEYDİBEYOĞLU
İzmir Katip Çelebi University

Jury Members :

Assoc. Prof. Dr. Mücahit SÜTÇÜ
İzmir Katip Çelebi University

Assoc. Prof. Dr. Derya DIŞPINAR
İstanbul University

Asst. Prof. Esra DOKUMACI
Dokuz Eylül University

Asst. Prof. Onur ERTUĞRUL
İzmir Katip Çelebi University

Date of Submission : 08.03.2019

Date of Defense : 08.04.2019





*To my family, my sister Sibel AYBARÇ,
my friends Emre TAYLAN and Elin SØRNES,*



FOREWORD

I would especially like to thank my advisor Dr. M. Ozgur Seydibeyoglu for both giving light to my way and shaping the thesis with his ideas. I would like to thank Dr. Derya Dispinar for both his time and his significant contributions to my thesis. I would like to thank Dr. Esra Dokumaci for her different point of view and ideas in thesis evaluation meetings. I would like to thank Dr Onur Ertugrul for his contributions and support during the thesis study from the production process to the examination of the samples. Also, I would like to thank Dr. Sercan Acarer for his contribution to simulation tests of this thesis. I thank the DEU EMUM team for their support in the implementation of the HIP process.

I would like to thank the CMS Company and R&D Center for providing all the facilities and laboratory equipment for carrying out this thesis. I would also like to thank Hakan Yavuz for his support about knowledge and experience especially in simulation studies. I would like to thank Bora Yay and Caner Kalender, who are always with me in laboratory studies. I would like to thank all of the employees in the CMS quality department to perform the mechanical tests.

I would like to thank my family, who deserved the biggest thank for their support and trust in every situation. Especially I would like to thank Dr. Sibel Aybarç my unique sister, who always trusted me and was with me. Thanks for always being there for me. I would like to thank to Emre Taylan, who is my chance, shared all my problems during this thesis, and allowed me to look at life differently. I would like to thank Elin Sørnes for her spiritual support and especially good foods during my thesis. I feel lucky to be together with such great and loving people. I would like to thank separately for all the spiritual support they have provided me.

March 2019

Uğur AYBARÇ



TABLE OF CONTENTS

	<u>Page</u>
FOREWORD	ix
TABLE OF CONTENTS	xi
ABBREVIATIONS	xiii
LIST OF TABLES	xv
LIST OF FIGURES	xvii
ABSTRACT	xvii
ÖZET	xxi
1. INTRODUCTION	1
1.1 Aluminum Metal Matrix Composite with SiC	2
1.2 Aluminum Metal Matrix Composite with Al ₂ O ₃	5
1.3 Aluminum Metal Matrix Composite with Graphene	8
2. EXPERIMENTAL	12
2.1 Materials	12
2.2 Preparation of Composites	13
2.2.1 Melting furnace	14
2.2.2 Stirring equipments	15
2.2.3 Hot isostatic process (HIP)	15
2.3 Characterization	17
2.3.1 Mechanical properties	17
2.3.1.1 Tensile test	17
2.3.1.2 Hardness test	18
2.3.1.3 Charpy impact test	18
2.3.2 Metallographical analysis	17
2.3.2.1 Optical microscopy	19
2.3.2.2 Scanning electron microscopy	20
2.3.2.2 Porosity measurement	20
3. RESULTS AND DISCUSSIONS	22
3.1 Determination of Stirring Method and Appropriate Mold Design.....	22
3.1.1 Simulation analysis	22
3.1.2 Simulation analysis of stirring methods.....	23
3.1.3 Simulation analysis of mold designs.....	26
3.1.4 The results of simulation analysis	27
3.1.4.1 The results of stirring methods.....	27
3.1.4.2 The results of mold design	33
3.1.5 Casting studies	36
3.1.6 The results of casting studies	38
3.1.6.1 Mechanical test results	38
3.1.6.2 Results of metallographic analysis.....	41
3.1.7 The determination of the appropriate stirring method and mold design... 45	45

3.2 The Effect of Reinforcement Particle On Mechanical Properties of Aluminum Matrix Composites	46
3.2.1 The production method of composite samples.....	46
3.2.2 Results and discussion.....	46
3.2.2.1 The evaluation effect of SiC and micro-Al ₂ O ₃ reinforcements.....	47
3.2.2.2 The evaluation on effects of micro-Al ₂ O ₃ and nano-Al ₂ O ₃ reinforcements	55
3.2.2.3 The evaluation effect of nano-Al ₂ O ₃ and graphene reinforcements .	60
3.2.3 Conclusions of the whole evaluation studies	65
3.3 The Effect Of Hot Isostatic Press On Mechanical Properties Of Aluminum Metal Matrix Composites	66
3.3.1 Experimental procedure	68
3.3.2 Results and discussions	68
3.3.3 Conclusions	75
4. CONCLUSION AND FUTURE WORK.....	76
REFERENCES	78
CURRICULUM VITAE	86

ABBREVIATIONS

YS	: Yield Strength
UTS	: Ultimate Tensile Strength
QI	: Quality Index
HIP	: Hot Isostatic Press





LIST OF TABLES

	<u>Page</u>
Table 1.1 : The summary of aluminum composite with SiC	2
Table 1.2 : The summary of aluminum composite with Al ₂ O ₃	6
Table 1.3 : The summary of aluminum composite with graphene.....	9
Table 2.1 : Chemical composition (wt. %) of matrix alloy - A356.....	12
Table 2.2 : Properties of reinforcement.....	12
Table 2.3 : Preheating process of reinforcements	13
Table 3.1 : Properties of materials used in simulation analysis	26
Table 3.2 : Percent values of porosity content	42
Table 3.3 : SDAS measurement of samples produced by different stirring types (μm).....	45
Table 3.4 : Grain size measurement of samples produced by different stirring types (μm).....	45
Table 3.5 : Grain size measurement of samples reinforced with SiC and Al ₂ O ₃ (μm).....	51
Table 3.6 : SDAS measurement of samples reinforced with SiC and Al ₂ O ₃ (μm)...	51
Table 3.7 : SDAS measurement of samples reinforced with micro and nano Al ₂ O ₃ (μm).....	57
Table 3.8 : Grain size measurement of samples reinforced with micro and nano Al ₂ O ₃ (μm).....	58
Table 3.9 : SDAS measurement of samples reinforced with nano-Al ₂ O ₃ and graphene (μm)	62
Table 3.10 : Grain size measurement of samples reinforced with nano-Al ₂ O ₃ and graphene (μm)	62
Table 3.11 : Macro grain size measurement of samples applied and unapplied HIP process (μm).....	69
Table 3.12 : SDAS measurements of samples applied and unapplied HIP process (μm).....	70



LIST OF FIGURES

	<u>Page</u>
Figure 1.1 : Classification of engineering materials.	1
Figure 2.1 : Morphology of reinforcements particle a) SiC, b) micro-Al ₂ O ₃ and c) nano Al ₂ O ₃	13
Figure 2.2 : Flow chart of casting process.	14
Figure 2.3 : a) Melting and b) preheating furnaces.....	14
Figure 2.4 : a) Mechanical and b) ultrasonic stirrer.....	15
Figure 2.5 : HIP machine.	16
Figure 2.6 : A set of HIP samples.	16
Figure 2.7 : Steps of HIP method.....	17
Figure 2.8 : Tensile test sample.	17
Figure 2.9 : Tensile test machine.	18
Figure 2.10 : Hardness test machine.	18
Figure 2.11 : Charpy impact test sample.	19
Figure 2.12 : Charpy impact test machine.	19
Figure 2.13 : a) Nikon Epiphot 200 and b) Clemex S2.0C.....	20
Figure 2.14 : Scanning electron microscope.	20
Figure 3.1 : Dimensions of the crucible.....	25
Figure 3.2 : Ultrasonic processing system.	25
Figure 3.3 : Mold types.	27
Figure 3.4 : Simulation test results of mechanical stirring types; a) horizontal section of crucible, b) vertical section of crucible, c) distribution of SiC particles.....	29
Figure 3.5 : Simulation test results of ultrasonic stirring types; a) horizontal section of crucible, b) vertical section of crucible, c) distribution of SiC particles.....	31
Figure 3.6 : Simulation test results of hybrid stirring types; a) horizontal section of crucible, b) vertical section of crucible, c) distribution of SiC particles.....	33
Figure 3.7 : Simulation test results of bottom-fed mold.	35
Figure 3.8 : Simulation test results of spoke mold.....	36
Figure 3.9 : Preheated spoke mold.....	37
Figure 3.10 : Solidification of preheated mold.	38
Figure 3.11 : Mechanical test results of sample produced by different stirring types; a) YS, b) UTS, c) elongation and d) QI of all samples.....	40
Figure 3.12 : Macrostructure of samples prepared by a) reference, b) ultrasonic, c) mechanical and d) hybrid stirring.	42
Figure 3.13 : Microstructure of samples produced by ultrasonic, mechanical and hybrid stirring methods.....	44

Figure 3.14 : Microstructure of composite samples with a) SiC and b) micro-Al ₂ O ₃ reinforcements	49
Figure 3.15 : Macrostructure of MMC samples with SiC and micro-Al ₂ O ₃ reinforcement.....	50
Figure 3.16 : SEM analysis of sample with 1wt%SiC.....	50
Figure 3.17 : Mechanical test results of samples reinforced with SiC and micro Al ₂ O ₃	52
Figure 3.18 : Porosity content of samples reinforced with SiC and micro Al ₂ O ₃	54
Figure 3.19 : Hardness test results of samples reinforced with SiC and micro Al ₂ O ₃	54
Figure 3.20 : Charpy impact test results of all samples reinforced with SiC and micro Al ₂ O ₃	55
Figure 3.21 : Microstructure of all samples reinforced with micro and nano Al ₂ O ₃	56
Figure 3.22 : Macrostructure of samples reinforced with micro and nano Al ₂ O ₃	57
Figure 3.23 : Percentage of porosity.	58
Figure 3.24 : Mechanical test results of samples reinforced with micro and nano Al ₂ O ₃	60
Figure 3.25 : Microstructure of samples reinforced with nano Al ₂ O ₃ and graphene.....	61
Figure 3.26 : Macrostructure of samples reinforced with nano Al ₂ O ₃ and graphene.	62
Figure 3.27 : Mechanical test results of samples reinforced with nano Al ₂ O ₃ and graphene.....	63
Figure 3.28 : Percentage of porosity.	64
Figure 3.29 : Macrostructure of samples with and without HIP process.....	68
Figure 3.30 : Microstructure of samples with and without HIP process.....	70
Figure 3.31 : Mechanical test results of samples with HIPed and un-HIPed.....	71
Figure 3.32 : The surface of a sample after HIP process.	72
Figure 3.33 : SEM images of samples before and after HIP process.....	72
Figure 3.34 : The variation of YS versus porosity content.	73
Figure 3.35 : The variation of UTS versus porosity content.....	73
Figure 3.36 : The variation of elongation versus porosity content.	73
Figure 3.37 : The variation of QI versus porosity content.	74

DEVELOPMENT OF CAST ALUMINUM METAL MATRIX COMPOSITES BY ADDITIONAL PROCESSES

ABSTRACT

It is seen that materials used traditionally today are insufficient to meet market expectations. For this reason, the interest on composite material increases day by day. The role of composite materials has become important in sectors, such as especially in automotive and aerospace industries, where a final product weight is of importance.

This thesis consists of four application parts. In the first part, a detailed literature review on aluminum metal matrix composites was discussed. In the second part, the appropriate stirring method was searched for the production of aluminum metal matrix composites. Therefore, mechanical stirring, ultrasonic stirring and ultrasonic added mechanical stirring (named: hybrid stirring) processes were applied. In this part, both simulation studies and casting applications were performed and the obtained results were compared. It was concluded that the best homogeneous stirring was achieved by hybrid mixing. Additionally in this part, studies were carried out to determine the casting mold suitable for the production of metal matrix composites. To determine the appropriate mold, spoke mold that was developed to simulate a wheel and the bottom filling casting mold given in the standards were examined with the help of casting simulations. It was concluded that spoke mold was affected less than mold and casting temperature. In the third part, it was tried to determine the effect of different additives (silicon carbide-SiC, micron and nano-sized alumina- Al_2O_3 and graphene) on the mechanical properties in the production of aluminum metal matrix composites using the appropriate stirring method and appropriate mold. The amount of additives were used as 0.075 wt%, 0.15 wt% and 0.25 wt% for graphene, 0.5 wt%, 1.0 wt% and 1.5 wt% for the others. All samples were heat treated with T6 thereafter mechanical tests were applied. In the last part, new samples were produced with 1.0 wt% SiC, 0.5 wt% nano-size Al_2O_3 and 0.25 wt% graphene additives, which had the highest mechanical properties in the third step, and these samples were heat treated with T6 and then hot isostatic press (HIP) process was applied. After these applications, mechanical tests were applied to whole samples. The highest mechanical properties were obtained with the addition of 0.5% nano-sized Al_2O_3 .

Key Words: A356 Aluminum Alloy, Aluminum Metal Matrix Composite, Ultrasonic Stirring, Hot Isostatic Press



DÖKÜM ALÜMİNYUM METAL MATRİKS KOMPOZİTLERİNİN İLAVE PROSESLERLE GELİŞTİRİLMESİ

ÖZET

Günümüz şartlarında geleneksel olarak kullanılan malzemelerin piyasa beklentilerini karşılamada yetersiz kaldığı görülmektedir. Bu nedenle özellikle kompozit malzemelere olan ilgili günden güne artış göstermektedir. Özellikle otomotiv ve havacılık sanayileri gibi nihai ürün ağırlığının büyük bir önem taşıdığı sektörlerde kompozit malzemelerin rolü önem taşımaya başlamıştır.

Gerçekleştirilen bu çalışma dört bölümden oluşmaktadır. İlk bölümde alüminyum metal matrisli kompozitler üzerine ayrıntılı bir literatür incelemesi yapılmıştır. İkinci bölümde, alüminyum metal matrisli kompozitlerin üretimi için uygun karıştırma yöntemi belirlenmeye çalışılmıştır. Bu nedenle mekanik karıştırma, ultrasonik karıştırma ve mekanik karıştırma işlemine ek olarak ultrasonik karıştırma işlemi (hibrit karıştırma) uygulanmıştır. Bu bölümde hem simülasyon çalışmaları hem de döküm uygulamaları gerçekleştirilmiş ve elde edilen sonuçlarla karşılaştırmalı olarak değerlendirilmiştir. En iyi homojen karışma durumu hibrit karıştırma işlemi ile elde edildiği sonucuna varılmıştır. Ayrıca aynı bölümde, metal matrisli kompozit üretimi için uygun döküm kalıbının belirlenmesi çalışmaları gerçekleştirildi. Bunun için standartlarda verilen alttan dolum döküm kalıbı ile bir jantı simüle etmesi amacıyla geliştirilen feder döküm kalıbı döküm simülasyonların yardımıyla incelendi. Feder kalıbının kalıp ve döküm sıcaklığından daha az etkilendiği belirlendi. Üçüncü bölümde belirlenen karıştırma yöntemi ve uygun kalıp kullanılarak alüminyum metal matrisli kompozitlerin üretiminde farklı katkıların (silisyum karbür-SiC, mikron ve nano boyutta alümina- Al_2O_3 ve grafen) mekanik özellikler üzerindeki etkisi belirlenmeye çalışılmıştır. Katkılar grafen için ağırlıkça %0.075, 0.15 ve 0.25 olarak diğer katkıları için %0.5, 1.0 ve 1.5 olarak kullanılmıştır. Elde edilen tüm numunelere T6 ısıl işlemi uygulanmış ve mekanik testlere tabi tutulmuştur. Son bölümde, en iyi mekanik dayanım özelliklerini veren %1.0 SiC, %0.5 nano boyutta Al_2O_3 ve %0.25 grafen katkıları ile yeni numuneler üretilmiş ve bu numunelere sıcak isostatik pres (HIP) işlemi ve sonrasında T6 ısıl işlemi uygulanmıştır. Bu uygulamalar sonrasında numuneler mekanik testlere tabi tutulmuştur. En yüksek mekanik özellikler %0.5 nano boyutlu Al_2O_3 ilavesi ile elde edilmiştir.

Anahtar Kelimeler: A356 Alüminyum Alaşımı, Alüminyum Metal Matris Kompozit, Ultrasonik Karıştırma, Sıcak İsostatik Pres



1. INTRODUCTION

Aluminum alloys have high thermal conductivity, high corrosion resistance, easy recyclability, sufficient strength characteristics, ductility, durability; and especially the lightweight [1-3]. Therefore, it can be largely used in many areas of industry such as aerospace, architectural construction, and especially in automotive sector [3;4]. However, when considering the demands of automotive sector are uprising day by day and aluminum alloys do not meet particular expectations. Therefore, manufacturing industry started to investigate alternative engineering materials. The classification of engineering materials is stated in Figure 1.1.

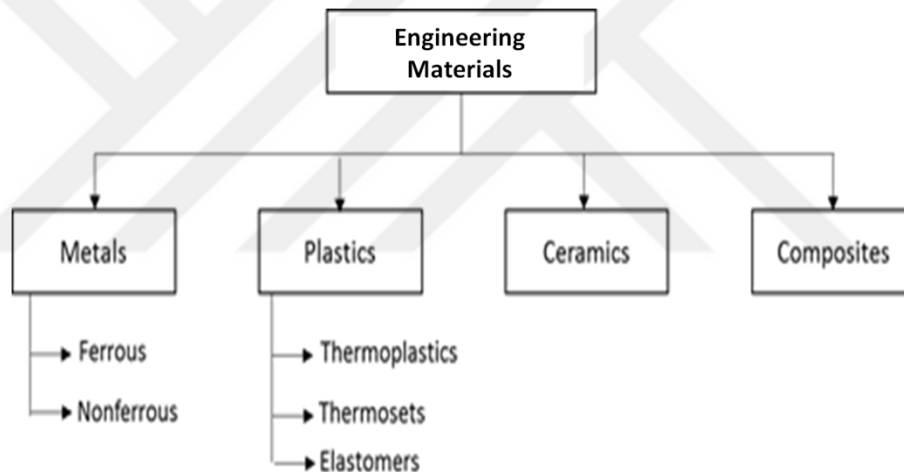


Figure 1.1 : Classification of engineering materials.

The group of composite material is one of the engineering materials containing two or more materials which are called reinforcement (for example; fibers, particulates or whiskers) materials and matrix (metals, plastics or ceramics) materials [5-7]. Notedly during the last 20 years, aluminum and its alloys have drawn attention in metal matrix composite systems [8-10]. For reinforcement materials, silicon carbide (SiC) and aluminum oxide (Al_2O_3) can be shown as the most widely used ones[8;11] and thus in this chapter, a literature survey was carried out on SiC, Al_2O_3 and graphene as reinforcements in aluminum metal matrix systems.

1.1 Aluminum Metal Matrix Composite with SiC

SiC is one of commonly used reinforcement material for aluminum metal matrix composites [8;12]. The summary of different investigations related to aluminum metal matrix composites with SiC reinforcement is given in Table 1.1.

Table 1.1 : The summary of aluminum composites with SiC.

Researchers	Additive Materials Particle Size	Rate Of Additive Materials	Preheat Conditions	Production Method	Ref.
Md. H. Rahman H.M. Mamun Al Rashed	53-74 μm	0%, 5%, 10%, 20%	800 °C for 2 hours	Stir casting	[13]
K. Karvanis D. Fasnakis A. Maropoulos S. Papanikolaou	325 mesh (~44 μm)	3%, 6%, 9%, 12%, 15%	1076 °C 1 hour 30 minutes	Centrifugal casting machine	[14]
K.L. Meena Dr.A. Manna Dr.S.S. Banwait Dr. Jaswanti	220-300-400 mesh (~69-40-37 μm)	5%, 10%, 15%	1100 °C for 1 hour 30 minutes	Stir casting	[15]
T. Ozben E. Kilickap O. Cakir	30-60 μm	5%, 10%, 15%	-	Pressure casting	[16]
M. Singla D.D. Dwivedi L.Singh V.Chawla	320 grit (~44 μm)	5%, 10%, 15%, 20%, 25%, 30%	1100 °C for 1- 3 hours	Stir casting	[17]
S. Johny James K. Venkatesan P. Kuppan R. Ramanujam	25 μm (Titanium di boride: 10 μm)	10% (Titanium di boride: 2.5% and 5.0%)	1000 °C for 2 hour	Stir casting	[18]
S.B. Prabu L. Karunamoorthy S.Kathiresan B. Mohan	60 μm	10%	800 °C for 2 hours	Stir casting	[19]
D. Sujan Z. Oo M.E. Rahman M.A. Maleque C.K. Tan	-	5%, 10%, 15%	-	Stir casting	[20]

Some researchers tried to clarify the effects of reinforcements in amount and particle sizes of reinforcements. One of them is Rahman et al. [13]. They investigated the effects on different amounts of SiC as 0, 5, 10 and 20 wt% on mechanical properties of composite materials. To produce composite samples, they concentrated on

mechanical stirring for 10 minutes at 500 rpm.; and they addressed hardness, tensile strength and wear resistance test to determine the mechanical properties of all samples, subsequently. They obtained the maximum results of hardness, tensile strength and wear resistance with 20 wt% SiC as $45,4 \pm 1,06$ HV, 77,56 MPa and nearly 0,005 cumulative mass loss, respectively. They declared that mechanical properties of composite ascended through increasing the amount of SiC.

Karvanis et al. [14] was interested in elucidating the effect of SiC particle on mechanical properties of aluminum metal matrix composites. So as to produce composite sample, they used a centrifugal casting machine and five different amounts of SiC additives as 3 wt%, 6 wt%, 9 wt%, 12 wt% and 15 wt%. They applied compressive strength, tensile strength and hardness tests to all composite samples. They declared that mechanical test results ascended through increasing the amount of SiC additives as tensile strength increased from 72,36 Pa to 119,38 MPa, and compressive strength increased from 140,86 MPa to 196,32 MPa.

Additionally, Meena et al. [15] tried to determine the effect of SiC additives in different amounts with various particle sizes. They used four different amounts of SiC as 5%, 10 wt%, 15 wt %, and 20 wt% and three different particle sizes as 220, 300 and 400 mesh. They worked with melt stirring method to produce composite samples and while doing so they addressed tensile strength, impact strength and hardness tests to all samples. They concluded that the results of whole tests were ascended through increasing the reinforced weight fraction but it was only limited to % elongation decrease.

Ozben et al. [16] used three different ratios as 5 wt%, 10 wt% and 15 wt% in SiC reinforcement to determine the mechanical properties of composite material by addressing hardness and impact tests to all samples. The outcomes of tests indicated that the maximum hardness and impact toughness were obtained as 65 HB and nearly 0,6 J, respectively. However, they explained that maximum tensile strength obtained from 10 wt% SiC; and over this interface bond between reinforcements and matrix was inadequate. They came to conclusion that increasing reinforcement ratio improves the mechanical properties such as, hardness and impact toughness, yet tensile strength pointed out different properties of some reinforced additives.

Singla et al. [17] conducted research on the effects of different amounts in SiC as 5 wt%, 10 wt%, 15 wt%, 20 wt%, 25 wt%, and 30 wt% on hardness and impact strength of composite samples. They applied two steps of stirring processes while using preheated aluminum scraps at 450° C for 3-4 hours and preheated SiC particles at 1100 °C for 1-3 hours. To obtain semi-solid state, aluminum scraps were heated above the liquidus then cooled just below liquidus in first step. Followingly, SiC particles were added and stirred manually. Afterwards, the melt was reheated and stirred with automatic stirrer to produce composite samples. To determine the hardness and impact strength, they addressed mechanical test to all composite samples by attaining the maximum hardness and impact strength with 25 wt% SiC additives as 45,5 BHN and 36 N-m, respectively. They expressed that the hardness and impact strength of composite refined with SiC escalation by increasing the amount of SiC additives.

Johny James et al. [18] investigated the effect of SiC, in which the particle size was 25 µm, on mechanical properties of aluminum alloy. Additionally, they used titanium di boride particles (average particle size of 10 µm) which was named as hybrid aluminum composite. In order to determine the effect, they melted the matrix material and added preheated SiC reinforcement as 2.5 wt% and 5.0 wt%. Besides, they added titanium di boride particles, which was preheated up to 200 °C, as 10 wt%. They addressed mechanical stirring for 15 minutes at 300 rpm. Subsequently, they produced samples and mechanical tests were applied to determine the change in mechanical properties. It was revealed that addition of SiC particle improved the strength of based alloy as 20%. One the other hand, while the addition of titanium increased, the reduction of strength was recorded as 50-60%. They also declared that titanium diboride improved both the surface roughness value and the wear resistance behavior.

Some researchers investigated the stirring processes detailly as such: stirring speed and duration time. One of them is Prabu et al. [19] who tried to determine the effects of stirring speed and time duration on mechanical properties of aluminum metal matrix composite. They worked with three different stirring speeds as 500, 600 and 700 rpm and three different time durations as 5, 10 and 15 minutes. To determine the effects of stirring processes, they used 10 wt% SiC (average particle size was 60 µm)

as a reinforcement. The outcome illustrated that hardness value of composite was non-uniform for a short stirring time and also at higher speed as 700 rpm. They concluded that the mechanical properties were directly affected by both stirring speed and time; when better hardness of composite could get at 10 minutes stirring time and at 600 rpm stirring speed.

Some researchers also used one reinforcement more in their researchs. Sujana et al. [20] addressed stir casting method and used both Al_2O_3 and SiC reinforcements to produce aluminum matrix composite. They worked with different weight fractions of both SiC and Al_2O_3 as 5 wt%, 10 wt% and 15 wt% by applying tensile strength, hardness and wear resistance tests to determine the mechanical properties of composite samples. They came into conclusion that the results of tensile strength and hardness increased as 258.8, 293.3 and 310.5 MPa and 30, 45 and 50 HR, respectively. To determine the wear resistances, they applied two different grinding speeds as 300 and 400 rpm with constant time and adhesive paper. They declared that wear resistance ascended through increasing the amount of SiC additives, yet decreased by increasing the grinding speed.

1.2 Aluminum Metal Matrix Composite with Al_2O_3

Al_2O_3 is also a commonly used reinforcement material for aluminum metal matrix composites [8]. The summary of different investigations related to aluminum metal matrix composites with Al_2O_3 reinforcement is given in Table 1.2.

Singh et al. [21] studied on the effects of particle sizes and amounts of reinforcements and process parameters for producing composite material as well. They used the Taguchi method to design the experiment with variables such as particle size, amount of reinforcement and stirring time. They determined variables from three different particle sizes of reinforcement as 75, 105 and 150 μm , three different weight percentages as 3 %, 6 % and 9 % and also three different stirring time for process parameters as 15, 20 and 25 minutes. Later, they produced composite samples and addressed hardness, tensile strength and impact strength tests to all. They concluded that increasing the stirring time and weight percentage of reinforcements had positive effect on mechanical test results, on the contrary increasing particle sizes had negative effects. They obtained the outcomes of

hardness, tensile strength and impact strength tests as increased from 29 HRB to 58 HRB and from 96 N/mm² to 147 N/mm² and from 12 Nm to 30,59 Nm, respectively.

Table 1.2: The summary of aluminum composites with Al₂O₃.

Researchers	Additive materials	Additive materials Particle Size	Rate of additive materials	Preheat conditions	Production method	Ref.
D. Sujan Z. Oo M.E. Rahman M.A. Maleque C.K. Tan	Al ₂ O ₃	400 μm	5%, 10%, 15%	-	Stir casting	[20]
L. Singh B. Ram A. Singh	Al ₂ O ₃	75 μm 105 μm 150 μm	3%, 6%, 9%	300 C for 1 hour	Stir casting	[21]
K.K. Alaneme M.O. Bodunrin	Al ₂ O ₃	28 μm	6%, 9%, 15%, 18%	250 C for 5 minutes	Stir casting	[22]
S. Mula P. Padhi S.C. Panigrahi S.K. Pabi S.Ghosh	nano Al ₂ O ₃	10 nm	2%		Ultrasonic chamber	[23]
S.A. Sajjadi H.R. Ezatpour H. Beygi	micro Al ₂ O ₃ nano Al ₂ O ₃	20 μm 50 nm	1%, 3%, 5%, 10% 1%, 2%, 3%	1100 C for 20 minutes	Stir casting Stir casting	[24]
M. Kok	Al ₂ O ₃	16 μm 32 μm 66 μm	7%, 15%, 23%	400 C for 10 minutes	Stir casting	[25]
N. Srivastava G. P. Chaudhari	Al ₂ O ₃	30-70 nm	1%, 2%, 3%	400 C	Manually mixed and ultrasonic vibration	[26]

Alaneme et al. [22] investigated the effect of Al₂O₃, with 28 μm particle size, on mechanical properties of composite by adding three different volume percentages as 6, 9, 15 and 18. They preheated the reinforcements for 5 minutes at 250 °C to improve the wettability between reinforcements and matrix materials. They applied stirring process as 300 rpm for 10 minutes. They declared that some mechanical properties (like tensile strength, yield strength, and hardness) ascended through increasing the ratio of additives, but some mechanical properties (like strain of fracture and fracture toughness) decreased by increasing the ratio of additives.

Sujan et al. [20] worked on stir casting method and used both Al_2O_3 and SiC reinforcements to produce aluminum matrix composite. They worked with different weight fractions on both SiC and Al_2O_3 such as 5 wt%, 10 wt% and 15 wt% by addressing tensile strength, hardness and wear resistance tests to determine the mechanical properties of composite samples; and declared the density of composite escalated from 2,73 to 3,02 by increasing the amount of reinforcement from 5% to 15% wt. And also tensile strength and hardness increased from 262,2 to 282,9 MPa and from 31 to 42 HR by extending the amount of reinforcement, respectively. They asserted that reinforced materials improve physical and mechanical properties of matrix metals. However, when compared to SiC reinforced aluminum, Al_2O_3 reinforced aluminum had higher wear rate.

Mula et al. [23] investigated the effect with nano-sized Al_2O_3 on composite mechanical properties. To produce nano-size Al_2O_3 , they practiced with $75\mu\text{m}$ Al_2O_3 powder and grinded it into a ball mill. Subsequently, they obtained nano Al_2O_3 , they used the non-contact ultrasonic casting method to produce composite samples with 2 wt% nano-sized Al_2O_3 . So as to determine mechanical properties, they addressed some mechanical tests such as hardness and tensile strength. They concluded that tensile strength and hardness results of composite samples increased respectively as nearly 57% and 92% when adding nano-sized dispersoids.

Sajjadi et al. [24] worked with two different particle sizes of Al_2O_3 as $20\mu\text{m}$ and 50 nm to investigate the effect on mechanical behaviour of composite. They used stir casting method and preheated the reinforcement as given in Table 1.2 by adding nano-sized and micro-sized reinforcement particles as 1 wt%, 2 wt%, 3 wt% and 1 wt%, 3 wt%, 5 wt%, 10 wt%, respectively. They analysed composite samples for their metallography and mechanical properties; and declared that wettability of particles correlated with size and percentage of reinforcement. Moreover, wettability was decreased by increasing the percentage and by reducing the particle size of reinforcement. However, the results of hardness, compressive strength and porosity ascended through increasing the amount of nano Al_2O_3 .

Kok [25] studied the effect of Al_2O_3 reinforcement by adding three different sizes and volume ratios as $16\mu\text{m}$, $32\mu\text{m}$, $66\mu\text{m}$ and 7%, 15%, 23%, respectively. To produce composites sample, pressure was applied following the vortex method. He

calculated the porosity and concluded that porosity was decreased by increasing both volume ratios and particle sizes. In addition, he asserted that composite which was reinforced with 66 μm has more homogeneity than the composite which was reinforced with 16 μm and 32 μm .

Srivastava et al. [26] investigated the effects of nano Al_2O_3 particles by using ultrasonic vibrations. They melted the matrix material and used a graphite rod mix on the reinforcement for 5 minutes. Later, they applied ultrasonic vibration for 3 minutes while adding nano particles as 1 wt%, 2 wt% and 3%; and in order to determine the ultrasonic vibration effect, they also produced 1 wt% without ultrasonic vibration. They addressed hardness and tensile tests to determine the mechanical properties. They concluded that the samples which were produced with ultrasonic vibration had more uniformed dispersion of reinforcement particles than the ones which are manually stirred. In comparison to the base alloy, sample was reinforced with 2 wt% showed the highest mechanical properties with YS and UTS as 81 % and 53 %, respectively. Additionally, they clarified that porosity content ascended through increasing the content of reinforcements. They clarified that mechanical properties of samples are improved due to thermal mismatch between matrix and reinforcements.

1.3 Aluminum Metal Matrix Composite with Graphene

During the last several years, graphene, which is a two dimensional carbon material, have taken attention of scientists since it contains high mechanical and chemical properties [27;28]. The summary of different investigations related to aluminum metal matrix composites with graphene reinforcement is given in Table 1.3.

Jagadish [29] worked with powder metallurgy to produce aluminum matrix composite with graphene. The researcher tried to explain the effects of four different amounts in graphene as 0.25 wt%, 0.5 wt%, 0.75 wt% and 1.0 wt%. To compare the effect of graphene reinforcement, reference sample was also produced without adding any reinforcements. Hardness and impact tests were addressed to determine mechanical properties of all samples. Outcomes of tests revealed that the reference sample had higher hardness value as 62.57 HRC while the maximum hardness was obtained with 0.5 wt% graphene as 52.06 HRC. Similar results were also obtained at

Charpy impact test. He declared that the impact test results decreased by increasing the amounts of graphene additives.

Table 1.3: The summary of aluminum composites with graphene.

Researchers	Additive materials	Rate of additive materials	Production method	Ref.
S. Venkatesan M.A. Xavier	Graphene	0.33%, 0.55% 0.77%	Stir casting	[27]
S.F. Bartolucci J. Paras M. A. Rafiee J. Rafiee S. Lee D. Kapoor N. Koratkar	Graphene	0,1%	Hot isostatic pressing, and hot extrusion	[28]
B. S. Jagadish	Graphene	0.25%, 0.5%, 0.75%, 1%	Powder metallurgy	[29]
P. Kumar S Aadithya K Dhilepan N Nikhil	Graphene (and SiC; fixed 5% wt.)	1%, 3%, 5%	Ultrasonic assisted stir casting	[30]
M.M. Narwate K.K. Mohandas	Graphene (aluminum with 10%fixed TiO ₂)	0,5%, 0,75%, 1,0%	Stir casting	[31]

The other research about graphene reinforcement was studied by Venkatesan et al. [27]. They applied three different amounts of graphene as 0.33 wt%, 0.55 wt% and 0.77 wt%. To produce composite samples, they practised stir casting method as 400 rpm for 5-10 seconds at 820 °C. They performed tensile test, hardness test and three-point bending tests; and concluded that outcomes of ultimate tensile strength, hardness and three-point bending increased from 145 MPa to 47 MPa, from 45 BHN to 57,1 BHN and from 210 MPa to 140 MPa by decreasing the amount of graphene, respectively. The test results revealed that optimum result was obtained with 0.33 wt% graphene additive.

Bartolucci et al. [28] investigated the aluminum which was reinforced with graphene platelets and multi walled carbon (MWCNT) nanotube as 0.1 wt% and 1.0 wt%, respectively. To produce composite samples, they applied milling, hot isostatic press and hot extrusion and also a reference sample was produced without reinforcement additives to compare the mechanical properties. They concluded that MWCNT

promoted the tensile strength up to 12% and graphene addition decreased hardness and strength values.

Kumar et al. [30] worked on constant amount of SiC reinforcement as 5.0 wt% and three different amounts of graphene as 1 wt%, 3 wt% and 5 wt% together. They also produced aluminum composite with 5.0 wt% SiC reinforcement in comparison to the reference sample. They melted aluminum and started stirring at 630 °C for 5 minutes then reheated at 900 °C; and applied ultrasonic cavitation for 10 minutes followingly. By the end of stirring process, they poured slurry in preheated metallic mould at 500 °C. They addressed tensile, hardness, flexural tests and impact test to determine mechanical properties of samples. They concluded that the outcomes of tensile test, flexural test and impact test ascended through increasing the amount of graphene additives. In addition, they declared that hardness of composite with 3 wt% graphene was at maximum.

Narwate et al. [31] also investigated the effects in three different amounts of graphene as 0.5 wt%, 0.75 wt% and 1.0 wt% with the constant amount of TiO₂ as 10 wt% reinforced aluminum. They melted matrix material and applied mechanical stirring for 5 minutes at 200 rpm. When a vortex was occurred, they added graphene reinforcement for 5-10 minutes in order to obtain samples. They addressed tensile and hardness tests to all samples. The maximum results of tensile and hardness tests were obtained with 1.0 wt% graphene additive as 112.7 MPa and 50 HRB, respectively.

As seen in the literature studies, the interest in aluminum metal matrix composites has increased day by day. Additionally, in these studies, the types and additions of the reinforcements are generally changed. But, the studies on determining the appropriate stirring method and mold selection for particle reinforced composite production are not discussed in detail. In this thesis, firstly, both the stirring method and the mold, which are suitable for the production of particle reinforced composite, are determined by simulation analysis supported by laboratory studies. By using the determined stirring method and mold, the composite samples were produced with the help of using SiC, micro-Al₂O₃, nano-Al₂O₃ and graphene reinforcements in different ratios. The effect of different reinforcements on the mechanical and metallurgical properties of the composite material were compared by using SiC and

micro-Al₂O₃ with similar particle size. By using micro-Al₂O₃ and nano-Al₂O₃ reinforcements, the effect of different particle size of the same reinforcement on the mechanical and metallurgical properties of the composite material was compared. nano-Al₂O₃ and graphene reinforcements were used to compare the effect of additives under micro-size. According to the test results, new samples were produced by using the reinforcement and the reinforcement ratios which had the highest quality index. The hot isostatic press (HIP) process was applied to the produced samples and the effect of the HIP process especially on the reducing of porosity and the effect on the mechanical properties of the composite materials were revealed comparatively.



2. EXPERIMENTAL

2.1 Materials

Table 2.1 exhibits the chemical composition of hypoeutectic aluminum alloy A356 (AlSi7Mg0.3) which was used as the matrix metal. A charge of 4 kg of A356 alloy was melted at 750°C in a graphite crucible at a resistance furnace during this study.

Table 2.1 : Chemical composition (wt. %) of matrix alloy - A356.

Alloy/Element	Si	Fe	Cu	Mn	Mg	Zn	Ti	Al
A356	7,3	0,1	0,1	0,05	0,3	0,05	0,1	Balanced

SiC, n- Al₂O₃, m- Al₂O₃ and graphene were used as reinforcement materials as illustrated in Table 2.2.

Table 2.2 : Properties of reinforcement.

Reinforcement	Particle size / properties	Amount of additive (wt.%)	Suppliers
SiC	50-56 µm	0.5, 1.0 and 1.5	Kuhmichel, Turkey
Al ₂ O ₃ (micro-Al ₂ O ₃)	65 µm	0.5, 1.0 and 1.5	Sermet Limited Company, Turkey
Al ₂ O ₃ (nano-Al ₂ O ₃)	79 nm	0.5, 1.0 and 1.5	Sermet Limited Company, Turkey
Graphene	99.5+%, 6 nm, S.A: 150 m ² /g Dia: 24µm	0.075, 0.25 and 0.25	Nanografi LLC, Turkey

To obtain an oxidized surface that improves wettability, reinforcement powders were preheated. Table 2.3 displays the preheating processes of all reinforcements separately.

Table 2.3 : Preheating process of reinforcements.

Reinforcement	Preheating temperature (°C)	Preheating time (minutes)
SiC	750	120
Al ₂ O ₃ (micro-Al ₂ O ₃)	750	120
Al ₂ O ₃ (nano-Al ₂ O ₃)	700	20
Graphene	600	30

Figure 2.1 shows that the morphology of reinforcements particle. The SEM micrograph in Figure 2.1 shows that SiC particles are more irregular in shape than the others. Additionally micro-Al₂O₃ particles are nearly the regular shape as round. Nano-Al₂O₃ particles are seen that also regular.

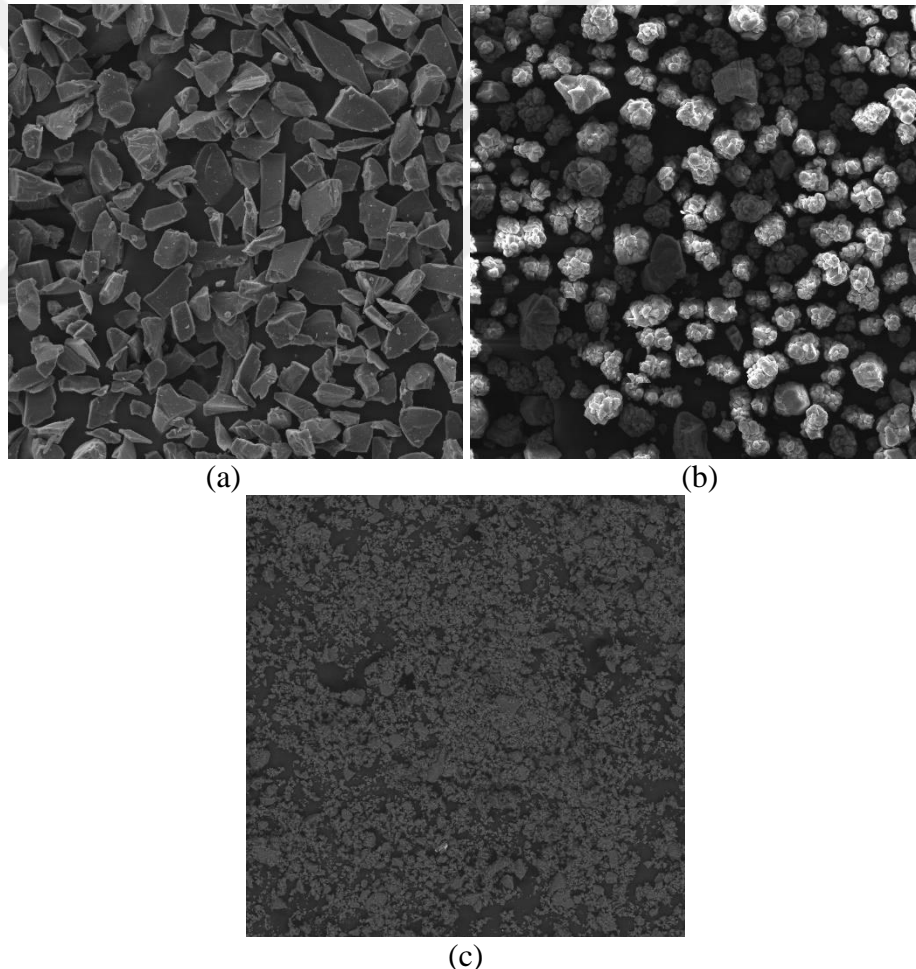


Figure 2.1 : Morphology of reinforcements particle a) SiC, b) micro-Al₂O₃ and c) nano-Al₂O₃

2.2 Preparation Of Composites

The composite samples were prepared by the way of casting processes of which the flow chart is demonstrated in Figure 2.2.

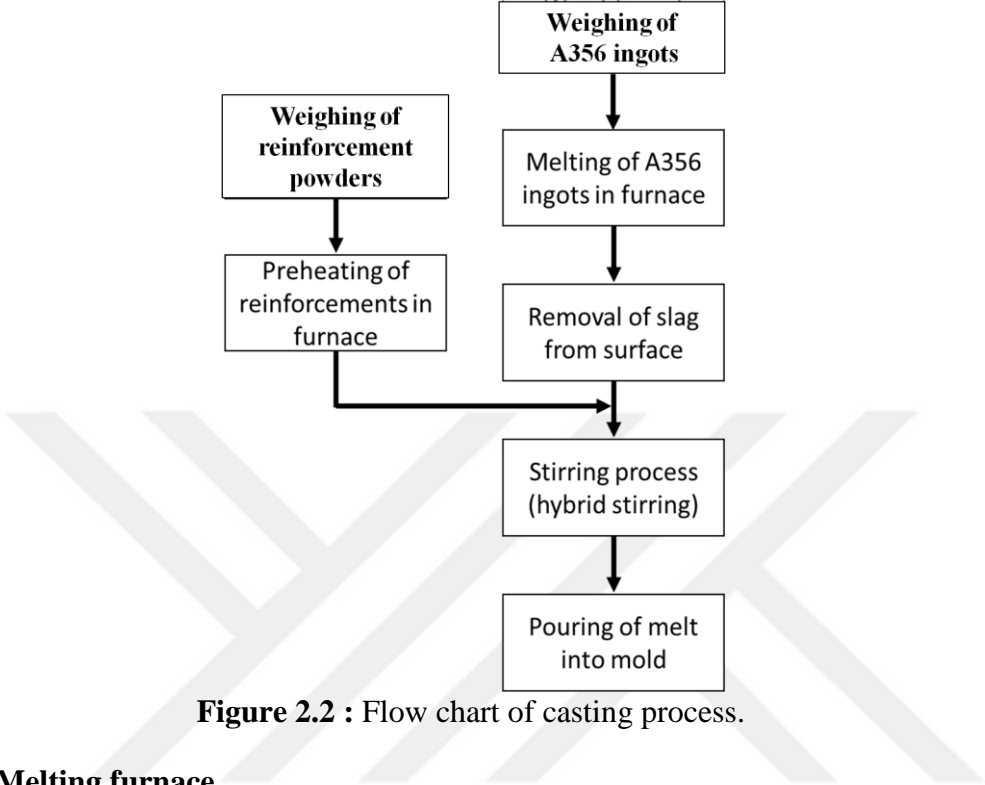


Figure 2.2 : Flow chart of casting process.

2.2.1 Melting furnace

Figure 2.3 a shows Protherm HLF400 brand melting furnace, which is located at CMS Light Alloy Wheels Co. Research and Development Center laboratory, was used in order to melt the matrix material. Figure 2.3 b shows Protherm brand melting furnace which is used to preheat the reinforcement materials.

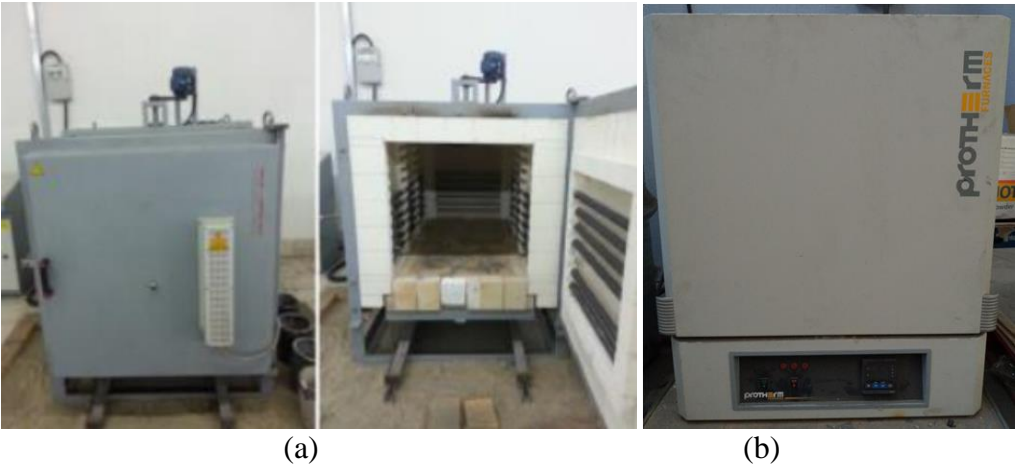


Figure 2.3 : a) Melting and b) preheating furnaces.

After all the samples were produced, T6 heat treatment process (solutionized at 540°C for 4 hours, then quenched in water at 80°C, artificially aged at 155°C for 3 hours) was applied.

2.2.2 Stirring equipments

Two different stirring equipments were used in this study such as mechanical stirrer and ultrasonic vibration. Mechanical stirring equipment was applied by Optimum B20-400 V brand machine at 600 rpm as given in Figure 2.4 a. The ultrasonic stirring was applied by Rtul brand machine, shown in Figure 2.4 b, which is capable of producing 3 kW of electric energy at a constant resonant frequency of 19.8 kHz.

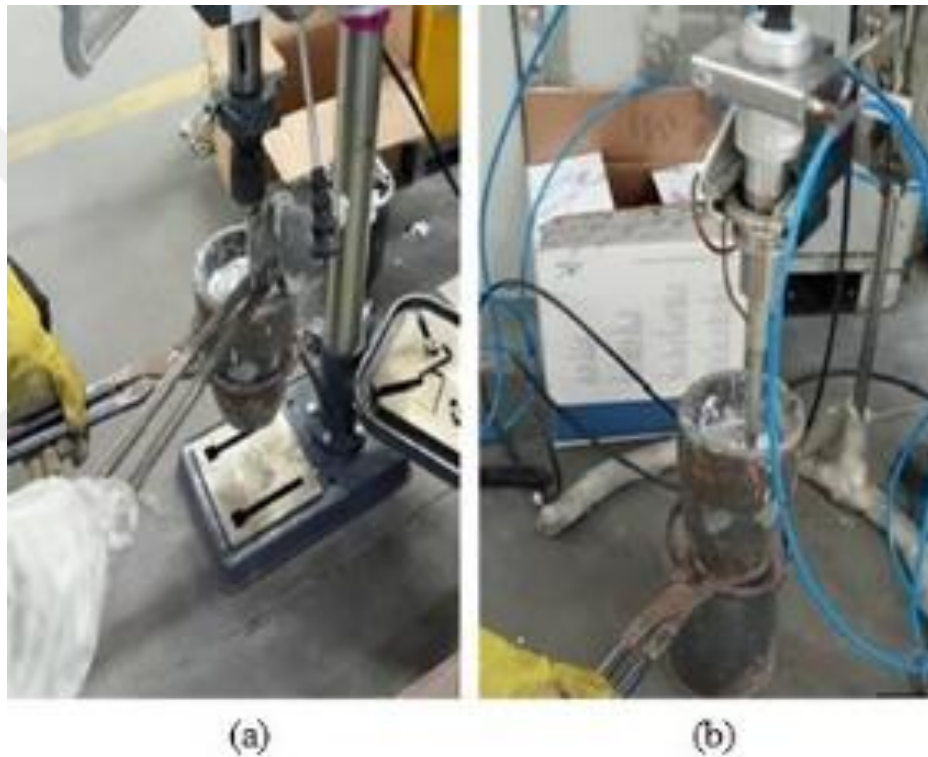


Figure 2.4 : a) Mechanical and b) ultrasonic stirrer.

2.2.3 Hot isostatic process (HIP)

HIP machine, which is ALP6-30H model of American Isostatic Presses company at Dokuz Eylul University Electronic Material Applying Center (EMUM), is given in Figure 2.5.



Figure 2.5 : HIP machine.

Before practicing the HIP method, all samples were machined as round to apply the same pressure on surface of samples while administering HIP condition. A group of samples, which were to be applied the HIP method, are demonstrated in Figure 2.6.



Figure 2.6 : A set of HIP samples.

The condition of HIP method was addressed under pressure of 100 MPa at 510°C for 2 hour and cooling condition was set as 50°C/minute. The steps of HIP method is given in Figure 2.7.

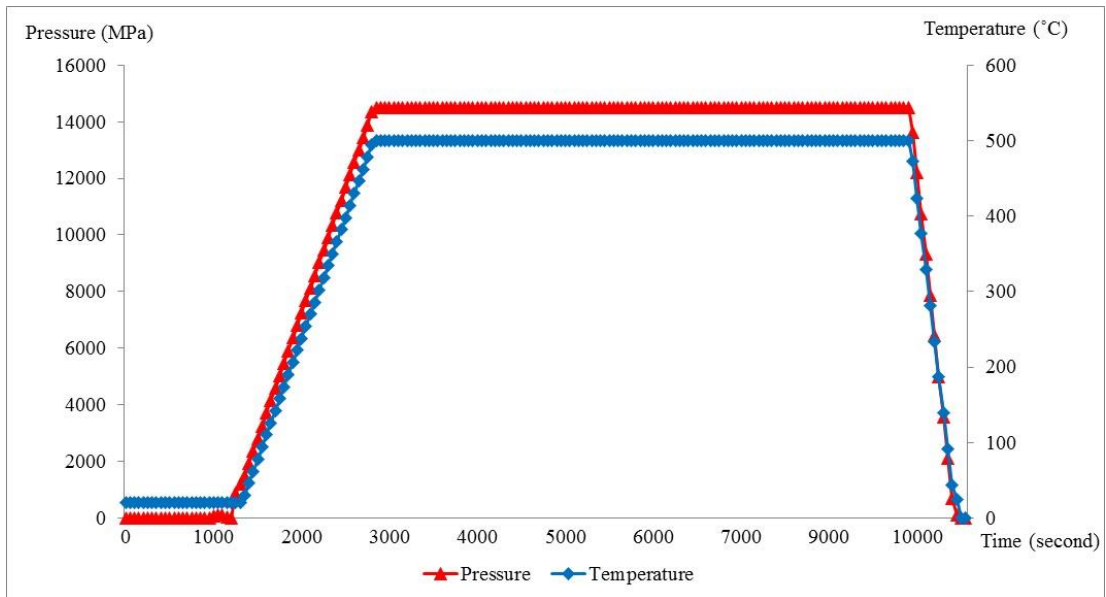


Figure 2.7 : Steps of HIP method.

2.3 Characterization

2.3.1 Mechanical properties

2.3.1.1 Tensile test

Tensile test samples were prepared in accordance with DIN EN ISO 6892-1 which is given Figure 2.8 and tests were applied in compliance with DIN EN 10002-1 by Zwick Z100 model tensile testing machine (Figure 2.9) for mechanical examinations. All dimensions in Figure 2.8 are in millimeters.

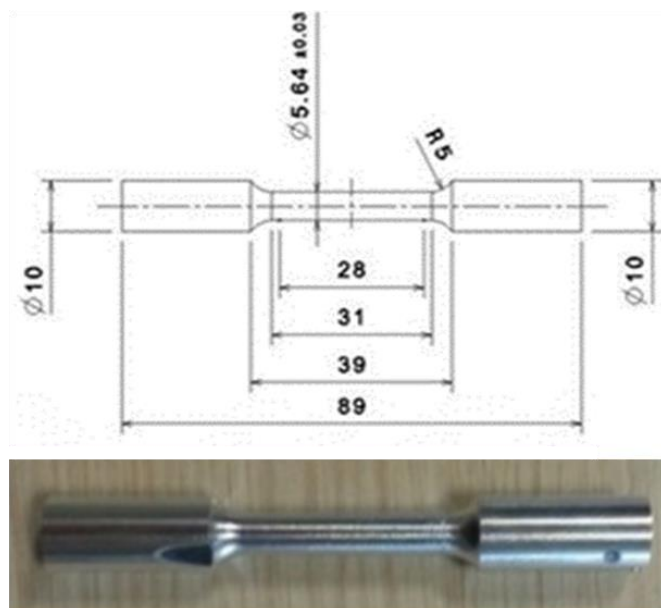


Figure 2.8 : Tensile test sample.



Figure 2.9 : Tensile test machine.

2.3.1.2 Hardness test

InfoTek TIME TH-600 machine, which was given in Figure 2.10, was used to measure the hardness of composite samples in accordance with DIN EN ISO 6506-1 standard.



Figure 2.10 : Hardness test machine.

2.3.1.3 Charpy impact test

Charpy Impact test samples (Figure 2.11) were prepared in equivalent to ASTM-E23 and INSTRON CEAST 9050 machines (Figure 2.12) that were operated to measure the impact energy. All dimensions in Figure 2.11 are in millimeters.

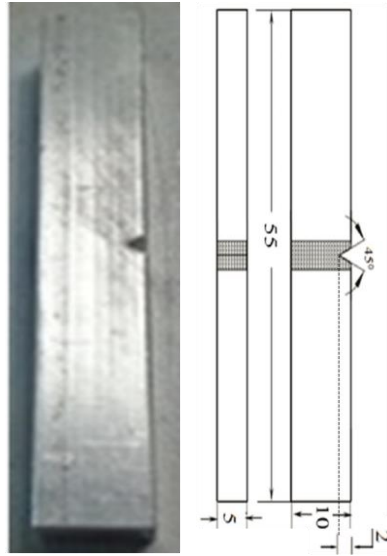


Figure 2.11 : Charpy impact test sample.



Figure 2.12 : Charpy impact test machine.

2.3.2 Metallographical analysis

2.3.2.1 Optical microscopy

To investigate the metallographic examinations, the samples were sectioned then grinded with SiC paper and polished with diamond paste. For metallographic analysis, the following etching solutions were used: 0.5% HF for micro and FeCl₃ for macro examinations. Nikon Epiphot 200 (Figure 2.13 a) and Clemex S2.0C (Figure 2.13 b) were used for microstructure and macrostructure analyses, respectively.

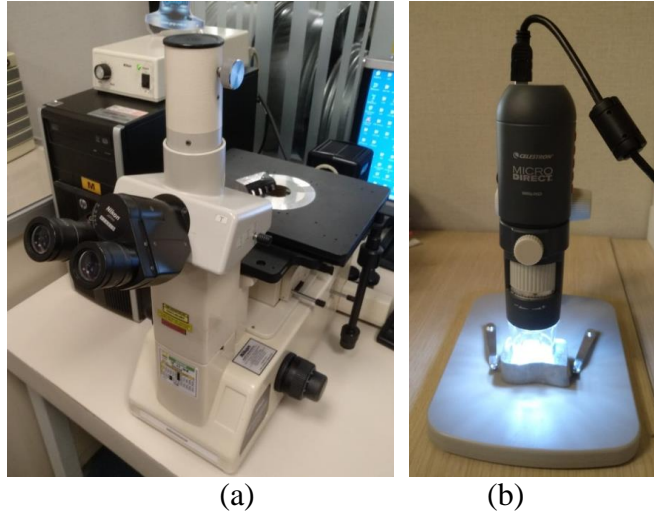


Figure 2.13 : a) Nikon Epiphot 200 and b) Clemex S2.0C.

2.3.2.2 Scanning electron microscopy

Carl Zeiss 300VP scanning electron microscope (Figure 2.14), which is located in Izmir Katip Celebi University Central Research Laboratories Application and Research Center, was used to investigate detailed views of interior structures of composite samples.



Figure 2.14 : Scanning electron microscope.

2.3.2.3 Porosity measurement

Porosity is calculated by using differences of density between measured principles (known as Archimedes' principle) and theoretical ones as given equation 2.1 [75; 76].

$$\% \text{ porosity} = (\rho_{\text{theoretical}} - \rho_{\text{measured}} / \rho_{\text{theoretical}}) * 100 \quad (2.1)$$

Theoretical density is calculated by rules of mixtures as given equation 2.2.

$$\rho_{\text{theoretical}} = \sum (f_i * \rho_i) = f_{\text{matrix}} * \rho_{\text{matrix}} + f_{\text{particle}} * \rho_{\text{particle}} \quad (2.2)$$

f is volume fraction and ρ is density of each material in composite.



3. RESULTS AND DISCUSSIONS

This study has three main parts. In the first part appropriate stirring method and mold design were dealt with and in the second part different reinforcement particles were taken into consideration to determine the effect on mechanical and metallographical properties of aluminum metal matrix composites. In the last part the effect of hot isostatic press on mechanical and metallographical properties of aluminum metal matrix composites were investigated.

3.1 Determination of Stirring Method and Appropriate Mold Design

The usage of aluminum alloys has been rapidly increased due to the high ductility, recyclability, high strength of weight ratio, high corrosion resistance and low-density properties [1-5]. Although aluminum has good properties after alloying process, the improvement of new developments in metal matrix composites has been observed with regards to the industrial demands [32]. To produce composite material, SiC particles [23-25;33;34] and aluminum alloys [5;6] have been selected respectively as reinforcement and matrix materials, especially during the last 20 years. There are many production techniques and alternative mold designs to produce composite material. In this chapter, which production technique and mold design were more appropriate to produce particle reinforced composite was explained with the help of simulation analysis and laboratory studies.

3.1.1 Simulation analysis

There are many fabrication techniques such as liquid metal infiltration, squeeze casting, powder metallurgy, spray decomposition and stir casting that can be used to produce composite materials for different types of reinforcement [24;35;36]. Yet, due to flexibility, budgetary and simplicity reasons, the stirring method is considered as one of the most preferred for the production of a discontinuous metal matrix composite [21;36-38].

Literature embraces many researchers who have studied on stirring method. Some of which were interested in stirring speed and time while others were interested in casting temperature and amount of reinforcements.

Prabu et al. [24] worked on the effect of mechanical stirring speed and time. They concluded that the homogeneous distribution of SiC was in direct relation with stirring process and it ascended through increasing stirring speed and time by applying the hardness test. Mathur et al. [39] worked on the constant stirring speed as 600 rpm and investigated the effects of different processes at temperatures as 700°C, 725°C and 750°C. They applied the tensile test to all samples and concluded that the tensile strength ascended through increasing casting temperature. Meena et al. [15] investigated the effects of different particle sizes of reinforcement as 220, 300 and 400 mesh and different weight fractions as 5%, 10%, 15%, and 20% on mechanical properties of composite samples. They addressed tensile and impact strength tests to determine the mechanical properties and concluded that the tensile and impact strength were increased, but elongation at fracture was decreased by increasing the amount of reinforcement.

During the last years, ultrasonic stirring method was also taken into consideration and researchers began to use this technique as an innovative method. Recent studies have begun to practice stir casting technique which was assisted with ultrasonic vibration to reduce segregation and to improve mechanical performance of metal matrix composite. This assisted method could be used especially on nano-particle reinforcement [40;41]. Kumar et al. [30] investigated the effect of ultrasonic stirring method to produce aluminum matrix composite by using SiC and graphene as reinforcements. They melted aluminum matrix, then cooled it down at the furnace to 630°C and added reinforcement particles with magnesium powder to improve the wettability of particles. They applied stirring process for 5 minutes at 630°C; and the charge was heated up to 900°C followingly by addressing ultrasonic cavitation for 10 minutes. They concluded that the mechanical properties were escalated by increasing the amount of graphene.

3.1.2 Simulation analysis of stirring methods

Simulation softwares are important tools for engineers to analyse the properties of final product and to determine production system parameters. They are commonly

used for predetermining the problems that could be encountered, especially in product design and production processes. By using simulation programs, engineers not only achieve faster results in product design, but also reduce trial costs during production. There are many simulation studies that are carried out in the literature about production of composite materials [42-45].

For the simulation analysis, aluminum and SiC (average particle size: 50-56 μm) were used as matrix and reinforcement materials, respectively. Literature survey was conducted to determine which content of reinforcement to be used. The particle size and content of SiC reinforcement were attributed to strengthening [46] and the typical application of SiC was used between 5-20 vol%. Yet, if the particulate amount increases, the viscosity of melt escalates as well; so that it is not easy to pour and to fill a mold cavity [47]. Therefore, SiC content was chosen to be around 1 wt. %. To produce composite samples, aluminum matrix was firstly melted then SiC reinforcement was added into molten aluminum while mechanical stirring process was being applied. Thereafter, it was stirred continuously for about 2 minutes to obtain a uniformed distribution of reinforcements [48]. The mechanical stirring time is an important part of the process. If the stirring time is higher, air or gas bubbles can be sucked into molten aluminum [49]; when all these circumstances are considered, stirring time was chosen as 2 minutes. Three different stirring methods such as mechanical, ultrasonic and hybrid (both mechanical and ultrasonic) were analysed by using simulation programs. Ansys Fluent was used in modeling the fluid flow for CFD analysis to characterize the distribution of reinforcement particles [44].

Figure 3.1 shows the geometry of crucible and dimension of stirring equipment parts. To create the simulation model, ANSYS CFD analysis was used. The assumptions which were used in the simulation studies are summarized as follows [44];

- ✓ SiC particles flow as a fluid because of its small size,
- ✓ SiC particles are uniformly distributed in the crucible at initial condition,
- ✓ Crucible is made of graphite which acts as an adiabatic solid wall,
- ✓ Fluids are treated as Newtonian fluids,
- ✓ Initial temperature is 1000 K
- ✓ Turbulence model is k- ϵ turbulence
- ✓ Mechanical stirrer is applied as 600 rpm axial speed

These assumptions were worked on each stirring methods. Figure 3.2 displays the applied ultrasonic processing system.

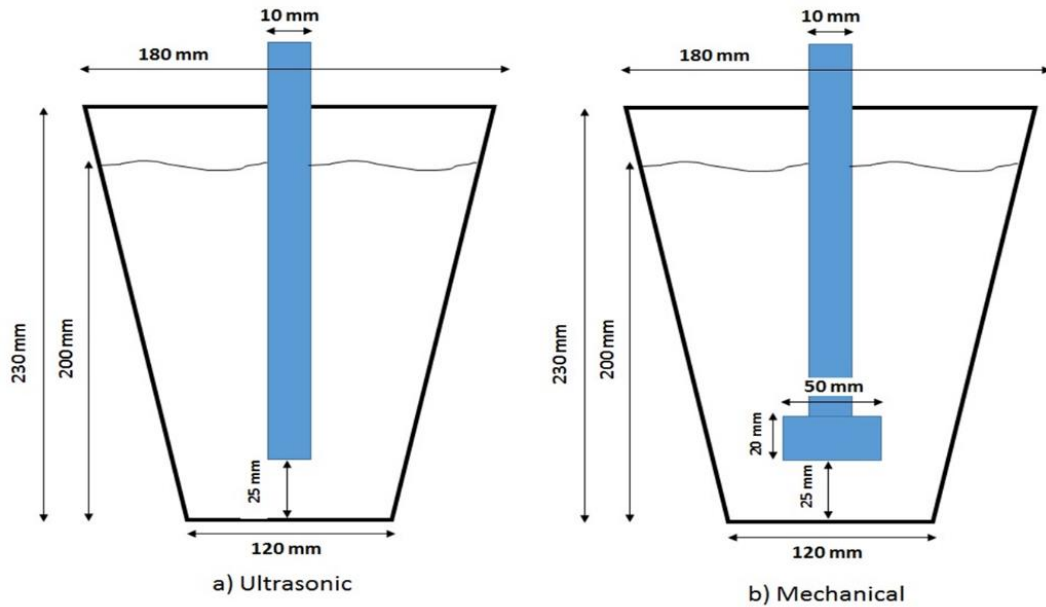


Figure 3.1 : Dimensions of the Crucible.

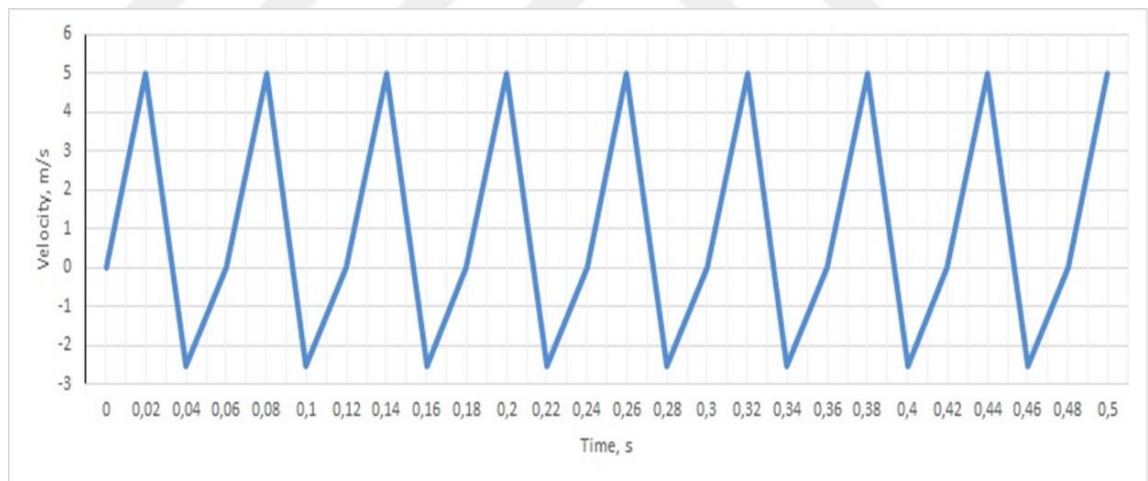


Figure 3.2. : Ultrasonic Processing System.

Simulation analysis were performed by using mechanical (for 2 minutes), ultrasonic (for 2 minutes) and hybrid (1 minute for mechanical and 1 for minute ultrasonic) stirring parameters.

Table 3.1 illustrates the material properties and solver parameters to perform the simulation studies.

Table 3.1 : Properties of materials used in simulation analysis [44].

Properties	Aluminum	SiC
Molecular weight (kg/kgmol)	26.891	40.11
Density (kg/m ³)	2720	3210
Specific Heat (J/kg-K)	963	750
Reference Temperature (K)	1000	1000
Standard state enthalpy (J/kg)	3,29E8	7,19E8
Viscosity (kg/m-s)	1.4x10 ⁻³	1x10 ⁻³
Particle size	-	50-56 μm

3.1.3 Simulation analysis of mold designs

The particle distribution in matrix is at a crucial importance for the performance of metal matrix composite [46]. Hashim et al. declared that particle distribution hinges on different steps of production processes as during stirring, after stirring (before solidification) and during solidification [47]. Especially during the solidification of metal matrix composite, if it is cooled rapidly, distribution of SiC particles are more homogeneous than slower cooling rate [44;47;49]. For a rapid cooling, both mold and casting temperatures should be determined at optimum. To determine the appropriate mold design, two different molds were analysed with the help of MAGMA simulation software.

Figure 3.3 a (known as bottom-fed mold) displays the mold which was built according to the ASTM B 108-03a and Figure 3.3 b (known as spoke mold) demonstrates the mold which was built to simulate wheel geometry [50].

In the direction of simulation analysis, aluminum and SiC (average particle size: 50-56 μm) were used as matrix and reinforcement materials, respectively. MAGMA simulation software was used to determine the effect of two different mold types. Three different casting temperatures (650°C, 750°C and 850°C) and three different mold temperatures (150 °C, 250 °C and 350°C) were applied conductively to determine the distribution and agglomeration of SiC particles. The assumptions of simulation analysis are summarized as follows;

- ✓ Filling time: 10 seconds,
- ✓ Heat transfer coefficient between liquid metal and mold: Magma database temperature dependent to heat transfer coefficients
- ✓ Particle specifications:
 - Particle size; 53 μm

- Density; 3,210 g/cm³
- ✓ Mold temperatures; 150, 250, 350°C
- ✓ Casting temperatures; 650, 750, 850°C.

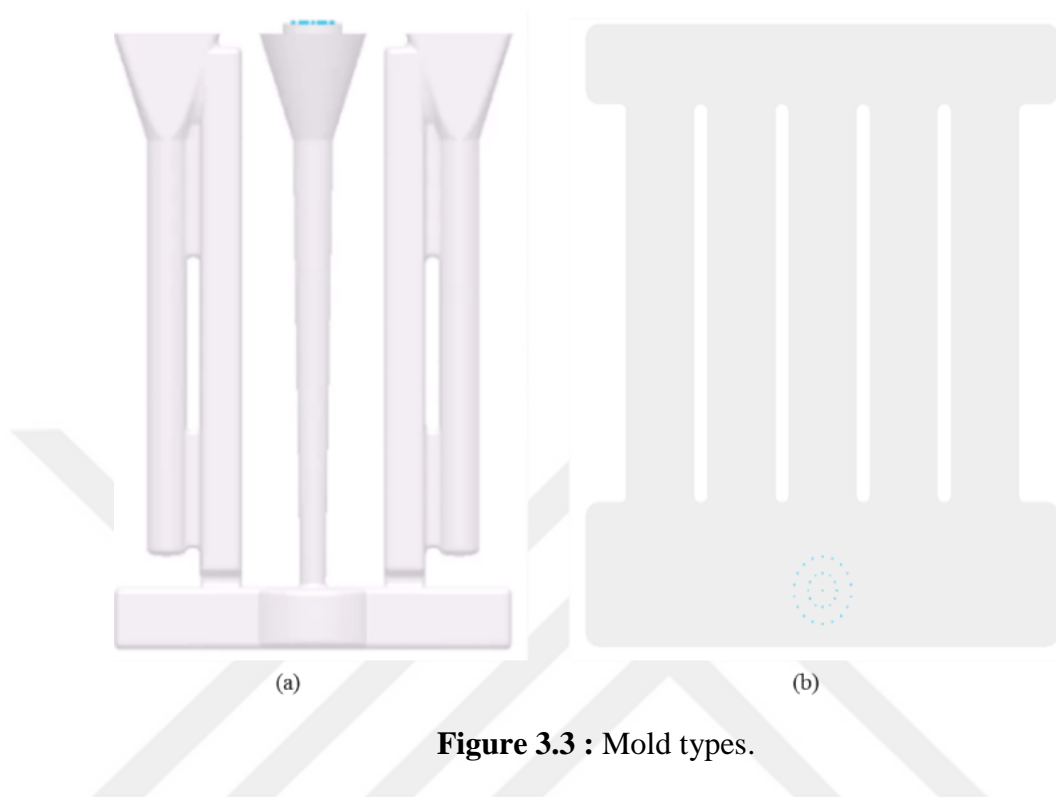


Figure 3.3 : Mold types.

After the simulation, color scale brings about a blue point, at where newly occurrences are observed, when reinforcement particles get into the mold; and yellow displays older ones.

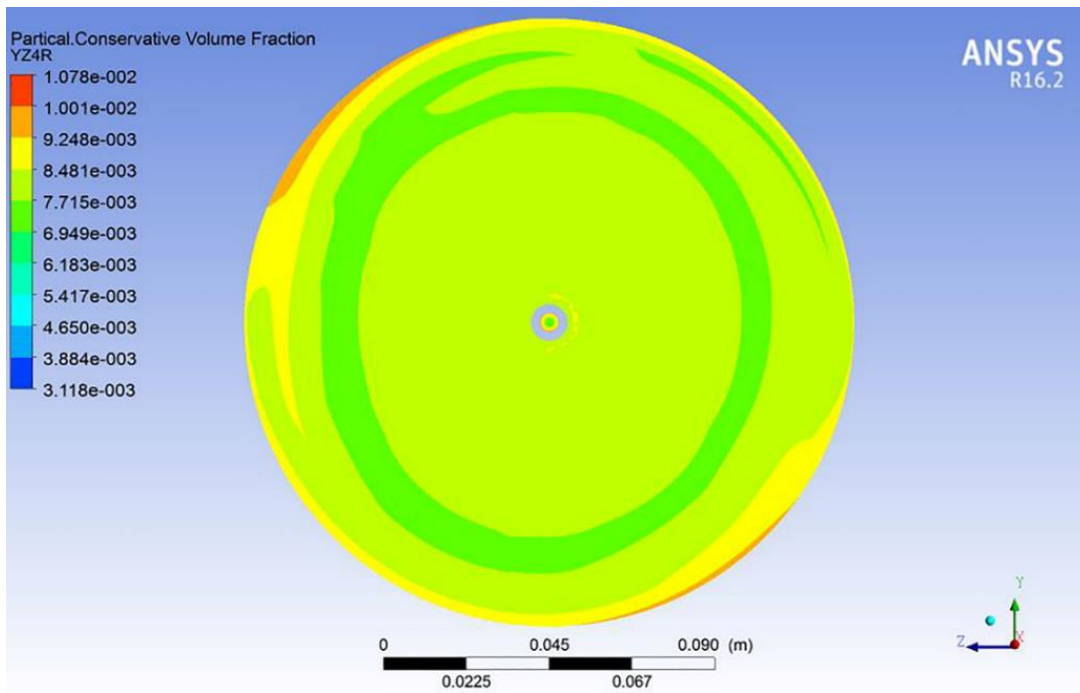
3.1.4 The results of simulation analysis

3.1.4.1 The results of stirring methods

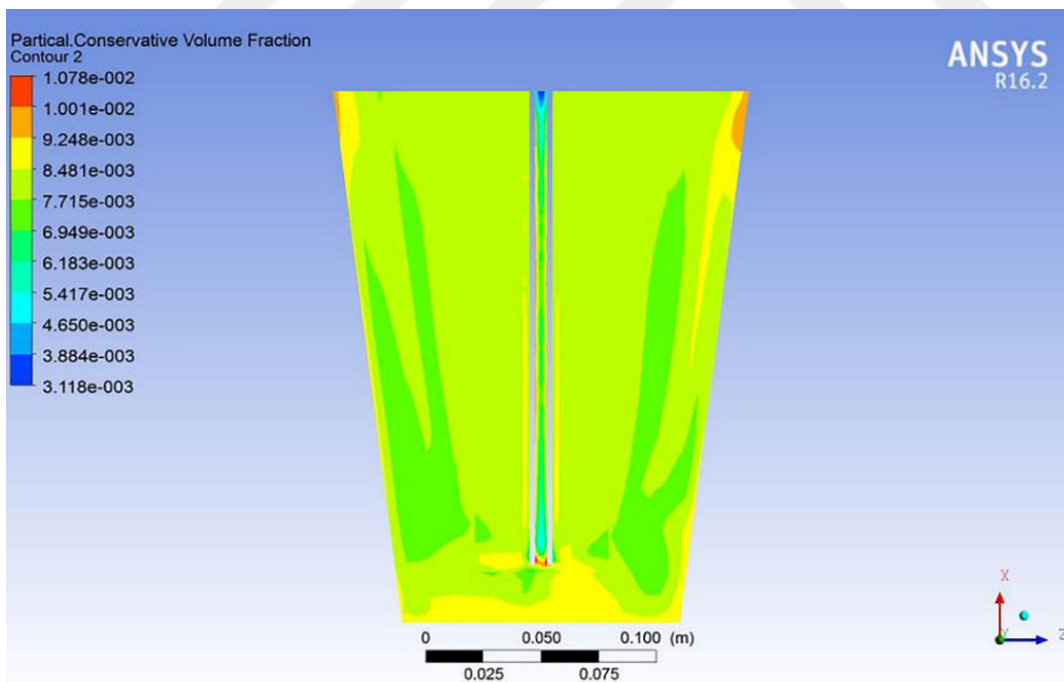
The simulation results and the volume fraction of SiC particles for mechanical, ultrasonic and hybrid stirring are demonstrated in Figure 3.4, Figure 3.5 and Figure 3.6, respectively. The results can be summarized as follows;

- ✓ For mechanical stirring (in Figure 3.4 a and b); SiC particles were distributed around the rotor due to vortex occurrence. Small pieces of agglomeration can be observed near the crucible wall. The distribution of SiC particles in aluminum alloy by using computational and experimental analysis were investigated by Naher et al. [51]. They declared that a uniformed distribution of SiC particles could be achieved by applying the highest stirring speed for

120-540 seconds. Figure 3.4 c displays the homogeneous distribution of SiC in the matrix as nearly 61 %.



(a)



(b)

Figure 3.4 : Simulation test results of mechanical stirring types; a) horizontal section of crucible b) vertical section of crucible c) distribution of SiC particles.

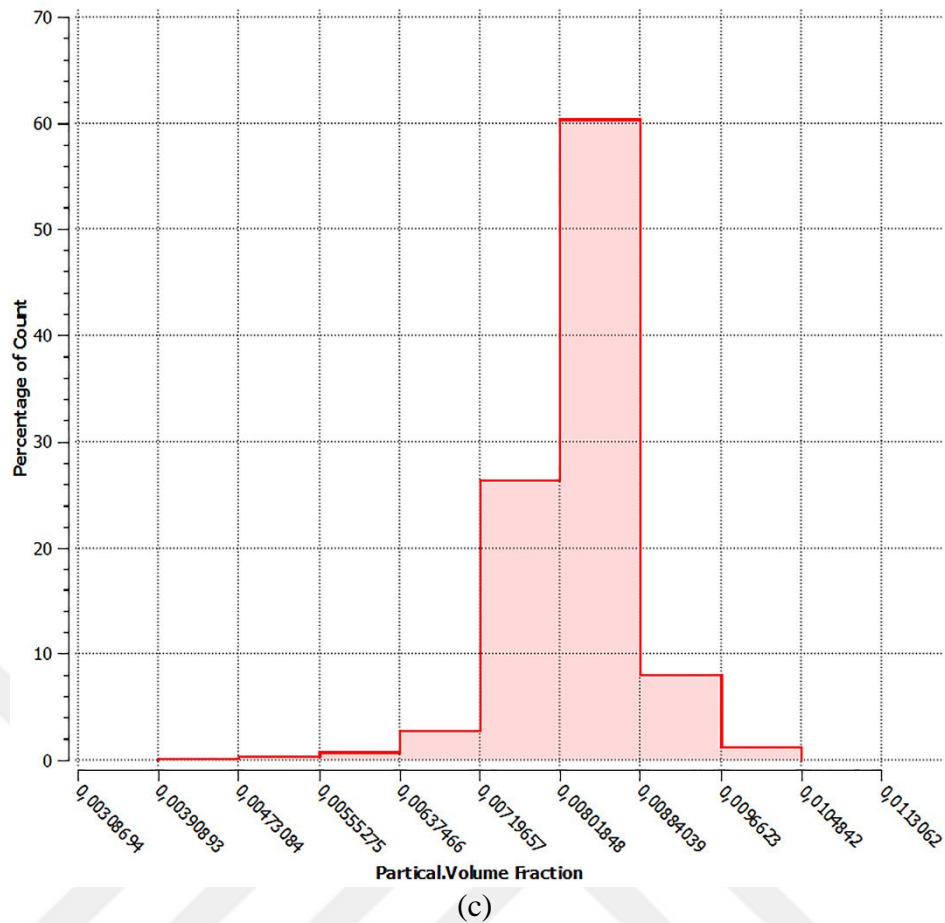


Figure 3.4 (continuation): Simulation test results of mechanical stirring types; a) horizontal section of crucible b) vertical section of crucible c) distribution of SiC particles.

- ✓ For ultrasonic stirring (in Figure 3.5 a and b); SiC particles were distributed from the bottom of crucible to the top by ultrasonic vibration. Correspondingly, it can be seen that SiC particles were homogeneously distributed at the bottom of crucible, but not to the whole volume of melt; and some agglomerated SiC particles were found especially near the crucible wall. Jia et al. [52] investigated nanocomposite enforcement via ultrasonic processing, and concluded that if the flow is stronger, the reinforcement particles are fewer and vice versa. Figure 3.5c demonstrates the homogeneous distribution of SiC in the matrix as nearly 57 %.

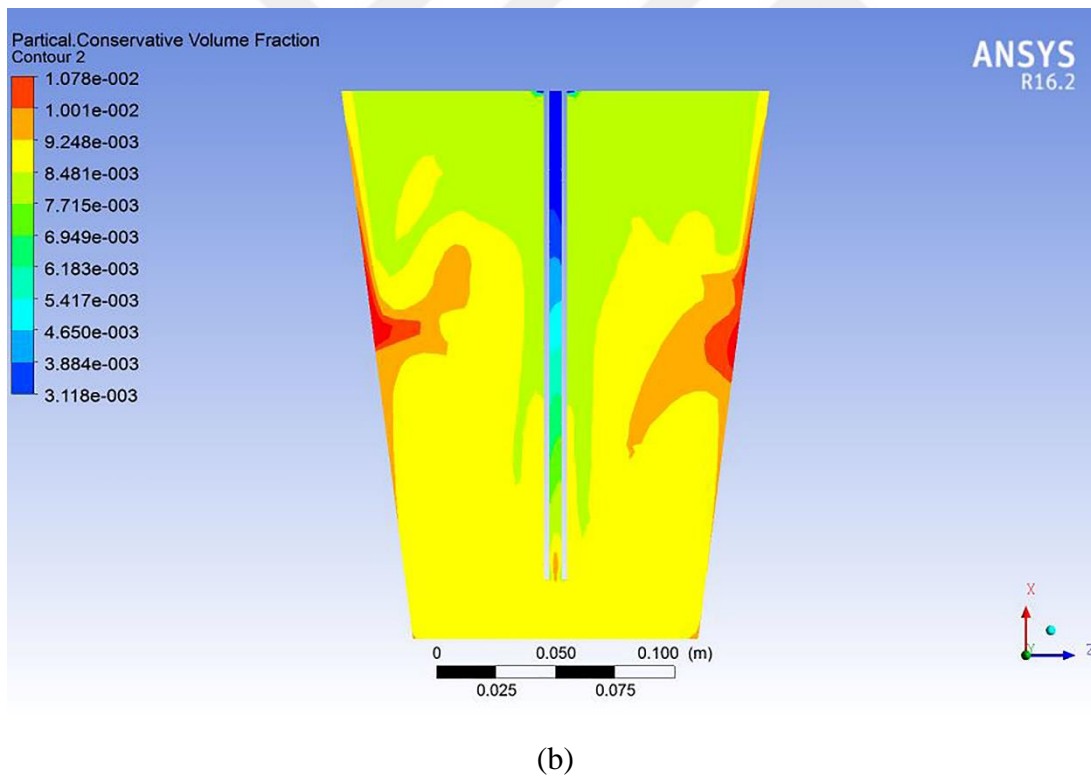
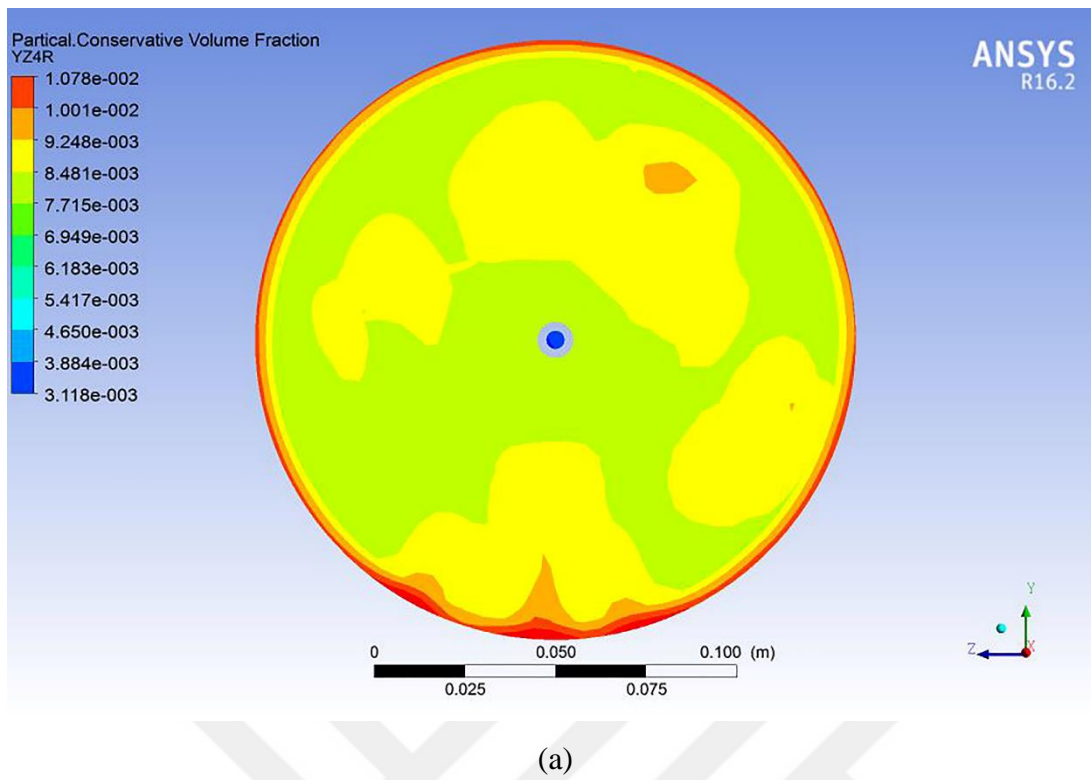


Figure 3.5 : Simulation test results of ultrasonic stirring types; a) horizontal section of crucible b) vertical section of crucible c) distribution of SiC particles.

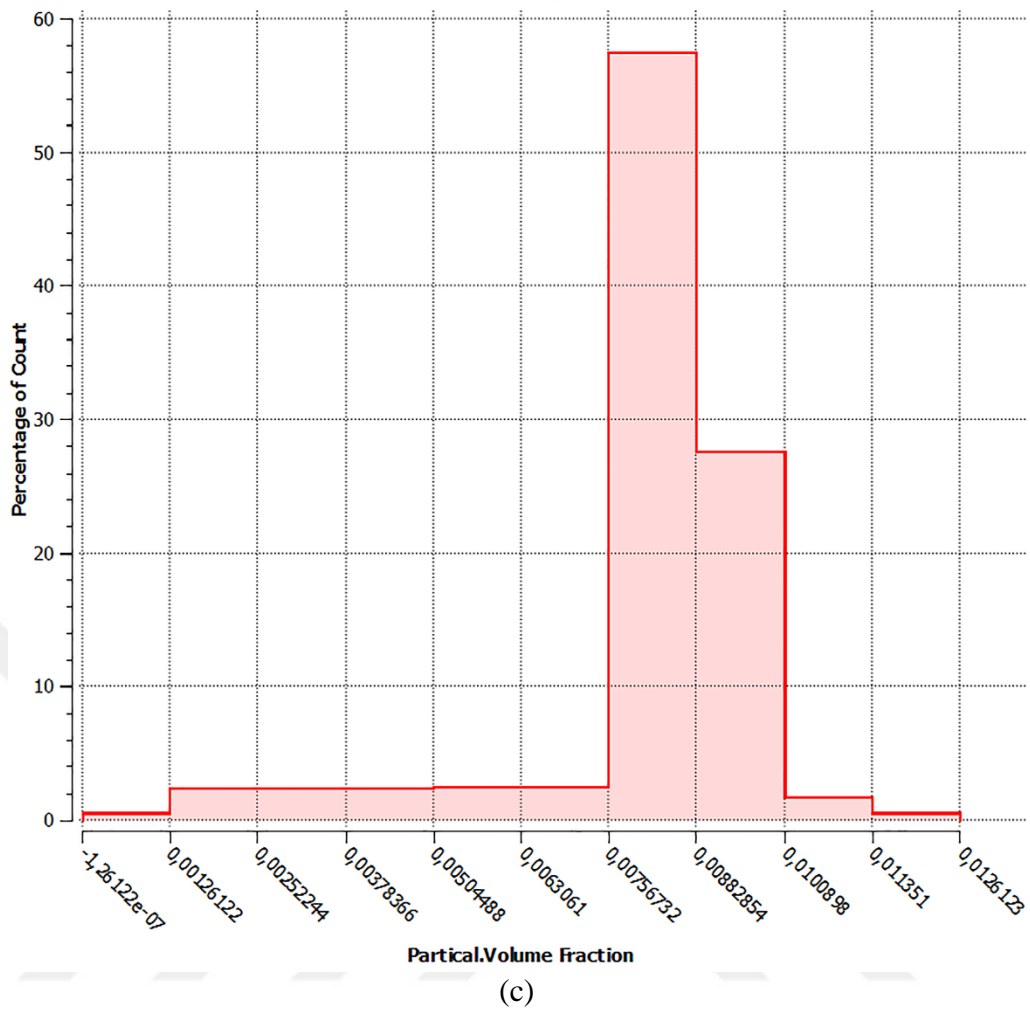


Figure 3.5 (continuation): Simulation test results of ultrasonic stirring types; a) horizontal section of crucible b) vertical section of crucible c) distribution of SiC particles.

- ✓ For hybrid stirring (in Figure 3.6 a and b); It can be seen that SiC particles were distributed homogeneously. Some SiC particles were observed to be placed near the crucible wall, but it was less than the ones of ultrasonic stirring. Figure 3.6 c shows the homogeneous distribution of SiC in the matrix as nearly 75 %.

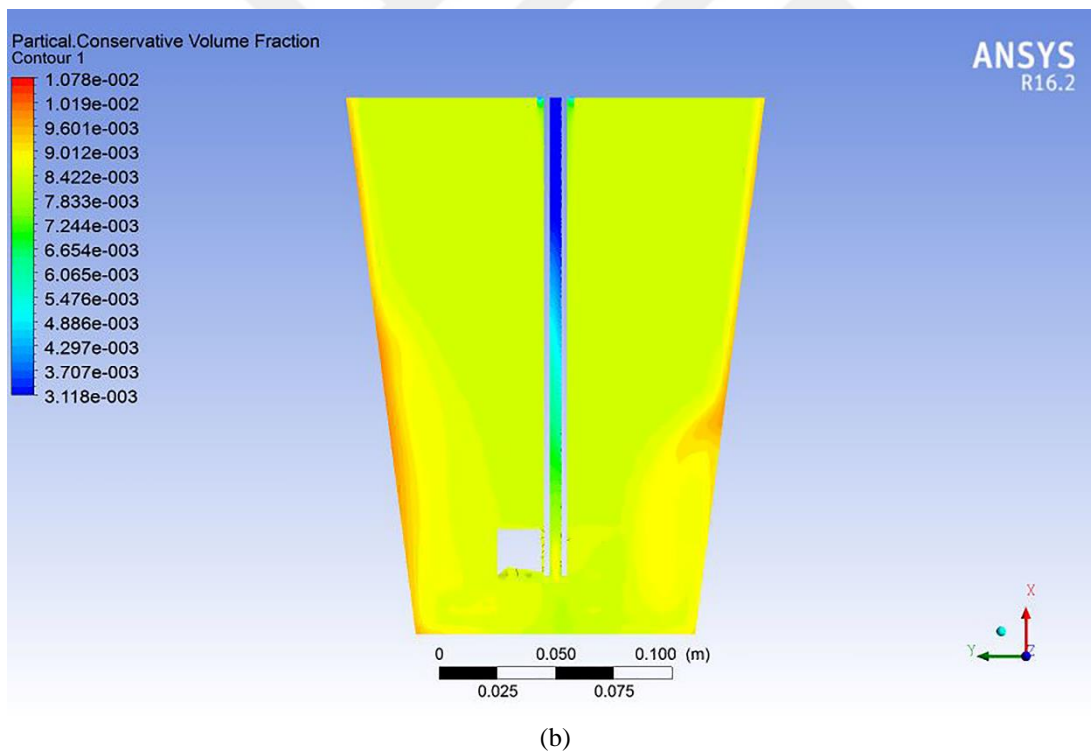
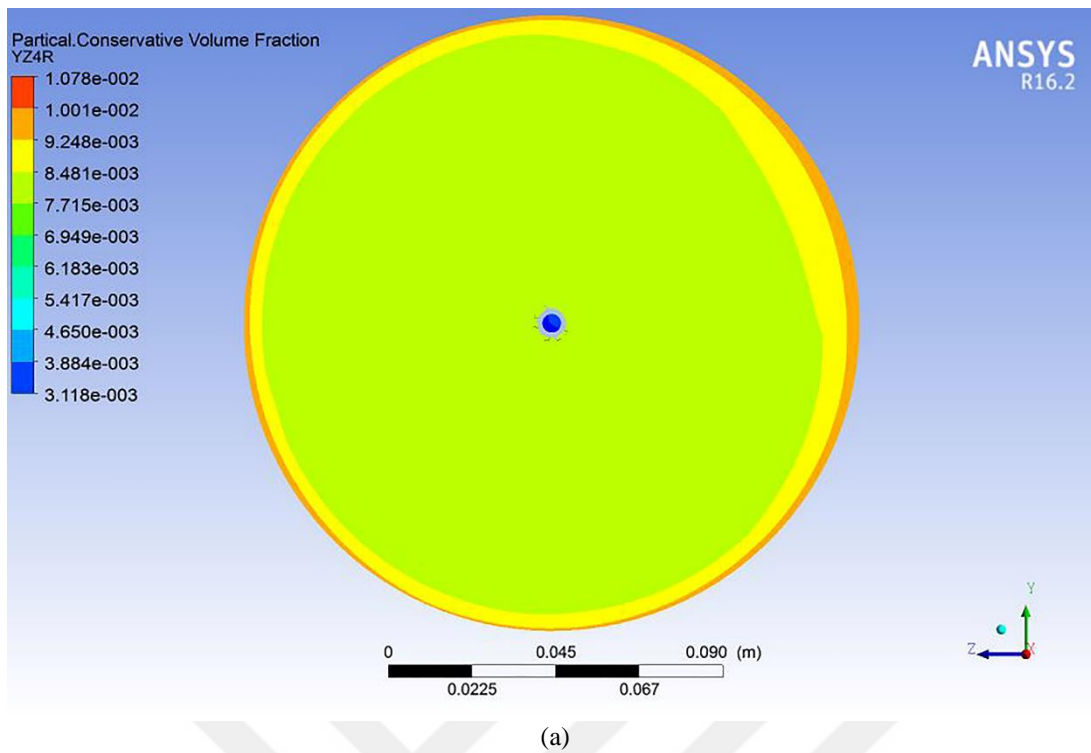


Figure 3.6 : Simulation test results of hybrid stirring types; a) horizontal section of crucible b) vertical section of crucible c) distribution of SiC particles.

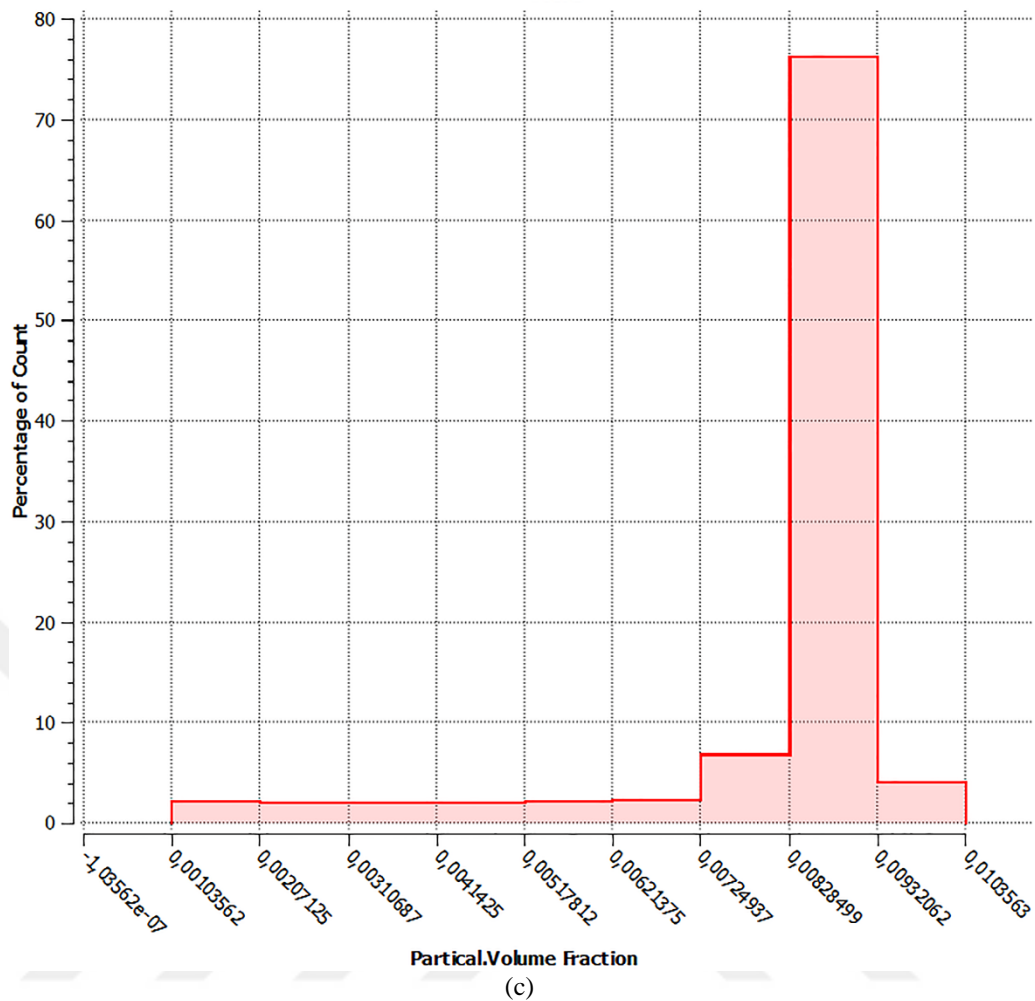


Figure 3.6 (continuation): Simulation test results of hybrid stirring types; a) horizontal section of crucible b) vertical section of crucible c) distribution of SiC particles.

As seen in Figure 3.6 more homogeneous distribution of reinforcement particles were obtained by using hybrid stirring type.

3.1.4.2 The results of mold design

Figure 3.7 and Figure 3.8 demonstrate the simulation results for different mold types; and also mold temperatures depending on the casting temperature. Figure 3.7 illustrates the different casting temperature and mold temperature for bottom-fed mold.

According to the simulation results, it can be clearly seen in Figure 3.7 that SiC particles float to the inner part of mold at 750 and 850°C; and agglomeration problem could be observed especially at higher casting temperature. In Figure 3.7 at 650°C,

distribution of SiC particles is more uniformed than the others. Furthermore if same casting temperatures are taken into consideration, it can be understood that percentage of SiC particle distribution is more systematic at lower casting temperature than higher casting temperature at the same mold temperatures. If the processing temperature increases up to 800°C, aluminum viscosity is decreased leading the reinforcement particle to distribute evenly [53]. Sozhamannan et al. [54] investigated the effect of processing parameters on metal matrix composites and found out that particles agglomerate due to viscosity on the grounds that viscosity decreases by increasing the casting temperature; so that SiC particles float over the aluminum melt. D.J. Lloyd et al. [55] studied on MMC which was produced by molten metal methods and declared that the reinforcement particle distribution is related to the solidification rate. When solidification rate is low, the reinforcing particles agglomerate. Thus it could be said that mold and casting temperatures are important if this mold is wanted to be used in order to produce MMC.

The mold used in Figure 3.7 was bottom-fed mold, on this wise melt must fill the mold against the gravity. Zakeri and Rudi investigated the aluminum composite with SiC and declared that viscosity of aluminum increases due to SiC reinforcement [56]. In view of this, it is difficult to arrange both mold and casting temperatures correctly, especially for bottom-fed mold. On the other hand, in Figure 3.8 it could be clearly seen that the distribution of particle is nearly the same in spoke mold whether both casting and mold temperature values are high or low.

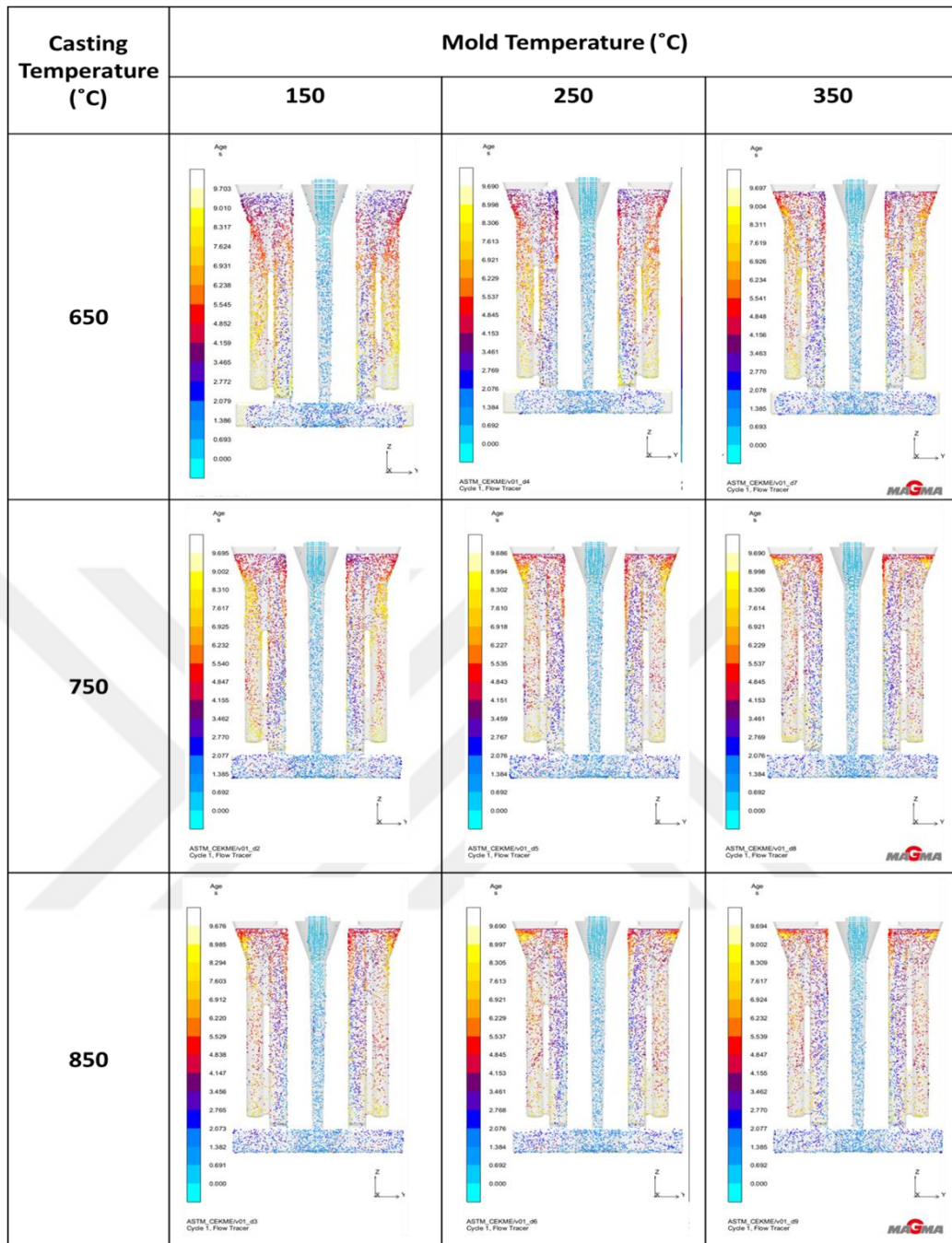


Figure 3.7 : Simulation result for bottom-fed mold.

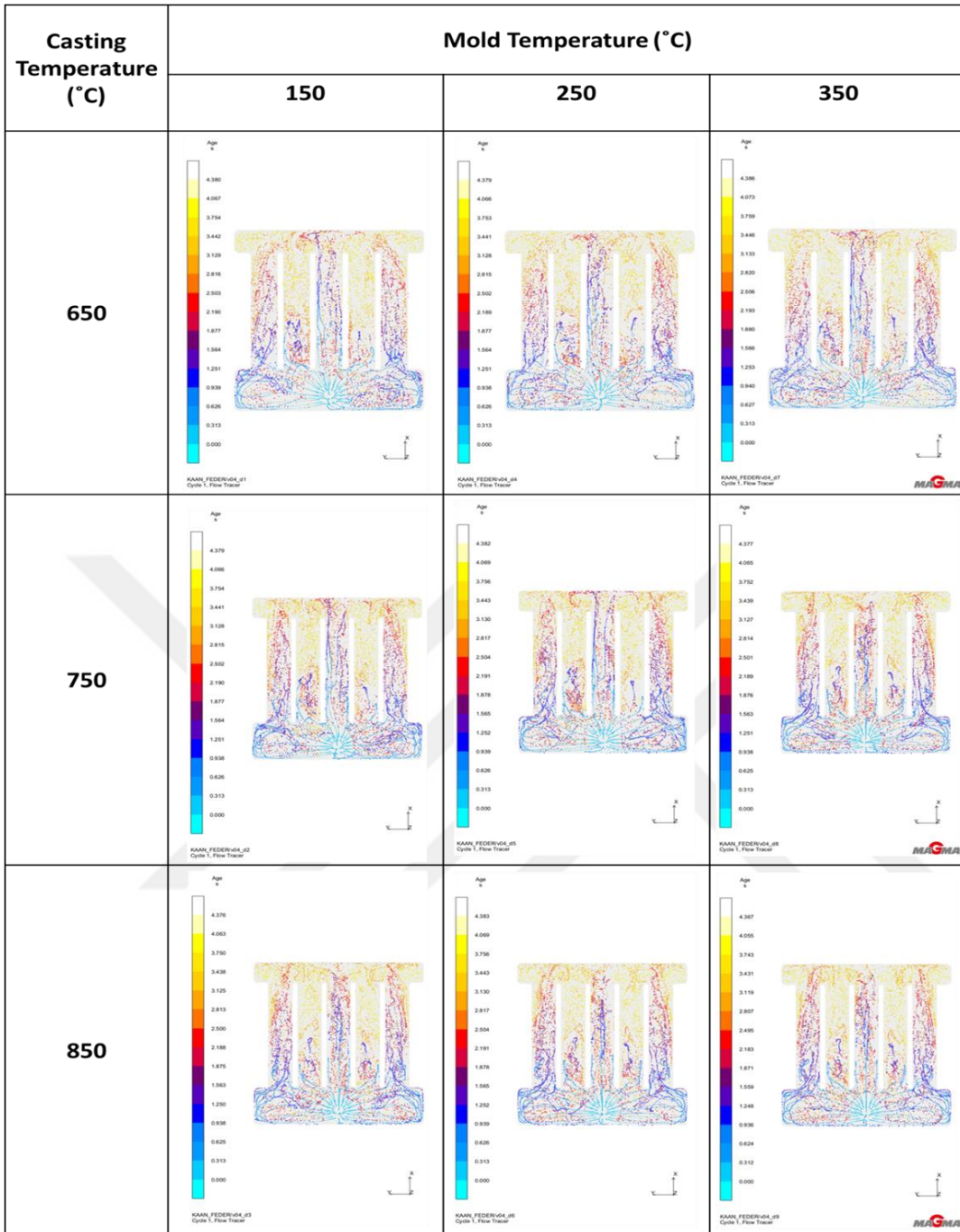


Figure 3.8 : Simulation result of spoke mold.

3.1.5 Casting studies

Laboratory studies were also conducted to prove the results of simulation analysis. Aluminum alloy of which the chemical composition was given in previous chapter, was used as the matrix material. To obtain composite material, silicon carbide powder with an average size of 50-56 μm was used as the reinforcement material. The flow chart of casting procedure is given in Figure 2.1. A charge of 4 kg of A356

alloy was melted at 750°C at a resistance furnace; and during melting process of alloy, SiC powders were weighed to be 1 wt. % of the charge. Later, SiC particles were preheated to 750°C for 2 hours at a separate furnace to obtain an oxidized surface, that improves their wettability.

After A356 was melted, the occurred dross was removed from the surface of melt and preheated SiC was added simultaneously during stirring process via using various stirring methods. Thereafter reinforcement was added into crucible, it was stirred continuously for 2 minutes to obtain a uniformed distribution of reinforcements [48]. If the stirring time was chosen higher, air or gas bubbles could be let in to the molten aluminum [49]. The stirring processes were applied as the same duration in simulation studies as 2 minutes for mechanical stirring and ultrasonic vibration, and 1 minute for each mechanical stirring and ultrasonic vibration (named as hybrid stirring).

Posterior to finishing the stirring processes, the composite was poured into the spoke mold, which was preheated to 320°C as given in Figure 3.9. The spoke mold was designed to simulate a wheel geometry. Samples 2, 3 and 4 represent the feeder of the wheel while the others represent the outer flange of wheel.



Figure 3.9 : Preheated spoke mold.

To analyze the mold solidification time, Magma Soft V5.3.1 was used. Figure 3.10 demonstrates the solidification behaviour of mold. It can be clearly seen that samples

1 and 5 are higher than the others due to the location of outer mold. To evaluate the results in accordance with the reference value of wheel mechanical tests, they are reported as an average of all these samples.

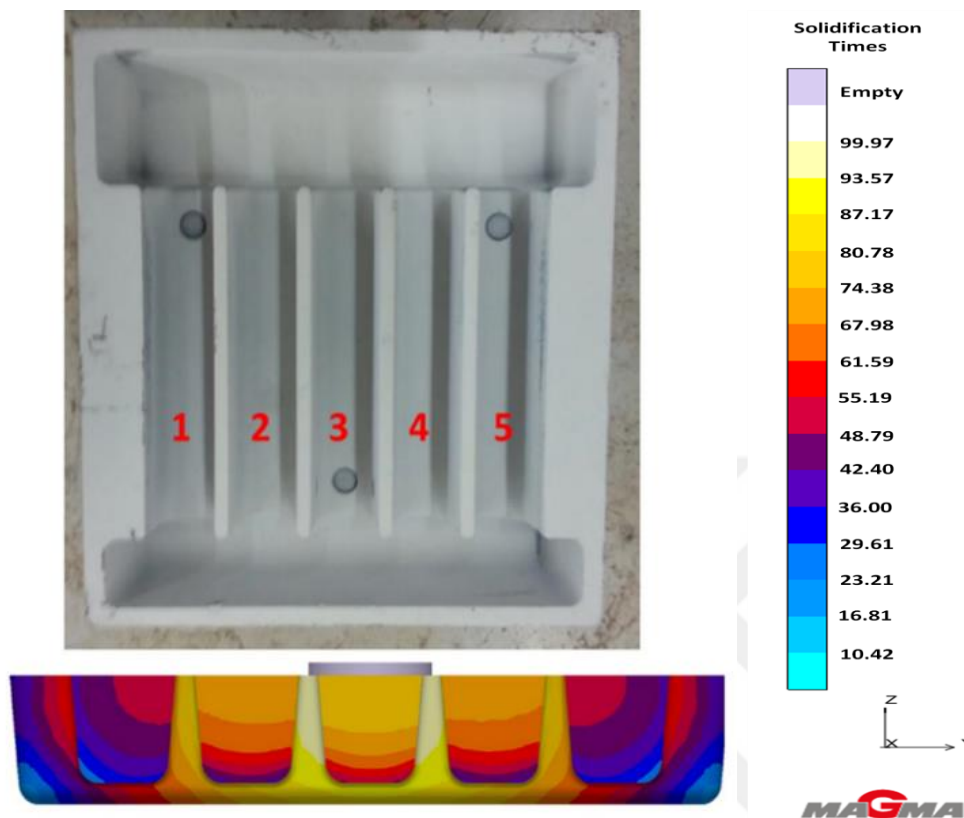


Figure 3.10 : Solidification time of preheated mold.

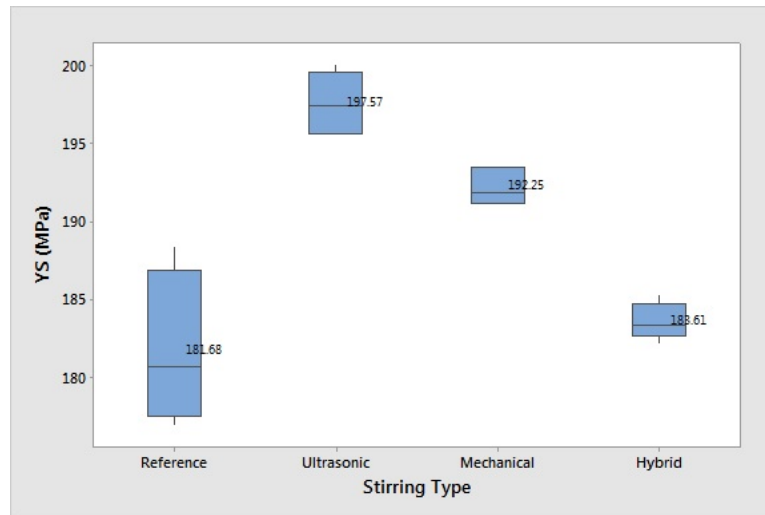
Reference samples were also poured without the addition of SiC in order to compare the efficiency of particle distribution in the matrix. In order to check the reproducibility of outcomes, two sets of casting were applied.

3.1.6 The results of casting studies

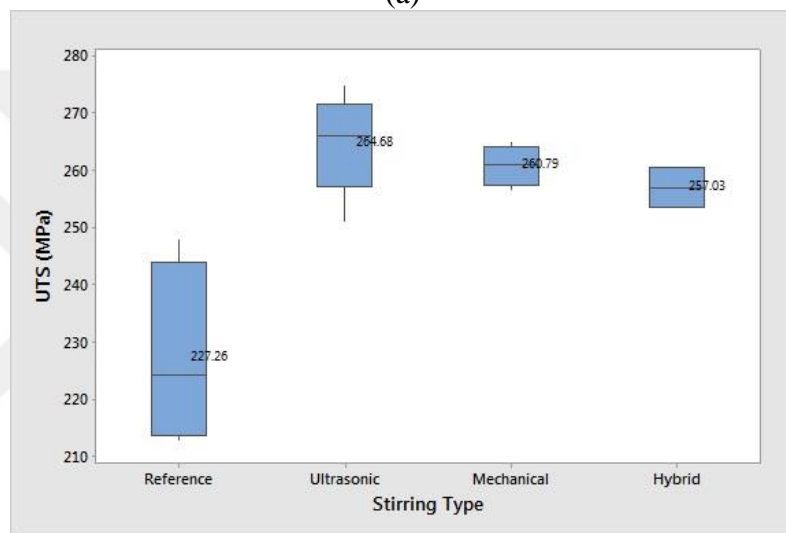
The results of casting studies can be taken into two categories as mechanical and metallographic examinations.

3.1.6.1 Mechanical test results

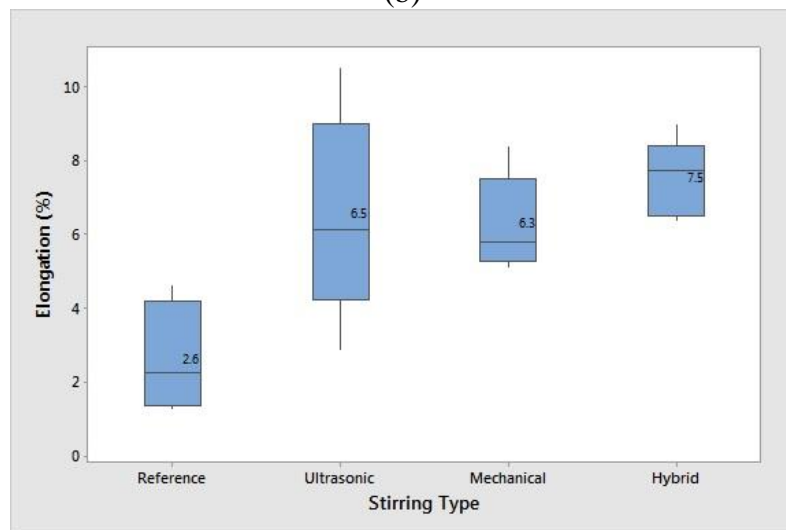
The mean and range distribution values of tensile test results of YS (Yield Stress), UTS (Ultimate Tensile Strength) and elongation at fracture of composite were produced by different stirring types that are presented in Figure 3.11.



(a)



(b)



(c)

Figure 3.11 : Mechanical test results of sample produced by different stirring types; a) YS, b) UTS, c) Elongation and d) QI of all samples.

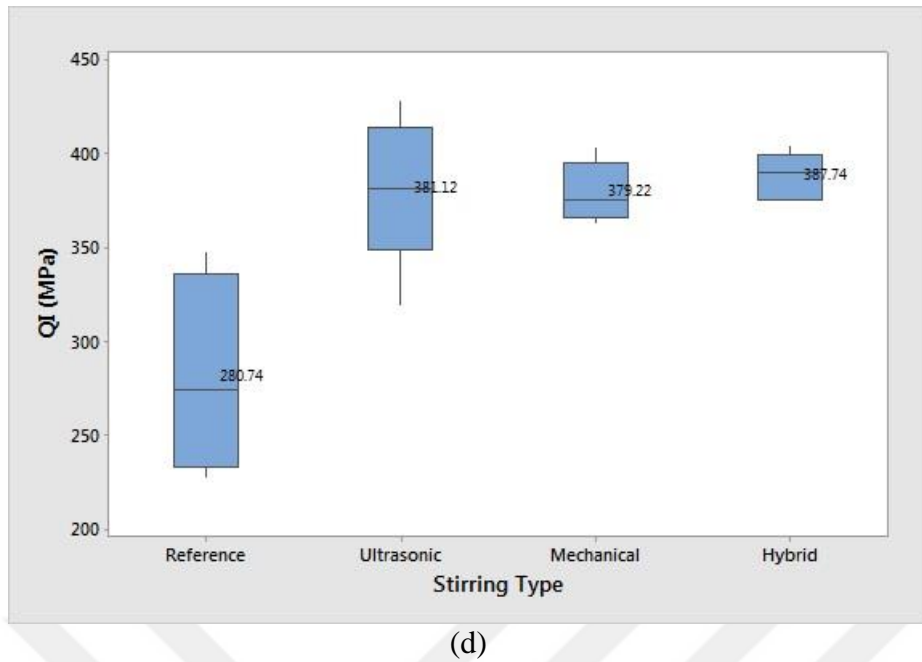


Figure 3.11 (continuation): Mechanical test results of sample produced by different stirring types; a) YS, b) UTS, c) Elongation and d) QI of all samples.

In Figure 3.11 a, it can be seen that YS value of the ultrasonic stirred samples is the highest. In comparison with reference samples, the increase of YS in ultrasonic, mechanical and hybrid stirring samples were obtained as 5.8%, 8.7% and 1.1%, respectively. It can be declared that YS value escalates by decreasing the average grain diameter or average arm spacing to the microstructure. It can also be observed clearly in Figure 3.13, Table 3.3 and Table 3.4 that samples, which are produced by using ultrasonic vibration, have the finest grain sizes and SDAS measurement results. Similar results were found by Liu et al. [57]. The UTS outcomes are given in Figure 3.11 b and the results that were obtained from them were similar at 257-265 MPa for all stirring types. In comparison to the result of reference sample, the increase of UTS in ultrasonic, mechanical and hybrid stirred samples were obtained as 16.5%, 14.9% and 13.1%, respectively. Jia et al. [41] declared that the escalation in the mechanical properties were by virtue of a mismatch between the thermal expansion coefficient and elastic modulus of the metal matrix and the reinforcement. If the scatter of tensile properties is taken into consideration, the outcomes attained from hybrid stirring are lower than the ones obtained from ultrasonic stirring ones. This is also related with the homogeneous distribution of reinforcement. It can be seen in Figure 3.13 that the reinforcement particles are located in the grain boundary,

especially the samples which were produced with ultrasonic stirring method. On the other hand, the elongation results of mechanically stirred samples are higher than the ultrasonic stirred ones. Jia [58] studied on the ultrasonic cavitation processing of Al based alloys and nanocomposites by conducting both experimental and simulation studies. The investigation illustrated the tensile strength and elongation values as 172.0 ± 5.9 MPa and 4.3 ± 0.5 %, respectively. He declared that the decrease in elongation values were in linked with the agglomeration of reinforcement.

When the elongation results are taken into consideration, it can be clearly seen that the hybrid stirred samples display the highest elongation value as 7.5%, followed by ultrasonic stirred samples; and mechanical stirred samples as the latest when compared with reference ones. Quality Index (QI), which is important for the evaluation of alloys, and of which engineers use to determine the suitable conditions for material selection [59], is calculated from the mechanical test results. This index [59;60] is subtracted by adopting tensile test results as they are demonstrated in equation 3.1:

$$QI = UTS + K * \log(\textit{elongation}) \quad (3.1)$$

QI; Quality index (MPa)

UTS; ultimate tensile strength (MPa)

K; constant (for A356 is equivalent to 150 MPa)

Elongation; (%)

QI, which is calculated by using equation 1, can be seen in Figure 3.11 d. In hybrid stirring process, it can be observed that more homogeneous distribution of reinforcement was achieved.

3.1.6.2 Results of metallographic analysis

Figure 3.12 and Table 3.2 demonstrate the macrostructure and the volumetric percentage in porosity of samples that are produced by using ultrasonic, mechanical and hybrid stirrings, respectively.

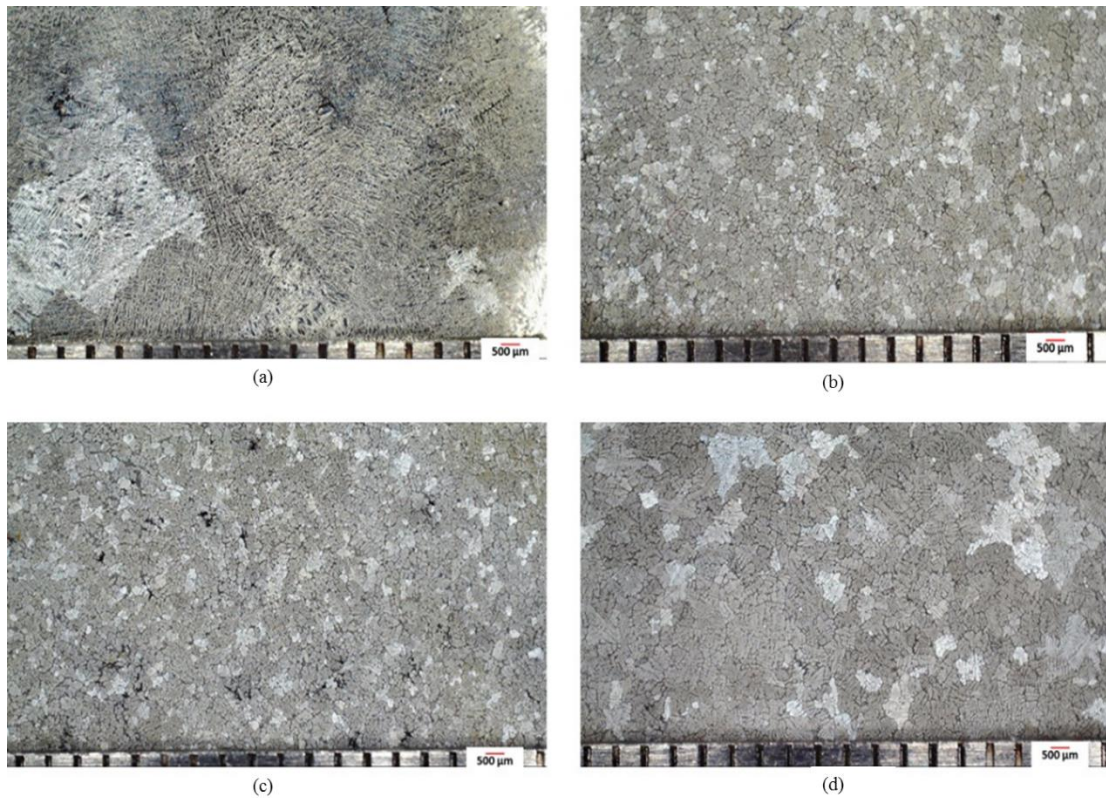


Figure 3.12 : Macrostructure of samples prepared by a) reference, b) ultrasonic, c) mechanical and d) hybrid stirring.

Table 3.2 : Percent values of the porosity content.

Stirring type	Percent porosity (%)
Reference	1.1
Ultrasonic	0.06
Mechanical	0.20
Hybrid	0.01

It can be clearly seen in Table 3.2 that ultrasonically stirred samples has less porosity than the mechanical stirred ones. It has been reported in many researches [53;61;62] that intermittent acoustic vibration caused by ultrasonic treatment which was generated in a melt result during the prevention of the local heating up while the latent heat was being released in the course of cooling period. Tsunekawa et al. [63] also stated that this situation promotes the decline in grain size as well as the decrease in porosity while wetting of non-metallic inclusions were increased. If the mechanical stirring samples are taken into consideration, the increased porosity content is clearly seen in the macrostructure as given in Figure 3.12 c. Hashim et al.

[64] tried to discuss this porosity formation in their research. A vortex is formed in mechanical stirring and it transfers both air bubbles and impurities into the melt leading an increase in porosity of samples. It can be observed that the macrostructure, which was subjected to ultrasonic stirring, has nearly no porosity in Figure 3.12 d. This is because the ultrasonic stirring was applied after the mechanical stirring. If any air bubbles also transferred into the melt during mechanical stirring, the ultrasonic cavitation would prevent the formation of porosity.

Figure 3.13 illustrates the microstructure of all samples at two different magnifications. Additionally, Table 3.3 and Table 3.4 show the SDAS and grain size measurement, respectively. It can be seen from these micrographs and measurements that the samples, which were produced with ultrasonic stirring, have the finest microstructure. Liu et al. [57] also investigated the effect of nano particle reinforcement addition by using ultrasonic process. They came into conclusion that 1 wt.% SiC reinforcement reduced the grain size due to they retarded the growth of grain. Moreover, it can be found in several researches on the literature about different matrix materials explaining the cavitation-enhanced nucleation and cavitation-induced dendrite-fragmentation that promotes the decrease in grain size [65;66].

Jia et al. [40] studied on the effect of solidification in microstructure alloy A356 with and without ultrasonic treatment; and concluded that the ultrasonic treatment provided a strong heat transfer from the melt. Therefore, finer grain size and higher eutectic growth could be obtained. However, in the same research, ultrasonic stirring fragmented the dendritic structure and fine globular structures were obtained. Atamanenko et al. [67] declared the similar effect of ultrasonic treatment on grain refinement of cast aluminum alloys by reporting the reinforcement particles were pushed via interface as well as engulfment. Same results were also acquired by Jia et al. [41]. The microstructural images of mechanical stirring had revealed that the dendritic structure was obtained and the reinforcement particles were generally engulfed due to vortex occurrence. Hashim et al. [64] illustrated that the vortex expedited to transfer the reinforcement particles into matrix via a pressure difference between the inner and the outer surfaces of the melt.

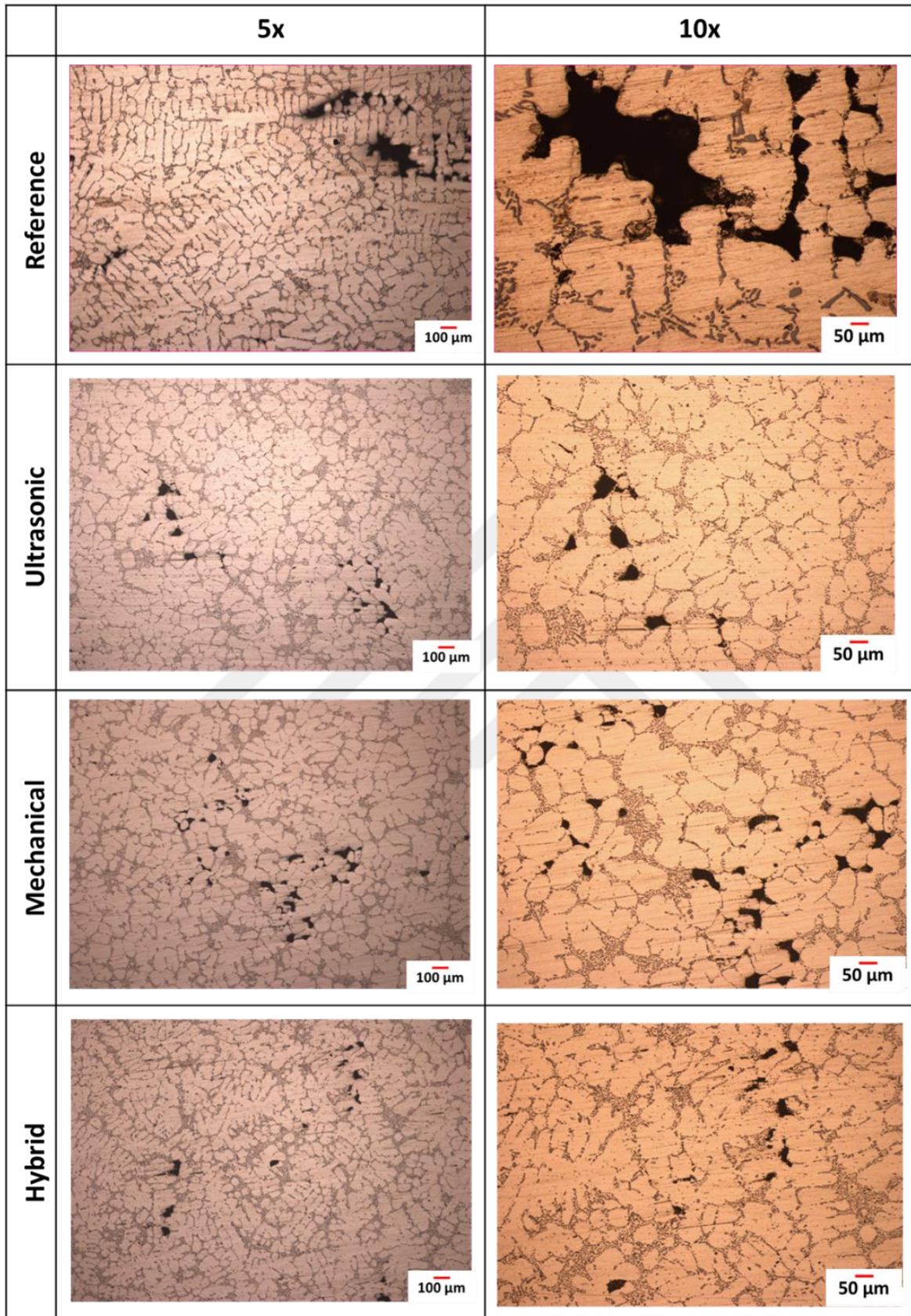


Figure 3.13 : Microstructure of samples produced by ultrasonic, mechanical and hybrid stirring methods.

Table 3.3 : SDAS measurement of samples produced by different stirring types (μm).

Stirring type	SDAS (μm)
Reference	$51,4 \pm 10,4$
Ultrasonic	$37,8 \pm 14,8$
Mechanical	$40,2 \pm 8,6$
Hybrid	$39,3 \pm 7,2$

Table 3.4 : Grain size measurement of samples produced by different stirring types (μm).

Stirring type	Grain size (μm)
Reference	1093 ± 178
Ultrasonic	488 ± 38
Mechanical	493 ± 62
Hybrid	604 ± 70

3.1.7 The determination of the appropriate stirring method and mold design

In this section, three different stirring methods as mechanical, ultrasonic and hybrid were applied to produce metal matrix composite. A356 aluminum alloy and SiC reinforcement were used as matrix and reinforcement materials, respectively. To investigate the difference between the methods, experimental and simulation studies were conducted. From the results of casting studies, ultrasonic stirring samples showed the highest YS owing to having finer microstructure; and the average UTS results were closer for all stirring types. Additionally, the scatter of UTS and elongation were found to be high for ultrasonic stirring. The hybrid stirring samples had the highest elongation at fracture values as 7,5% when the highest QI value was calculated for the hybrid stirred castings as 387 MPa. This index is particularly important for material selections in applications of automotive and aerospace industry. According to the simulation results, the best mechanical results were obtained by practicing the hybrid method. It can be also understood from simulation outcomes that hybrid stirring method demonstrated the most homogeneous mixing where the distribution of SiC in matrix was 76%. The mechanical and ultrasonic stirring results exhibited nearly 61% and 56% of distribution, respectively.

However, it was determined which mold type is appropriate for composite producing; bottom-fed or spoke mold to use in simulation studies. It was come to the conclusion that spoke mold was more appropriate than bottom-fed mold to produce particle reinforced metal matrix composite.

3.2 The Effect Of Reinforcement Particle On Mechanical Properties Of Aluminum Matrix Composites

In this chapter, the effects of different reinforcement additives on the mechanical and metallurgical properties of aluminum metal matrix composites are discussed. SiC, n- Al₂O₃, m- Al₂O₃ and graphene were used as reinforcement materials. The same casting process, mechanical tests procedures and metallographic analysis given in previous chapter was applied to produce all composite samples with different reinforcement additives. Obtained results were worked with in order to compare each reinforcement.

3.2.1 The production method of composite samples

Preheated reinforcement particles were respectively added into the melt with mechanical stirring by including ultrasonic vibration for 2 minutes as determined in Chapter 3.1. After the stirring process was finished, the melt with different reinforcements was poured into the mold, which is determined in Chapter 3.1, and preheated to 320°C.

3.2.2 Results and discussion

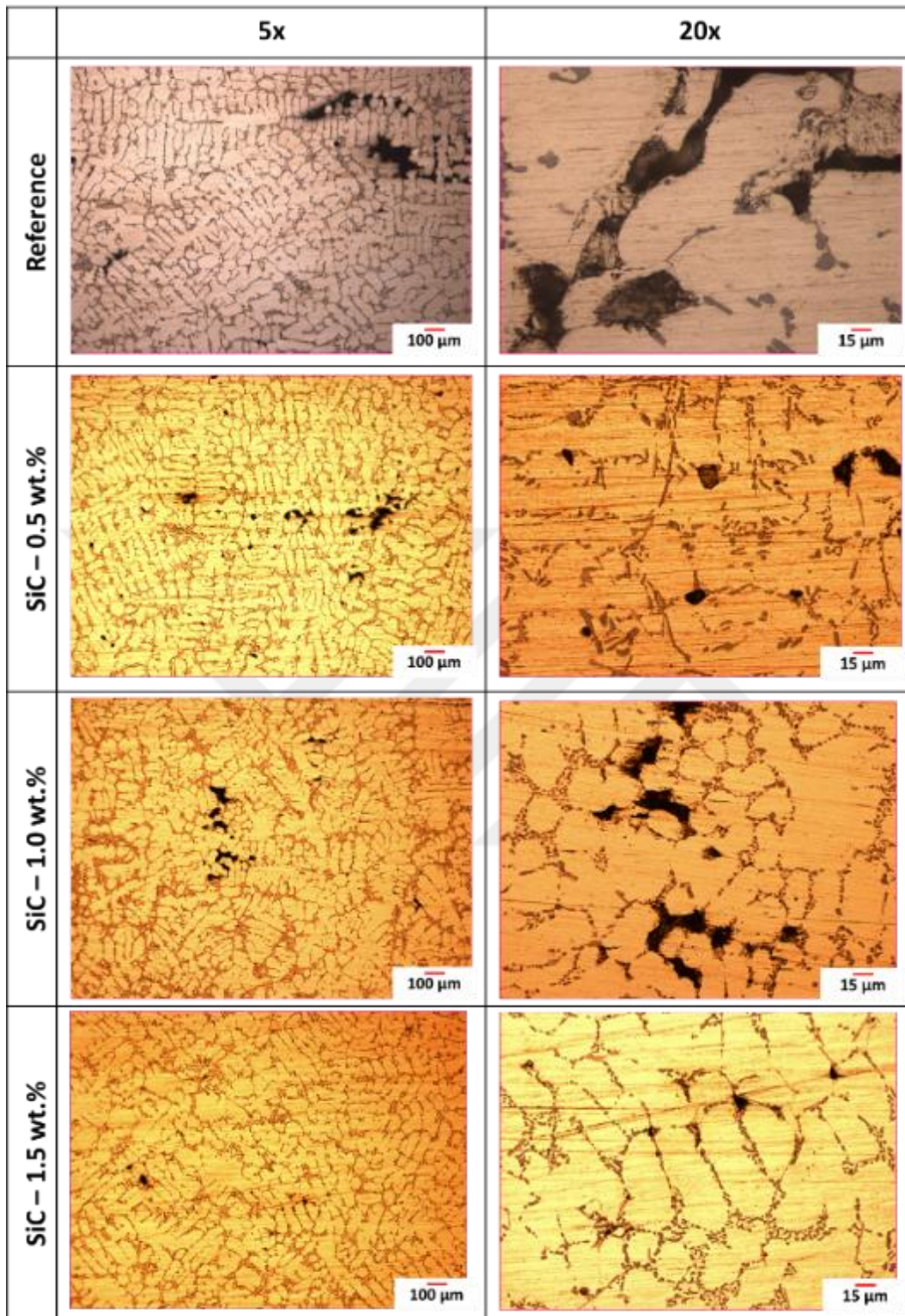
By using the obtained test results, comparative types of reinforcements were evaluated.

- SiC and m- Al₂O₃ reinforcements were used to determine the effects of different reinforcements with the same particle size.
- m- Al₂O₃ and n- Al₂O₃ reinforcements were used to determine the effects of different particle sizes with the same reinforcement type.
- n- Al₂O₃ and graphene reinforcements were used to determine the effects of nano particle sizes with the different reinforcements.

3.2.2.1 The evaluation effect of SiC and micro-Al₂O₃ reinforcements

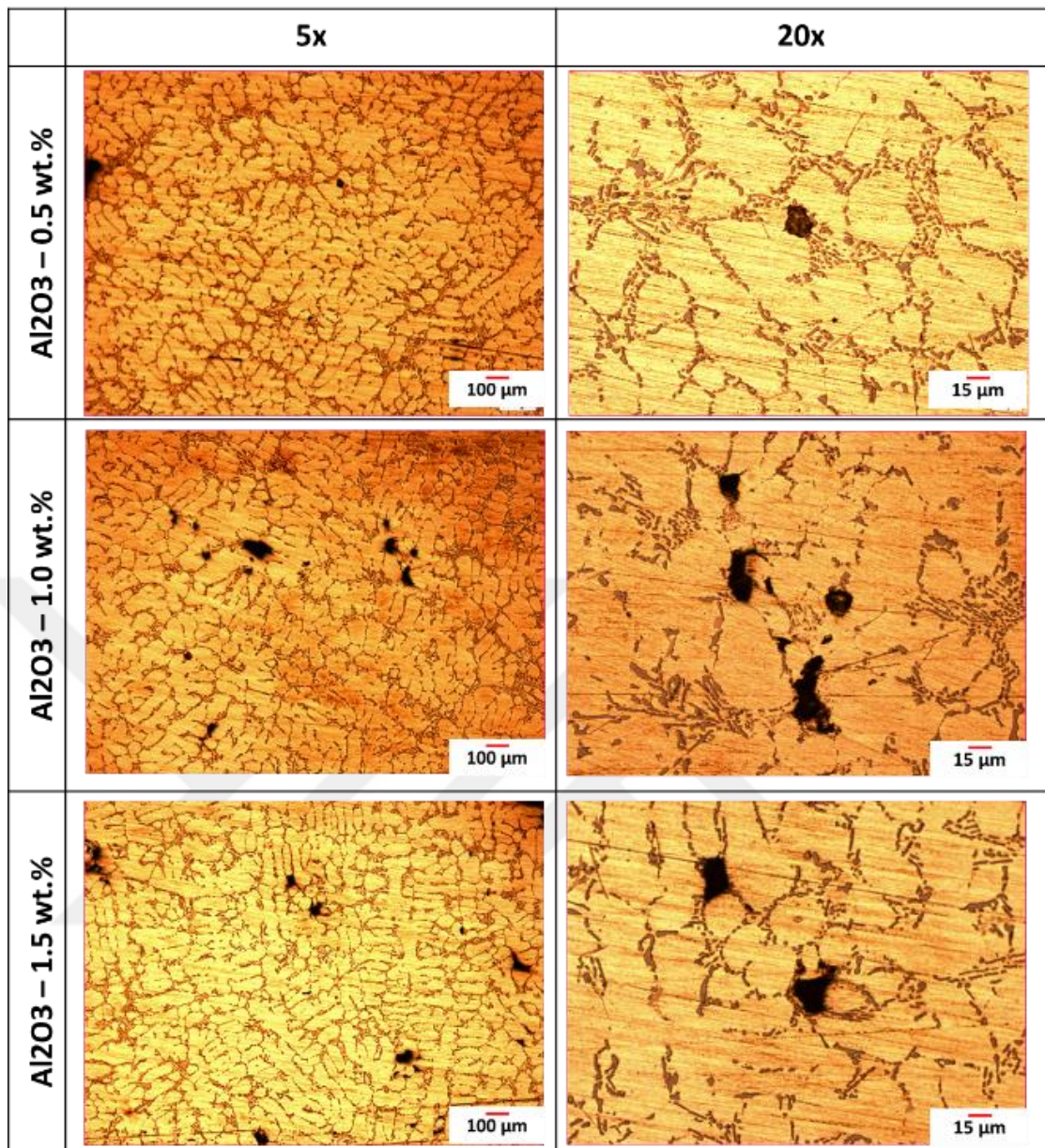
The microstructure and macrostructure images of all composite samples which were reinforced with SiC and micro-Al₂O₃ are demonstrated in Figure 3.14, Figure 3.15, respectively. Figure 3.16 elaborates the SEM analysis of composite sample which is reinforced with 1wt% SiC. However, the grain size and secondary dendritic arm spacing (SDAS) measurements are given in Table 3.5 and Table 3.6, respectively.

Considering Table 3.5 and Table 3.6, it can be said that addition of SiC makes microstructure finer than addition of Al₂O₃. On the grounds that SiC improves the solidification velocity due to having higher thermal conductivity. The thermal conductivity of SiC and Al₂O₃ are 126 W/mK and 35.6 W/mk, respectively [68]. The differences of thermal conductivity of reinforcements affect the microstructure during the solidification period. Hernandez-Sandoval et al. [69] investigated the effects of Al₂O₃ and SiC reinforcements by adding 5 wt%, and concluded that the average grain size of composite, which is reinforced with SiC particle, is finer than the one that is reinforced with Al₂O₃ particle.



(a)

Figure 3.14 : Microstructure of composite samples with a) SiC and b) micro- Al_2O_3 reinforcements.



(b)

Figure 3.14 (continuation): Microstructure of composite samples with a) SiC and b) micro-Al₂O₃ reinforcements.

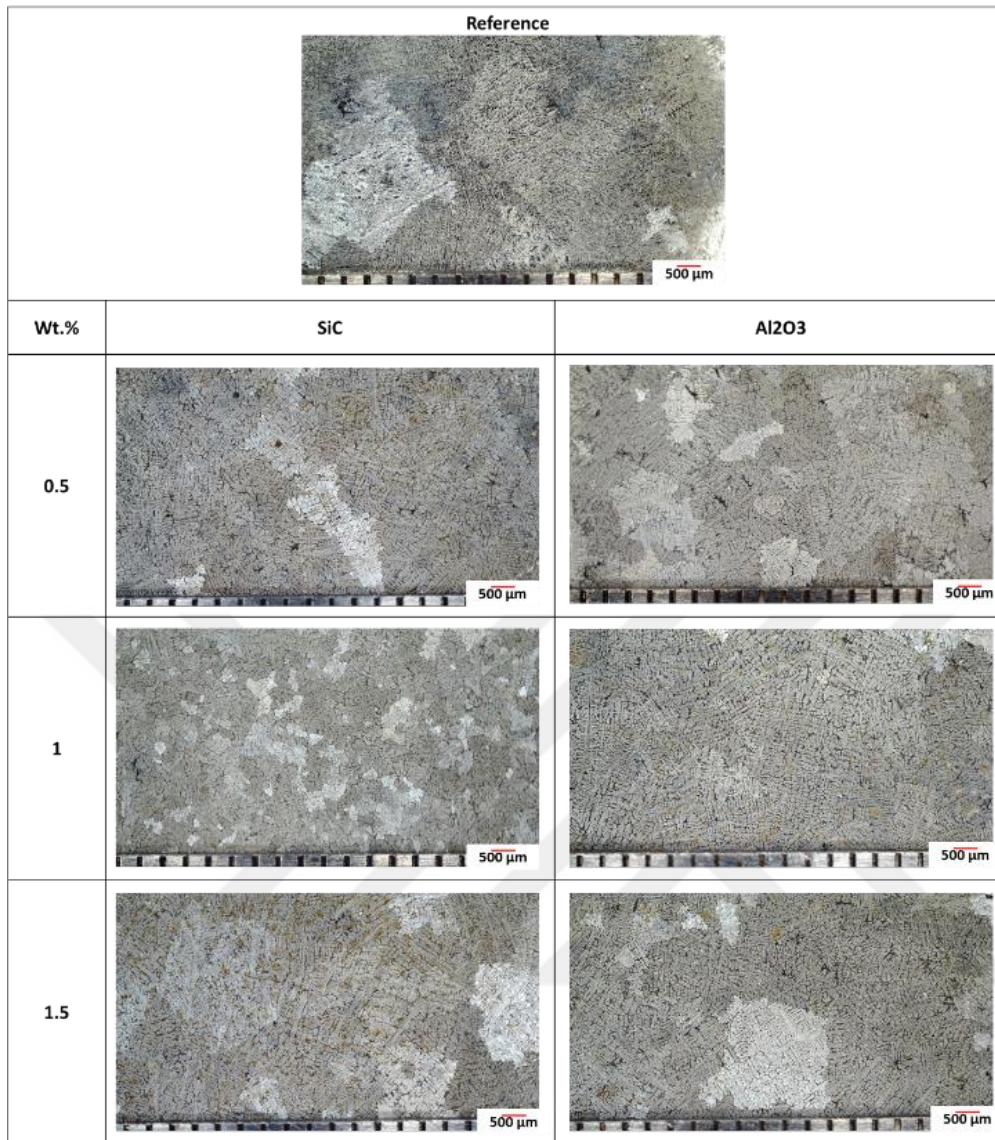


Figure 3.15 : Macrostructure of MMC samples with SiC and micro-Al₂O₃ reinforcement.

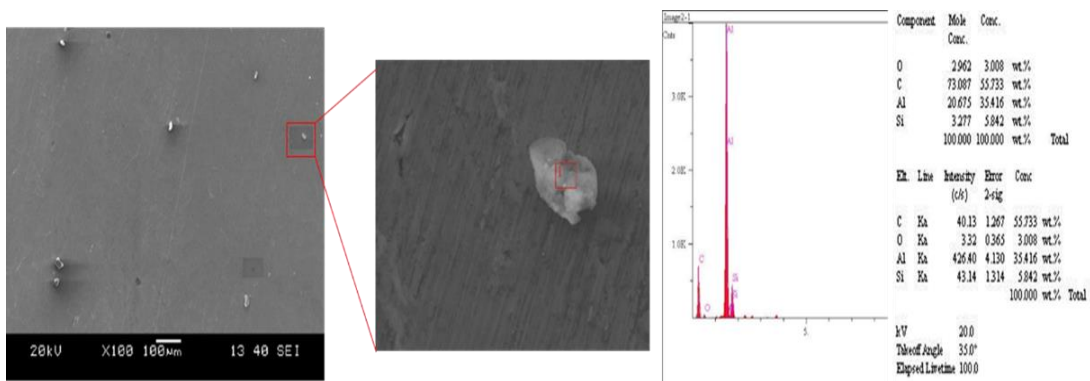


Figure 3.16 : SEM analysis of sample with 1wt% SiC.

Table 3.5 : Grain size measurement of samples reinforced with SiC and micro-Al₂O₃ (μm).

Samples		Grain size measurement (μm)
Reference		1093 ± 178
SiC (wt.%)	0.5	1089,12 ± 132
	1	592,77 ± 52
	1.5	1155,90 ± 178
micro-Al ₂ O ₃ (wt.%)	0.5	1462,08 ± 217
	1	1525,87 ± 166
	1.5	1226,13 ± 257

Table 3.6 : SDAS measurement of samples reinforced with SiC and micro-Al₂O₃ (μm).

Samples		SDAS measurement (μm)
Reference		51.4 ± 10.4
SiC (wt.%)	0.5	40,9 ± 8,4
	1	37,5 ± 7,9
	1.5	42,38 ± 9,9
micro-Al ₂ O ₃ (wt.%)	0.5	43,6 ± 7,9
	1	49,3 ± 9,6
	1.5	47,5 ± 8,2

The coefficient of thermal expansion has also a crucial importance to produce particle reinforcement composites. As a consequence of the thermal mismatch stress, dislocation density can be increased [70]. Through differences of thermal expansion between reinforcement particle and matrix material, stress occurs. Bindumadhavan et al. [48] explained that aluminum composite's coefficient of thermal expansion with SiC is much higher than the one of reinforcement particle's. The coefficient of thermal expansion of SiC and micro-Al₂O₃ are 4 μm/m°C and 7.1 μm/m°C, respectively [68]. In order to avoid SiC enhancement on the mechanical properties of aluminum matrix composite [68], Figure 3.17 illustrates the mechanical test results of aluminum metal matrix composite which was reinforced with SiC and micro-Al₂O₃, individually.

Elongation and ultimate tensile strength (UTS) are more important factors to determine the quality of a wheel since original equipment manufacturers need some amount of plastic deformation before fracture. Thus they determine the values of elongation and UTS as minimum 2.0-4.5% and 200 - 230 MPa, respectively [71].

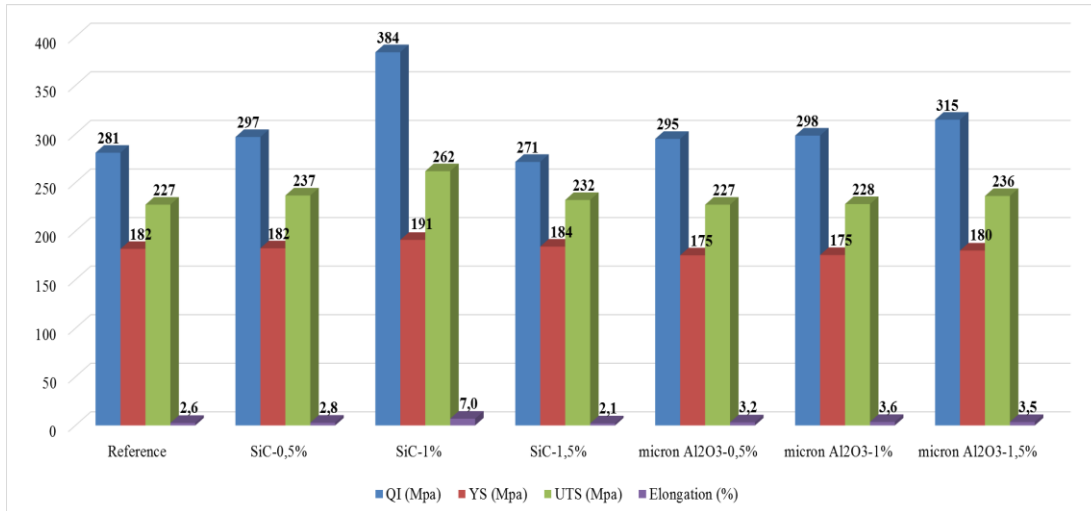


Figure 3.17 : Mechanical test results of samples reinforced with SiC and micro- Al_2O_3 .

It could be clearly seen from Figure 3.17 that the average mechanical results of SiC addition was higher than micro- Al_2O_3 . The mechanical properties of composite which is reinforced with micro- Al_2O_3 escalates with increasing the micro- Al_2O_3 content in the matrix. For SiC additions, the maximum mechanical properties were obtained with 1 wt. % additive. This result was also in correlation with the microstructure analysis. Furthermore, minimum grain size was attained with the same amount of SiC. Emamy et al. [72] investigated the effects on different amounts of micro- Al_2O_3 and SiC reinforcement on aluminum composite's mechanical properties. The effect of grain refinement was also studied. They concluded that as the reinforcement was increased, the mechanical properties were decreased, whereas average UTS results were between 240 MPa to 170 MPa for SiC addition and 260 MPa to 220 MPa for micro- Al_2O_3 addition. QI helps to analyse the mechanical properties by including the UTS and elongation at the same time. When QI results were taken into consideration, the maximum value would have obtained with 1 wt. % addition of SiC.

The differences between the mechanical properties of different test conditions could be generated by two reasons. One of them was the amount of addition and the other one was porosity. Rajeswari et al. [73] tried to produce aluminum metal matrix composite with the combination of SiC and micro- Al_2O_3 reinforcements. It was found that SiC and micro- Al_2O_3 particles were floating towards the melt surface due to the density difference and surface tension. In that case, the composite material is not easily obtained if high amounts of reinforcements are used. For higher amount of

reinforcement, a stirring process is required which also aids the homogeneity [74]. Yet, if stirring time is exceeded, amount of porosity will increase due to a vortex occurrence, which negatively affects the mechanical properties. Porosity is calculated by using differences of density between measured principles (known as Archimedes' principle) and theoretical ones as given equation 3.2 [75;76].

$$\% \text{ porosity} = (\rho_{\text{theoretical}} - \rho_{\text{measured}} / \rho_{\text{theoretical}}) * 100 \quad (3.2)$$

Theoretical density is calculated by rules of mixtures as given equation 3.

$$\rho_{\text{theoretical}} = \sum(f_i * \rho_i) = f_{\text{matrix}} * \rho_{\text{matrix}} + f_{\text{particle}} * \rho_{\text{particle}} \quad (3.3)$$

f is volume fraction and ρ is density of each material in composite.

Porosity values were calculated by using equation 3.2 and equation 3.3 and illustrated in Figure 3.18. It could be clearly seen that the composite samples, which were reinforced with SiC, had lower porosity content than the composite samples that were reinforced with micro- Al_2O_3 ones in Figure 3.18. As discussed earlier, these samples had also revealed the highest mechanical properties.

The hardness and Charpy impact test results are demonstrated in Figure 3.19 and Figure 3.20, respectively. When these results are taken into consideration, the maximum test result was obtained with 1 wt. % SiC addition. For micro- Al_2O_3 addition, the impact test results increased linearly by raising the amount of addition. However, for SiC addition, maximum test result was obtained from 1 wt. % SiC additive. These results were also related to the porosity content and mechanical test results. Through increasing porosity contents, inhomogeneous stress distributions occur around pores that causes a damage on composite material due to the creation of weakness in inhomogeneous regions [77;78].

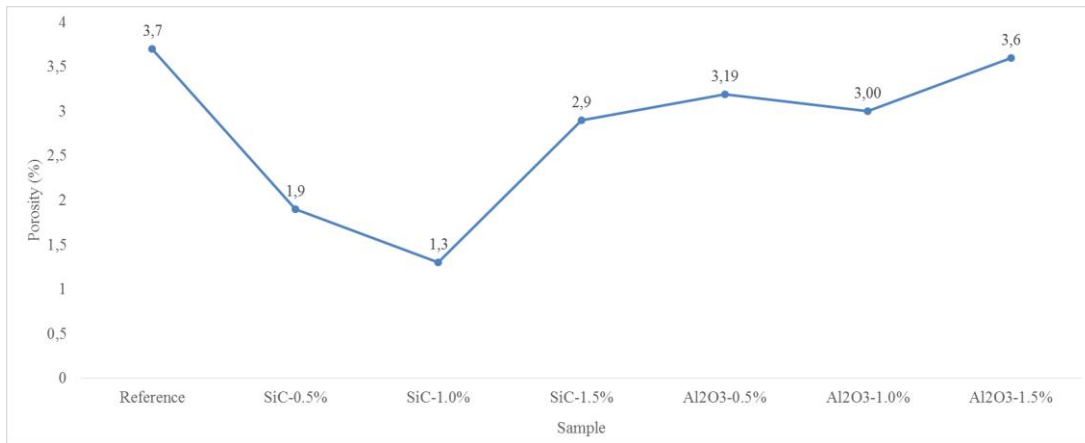


Figure 3.18 : Porosity content of samples reinforced with SiC and micro-Al₂O₃.

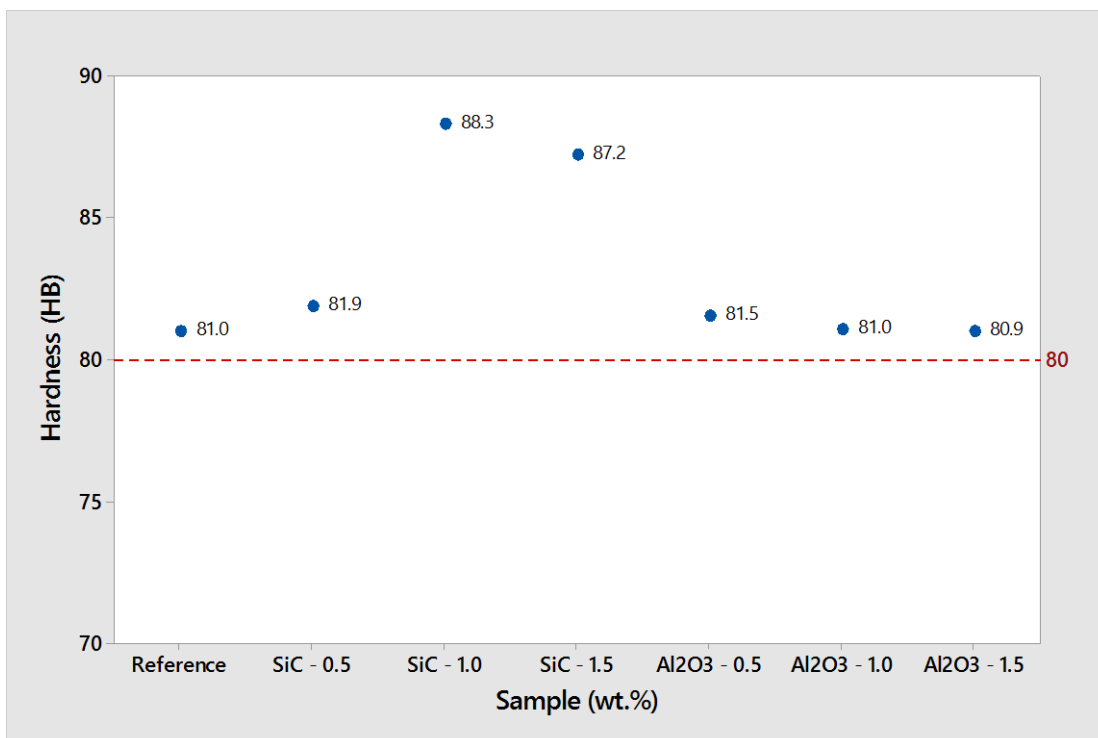


Figure 3.19 : Hardness test result of samples reinforced with SiC and micro-Al₂O₃.

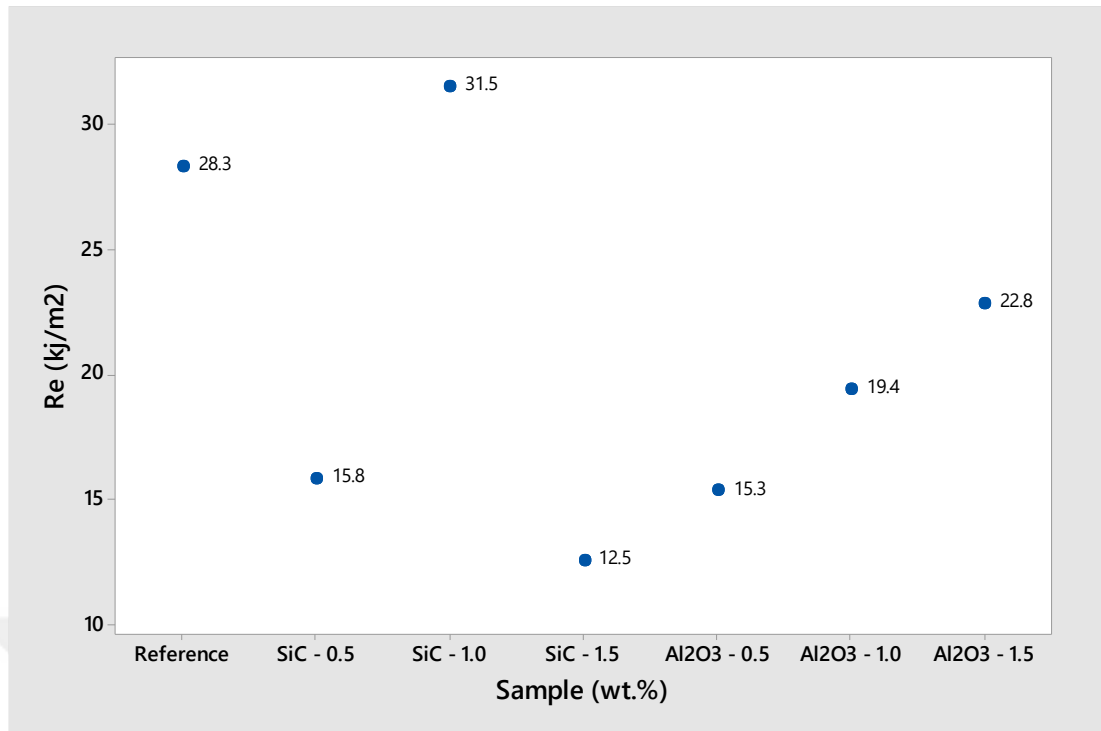


Figure 3.20 : Charpy impact test results of all samples.

3.2.2.2 The evaluation on effects of micro-Al₂O₃ and nano-Al₂O₃ reinforcements

The microstructure and macrostructure images of all composite samples, which were reinforced with micro-Al₂O₃ and nano- Al₂O₃, are illustrated in Figure 3.21, Figure 3.22, respectively. On the other hand, the grain size and secondary dendrit arm spacing (SDAS) measurements are given in Table 3.7 and Table 3.8, respectively.

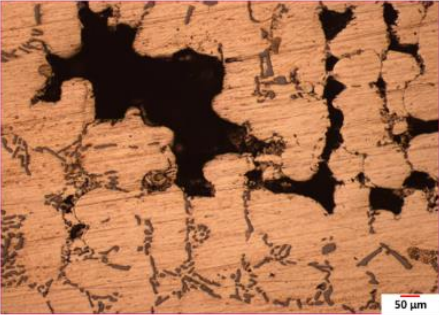
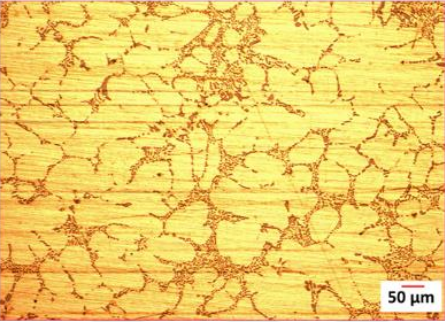
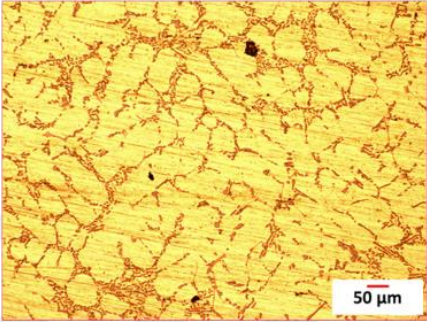
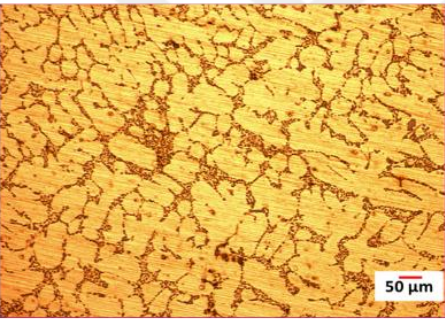
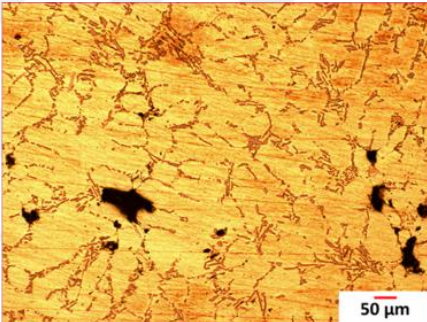
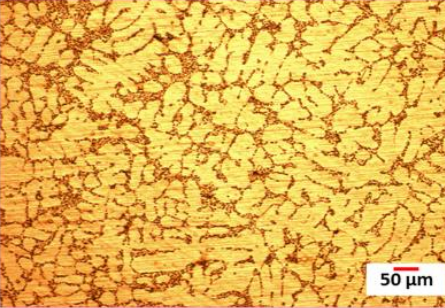
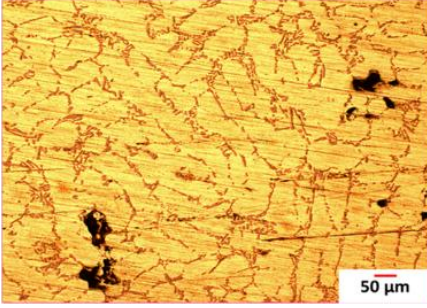
	10x	10x	
Reference			Reference
n-Al ₂ O ₃ – 0.5 wt. %			m-Al ₂ O ₃ – 0.5 wt. %
n-Al ₂ O ₃ – 1.0 wt. %			m-Al ₂ O ₃ – 1.0 wt. %
n-Al ₂ O ₃ – 1.5 wt. %			m-Al ₂ O ₃ – 1.5 wt. %

Figure 3.21 : Microstructure of samples reinforced with micro and nano Al₂O₃.

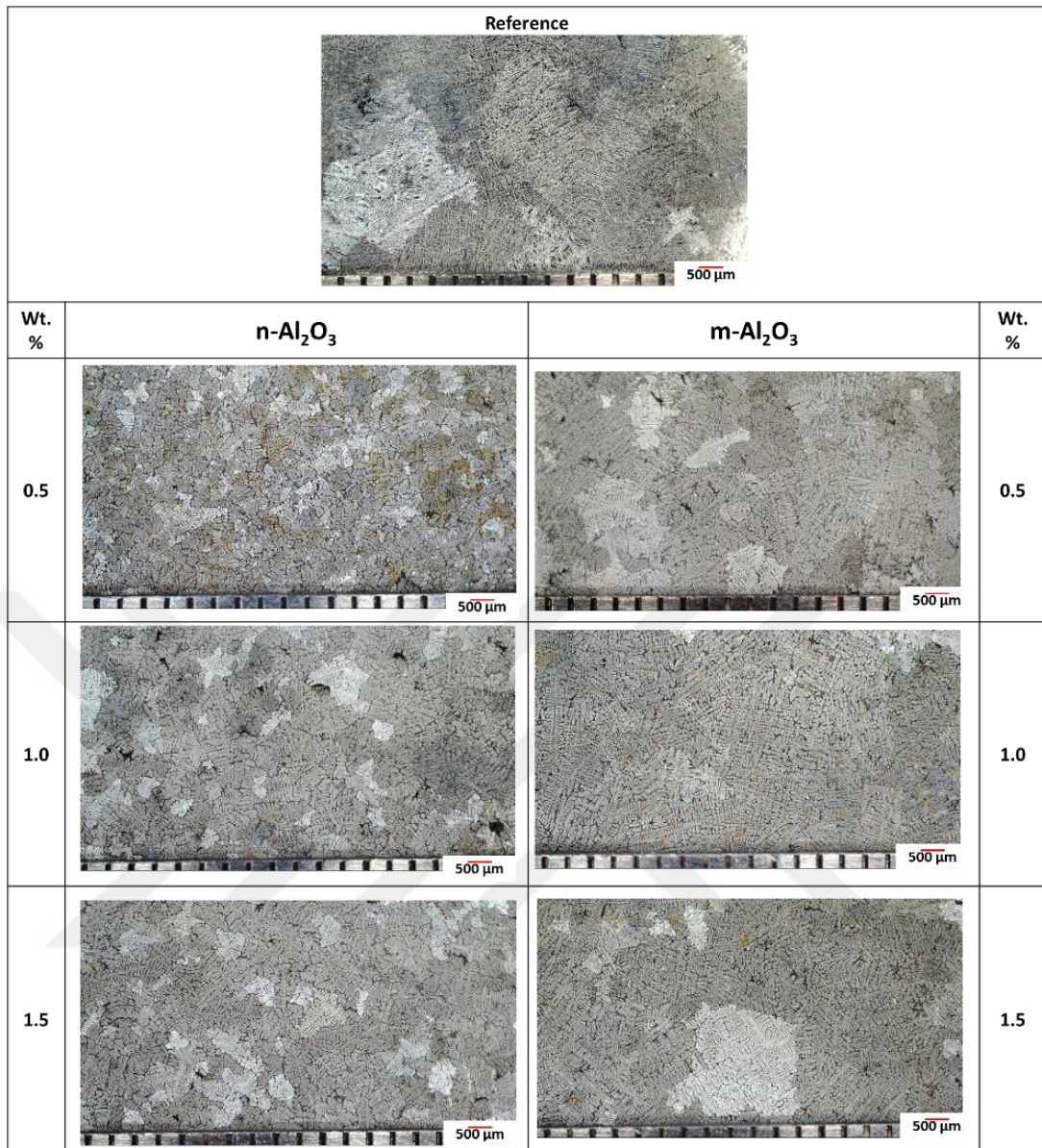


Figure 3.22 : Macrostructure of samples reinforced with micro and nano Al_2O_3 .

Table 3.7 : SDAS measurement of samples reinforced with micro and nano Al_2O_3 (μm).

Samples		SDAS measurement (μm)
Reference		51 ± 10
micro- Al_2O_3 (wt.%)	0.5	44 ± 8
	1.0	49 ± 10
	1.5	48 ± 8
nano- Al_2O_3 (wt.%)	0.5	32 ± 7
	1.0	34 ± 6
	1.5	32 ± 6

Table 3.8 : Grain size measurement of samples reinforced with micro and nano Al_2O_3 (μm).

Samples		Grain size measurement (μm)
Reference		1093 ± 178
micro- Al_2O_3 (wt.%)	0.5	1462 ± 217
	1.0	1526 ± 166
	1.5	1226 ± 257
nano- Al_2O_3 (wt.%)	0.5	756 ± 53
	1.0	782 ± 131
	1.5	887 ± 219

SDAS and grain size measurements show that the group of samples, which were reinforced with nano particles, have finer grain size and secondary dendrite arm spacing. The reason is due to the fact that nano- Al_2O_3 had relatively higher thermal conductivity. The thermal conductivity of nano and micron Al_2O_3 are 40 W/mK [79] and 35.6 W/mK, respectively [68]. If the thermal conductivity is higher, the solidification velocity is also elevated. Therefore, grain size is getting finer. As it is observed from the grain size measurement results of samples, which are reinforced with nano- Al_2O_3 , it is getting coarse when increasing the amount of nano particle additives. The minimum result was obtained with 0.5 wt% nano- Al_2O_3 .

As it can be observed in micro and macro structure photographs that the reference sample has large porosities. Figure 3.23 displays a percentage of porosity that is calculated with the help of using differences in density between measured and theoretical as given afore.

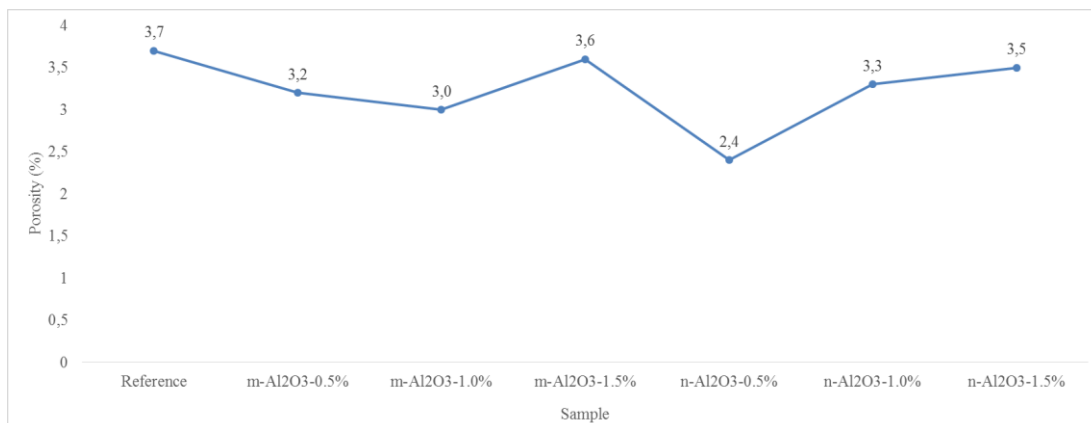


Figure 3.23 : Percentage of porosity.

The group of samples, which were reinforced with nano- Al_2O_3 , have a lower percentage of porosity than the sample that was reinforced with micro- Al_2O_3 . It is seen that the amounts of porosity and shrinkage are ascending through the increase of nano- Al_2O_3 addition. Ezatpour et al. [80] concluded that the porosity percentage escalates both by increasing the stirring time and the amount of nano- Al_2O_3 additives. They used the same amount of additives and obtained the highest percentage of porosity with 1.5% wt nano- Al_2O_3 as 4%. In current study, the maximum porosity value was obtained with 1.5% wt as 3.5%. This could be a consequence of the ultrasonic stirring as Babu et al. [81] explained that the surface tension between additives and matrix material could be decreased by ultrasonic stirring.

If the mechanical test results are examined as given in Figure 3.24, the group of samples, which were reinforced with nano- Al_2O_3 , show higher results than the group of samples that were reinforced with micro- Al_2O_3 . When each addition group is compared in itself, it is seen that the addition of 0.5%wt nano- Al_2O_3 displays the highest UTS and elongation values. One of the reasons for this is the agglomeration due to the increased amount of reinforcement and the distribution of reinforcements to the internal structure. Another effect may also have considered to be percentage of porosity. When the hardness measurement results are analyzed, the results decrease by increasing the amount of nano- Al_2O_3 . The highest value was measured in the addition of 0.5% wt of nano- Al_2O_3 as 87,7 BH. When the samples with micro- Al_2O_3 reinforcement are examined, hardness test results are nearly the same. When these values are taken into consideration, samples which are reinforced with nano- Al_2O_3 addition, meet all requirements of car manufacturers.

Figure 3.24 also demonstrates the Charpy impact test results; as for micro- Al_2O_3 addition, test results ascended through increasing the amount of additives, but the results for nano- Al_2O_3 were observed to be the opposite. Although the outcomes decreased by increasing the amount of nano- Al_2O_3 , the maximum test result was obtained with 0.5%wt nano- Al_2O_3 additive. Porosity content was also significant on these results. By virtue of porosity content, inhomogeneous stress distribution ensue around pores and this incline lead to damage of composite material [77;78].

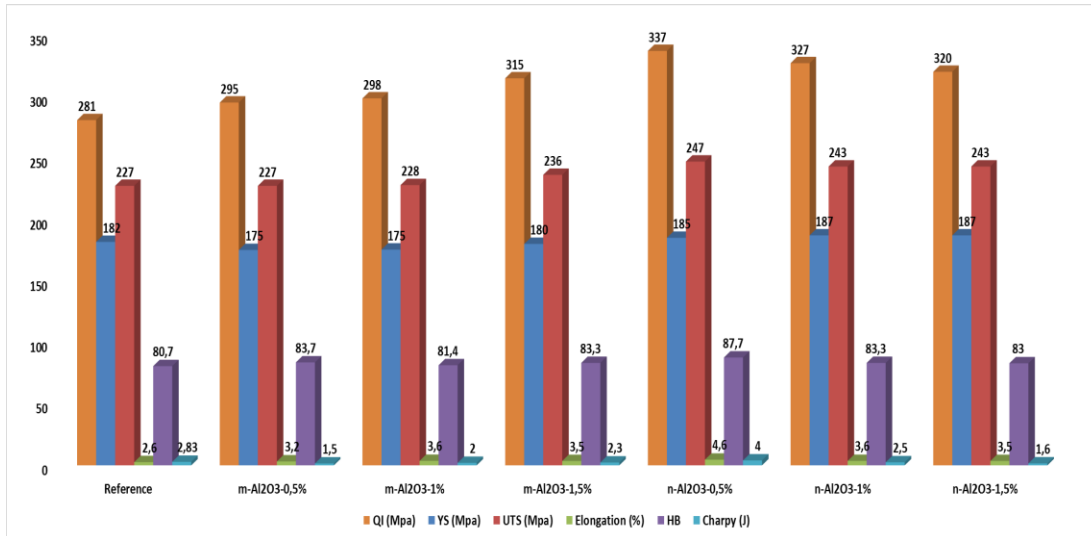


Figure 3.24 : Mechanical test results of samples reinforced with micro and nano Al_2O_3 .

3.2.2.3 The evaluation effect of nano- Al_2O_3 and graphene reinforcements

The microstructure and macrostructure images of all composite samples that are reinforced with mano- Al_2O_3 and graphene are shown in Figure 3.25, Figure 3.26, respectively. However, the grain size and secondary dendrit arm spacing (SDAS) measurements are given in Table 3.9 and Table 3.10, respectively.

The reference sample appears to have large porosities. This is also a reason for obtaining low values, especially in mechanical test results. Figure 3.25 and Figure 3.27 demonstrate that the coarse aluminum dendrites are getting finer by increasing the amount of nano- Al_2O_3 reinforcement, yet the same condition could not be said for graphene. Although there is a reduction of dendrites in microstructural images, there is no significant improvement. Considering the outcome of SDAS measurement in Table 3.9, it is easily seen that the results are close to each other. This also means that there is no mold-based effect in cooling process. Therefore, it can be concluded that the mechanical test results are directly related to the internal structure of the produced composite. In Figure 3.26, it is observed that there is an increase of porosity and shrinkage in the interior structure with addition of nano- Al_2O_3 . This also proves the results of the calculated porosity given in Figure 3.28. Moreover, similar situation is valid for graphene and it is understood from Table 3.9, there is no regular change of particle size analysis by increasing the amount of graphene. For nano- Al_2O_3 samples, the grain size ascended through increasing the amount of additive. This may be due to the occurrence of agglomeration in the added particles. The

lowest grain sizes of samples with nano- Al_2O_3 and graphene were obtained with the amounts of 0.5% wt and 0.075% wt, respectively.

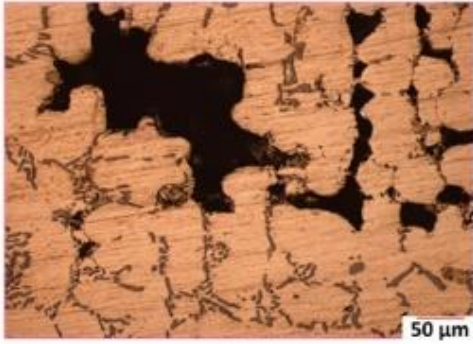
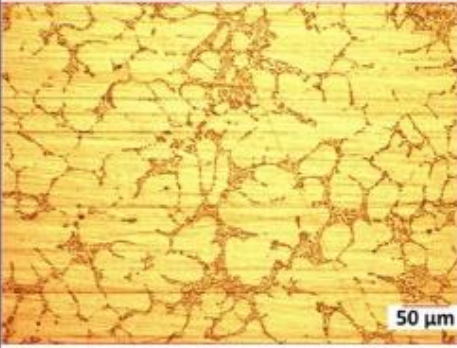
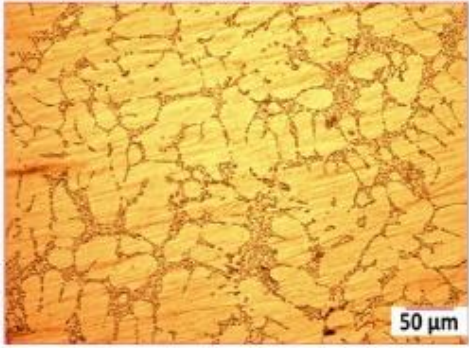
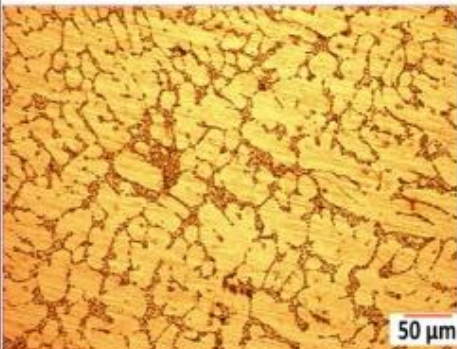
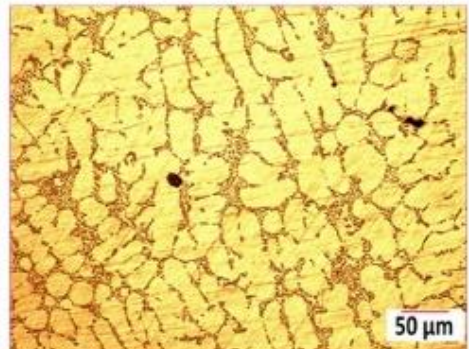
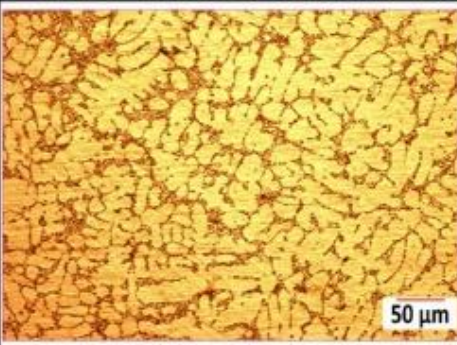
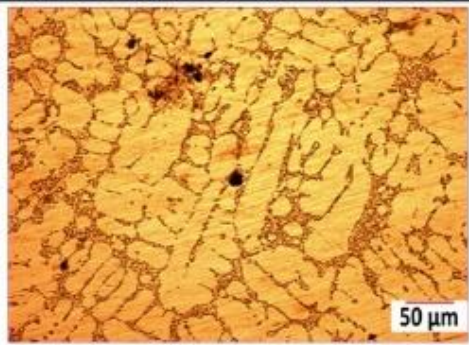
	10x	10x	
Reference			Reference
nano Al_2O_3 – 0.5 wt. %			graphene – 0.075 wt. %
nano Al_2O_3 – 1.0 wt. %			graphene – 0.15 wt. %
nano Al_2O_3 – 1.5 wt. %			graphene – 0.25 wt. %

Figure 3.25 : Microstructure of samples reinforced with nano Al_2O_3 and graphene.

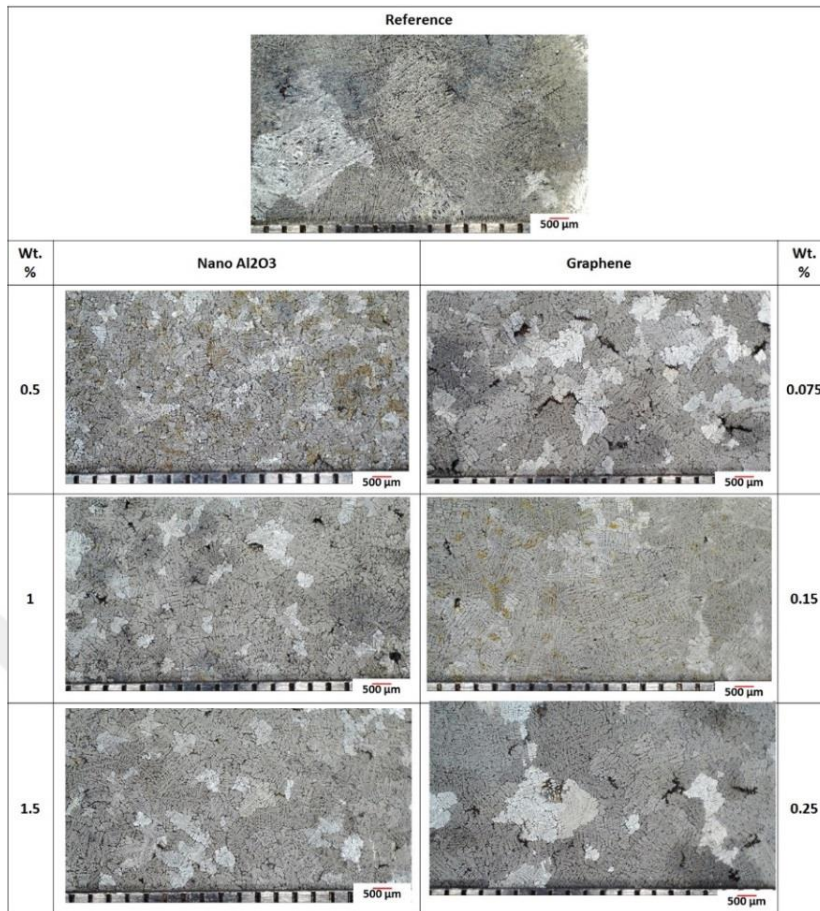


Figure 3.26 : Macrostructure of samples reinforced with nano Al₂O₃ and graphene.

Table 3.9 : SDAS measurement of samples reinforced with nano Al₂O₃ and graphene (μm).

Samples		SDAS measurement (μm)
Reference		51.4 ± 10.4
nano-Al ₂ O ₃ (wt.%)	0.5	32.2 ± 6.5
	1.0	33.8 ± 6.1
	1.5	32.4 ± 6.2
Graphene (wt.%)	0.075	38.8 ± 7.7
	0.15	33.1 ± 6.2
	0.25	34.6 ± 5.6

Table 3.10 : Grain size measurement of samples reinforced with nano Al₂O₃ and graphene (μm).

Samples		Grain size measurement (μm)
Reference		1093 ± 178
nano-Al ₂ O ₃ (wt.%)	0.5	755.5 ± 53
	1	781.7 ± 131
	1.5	887.3 ± 219
Graphene (wt.%)	0.075	948.4 ± 195
	0.15	2226.14 ± 609
	0.25	1925.9 ± 429

When the mechanical test results are examined as given in Figure 3.27, the addition of nano- Al_2O_3 displays higher results than the samples with graphene. The most important reason for this is the particle size of reinforcement materials. Suthar et al. [82] declared that agglomeration could be seen with small particle sizes due to the fact that they have more surface area. When each addition group is compared in itself, the addition of 0.5% wt nano- Al_2O_3 shows the best UTS and elongation values. One of the reasons for this is the agglomeration due to the increased amount of reinforcement and the distribution of reinforcements in the internal structure. Another effect may also have considered to be percentage of porosity.

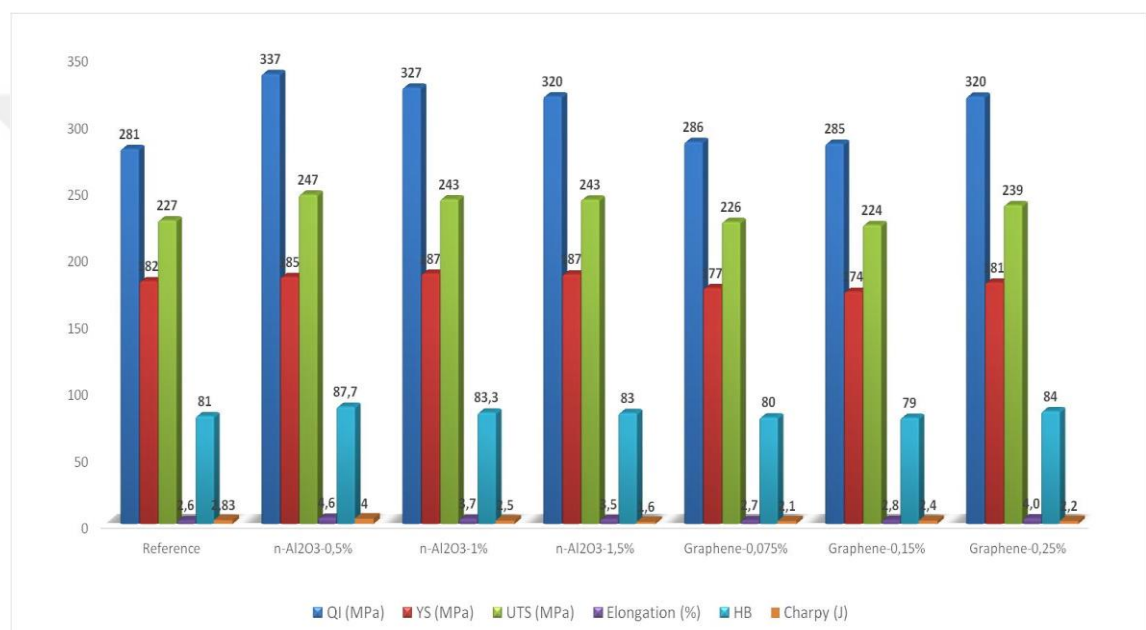


Figure 3.27 : Mechanical test results of samples reinforced with nano Al_2O_3 and graphene.

When the percentage of porosity, given in Figure 3.28, is examined, porosity ascended through increasing the amount of nano- Al_2O_3 . If samples with graphene is considered, the best test results were obtained with the amount of 0.25% wt. It could be said that percentage of porosity values are effective. The amount of porosity decreases by increasing the amount of graphene addition. The porosity values depend not only on the amount of additives, but also on the type and duration of applied stirring processes during additions. Oztop et al. [76] elucidated that percentage of porosity escalates by increasing the amount of graphene reinforcement while using mechanical stirring system. However, they used only mechanical stirrer during the stirring process and carried out the process for a total of 6 minutes. Hashim et al. [64]

and Su et al. [83] reported that the porosity was formed by the ingress of gases. Therefore, the escalation in the mechanical stirring cycle and duration increases the amount of porosity due to the inlet of air into melt. In this study, percentages of porosity values were obtained as a result of graphene additions are lower than the results of Oztop et al. [76] study. The biggest reason of this is that dissolved gases in the molten metal are floated to the surface of melt by applying ultrasonic vibration. Considering the QI calculated, the results of the group with nano- Al_2O_3 additives were higher than the group with graphene additives. Increasing the amount of nano- Al_2O_3 leads to a decrease in the QI. For samples with graphene, it is seen that the highest result was attained with the highest amount of reinforcement. When the hardness test results are analyzed, it is observed that the results decrease by increasing the amount of nano- Al_2O_3 . The highest value was measured as 87,7 BH with the addition of 0.5% wt to nano- Al_2O_3 . On the other hand, hardness test results of the samples with graphene escalated by increasing the amount of additives. The highest value was measured as 85.12 BH with the addition of 0.25% wt of graphene.

Percentage of porosity which is calculated by using aforementioned equations are displayed in Figure 3.28.

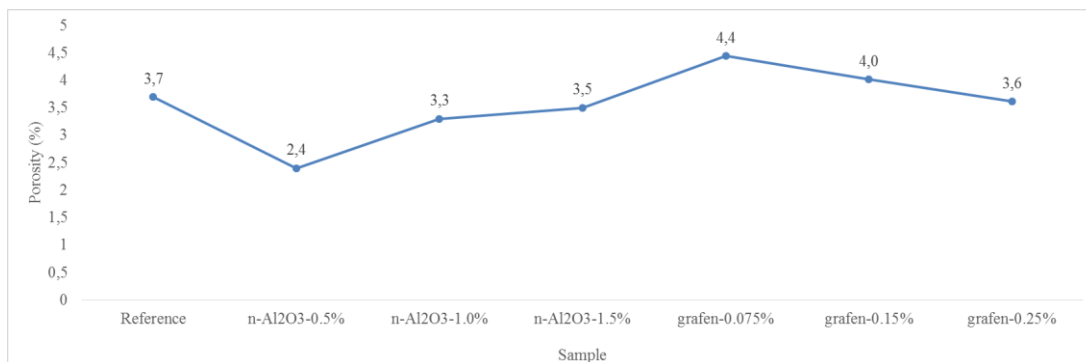


Figure 3.28 : Percentage of porosity.

Ezatpour et al. [80] declared that porosity percentage escalates not only by increasing the stirring time but also by the amount of nano- Al_2O_3 reinforcement. They added the same amount of nano- Al_2O_3 and get the highest percentage of porosity, as nearly 4%, with 1,5% wt addition of nano- Al_2O_3 . In current study, maximum percentage of porosity was obtained with the amount of 1,5%wt addition as 3,47%. It could be thought that this result was attained due to the ultrasonic stirring, added mechanical stirring. Babu et al. [81] elucidated that cavitation bubbles formed by ultrasonic

stirring decrease the surface tension between reinforcement and matrix material, and improve the wettability. This could be the reason of attaining lower porosity values than the literature.

3.2.3 Conclusions of the whole evaluation studies

With the help of using mechanical test results and metallographic investigations, comparative types of reinforcements were evaluated as follows;

- Aluminum metal matrix composite with SiC particles have higher mechanical properties than the ones with Al₂O₃ particles,
- Aluminum composite with 1 wt. % SiC has the lowest porosity and as a result the highest mechanical properties were obtained.
- Aluminum metal matrix composite with nano-Al₂O₃ particles have higher mechanical properties than the ones with micro-Al₂O₃ particles,
- Aluminum composite with 0.5 wt. % nano-Al₂O₃ has the lowest porosity and as a result the highest mechanical properties were attained.
- The maximum impact test result was also obtained from the one which was reinforced with 0.5% nano-Al₂O₃ additive.
- Aluminum metal matrix composite with nano-Al₂O₃ particles have higher mechanical properties than the ones with graphene particles.
- Aluminum composite with 0.5 wt. % nano-Al₂O₃ has the lowest porosity and as a result the highest mechanical properties were attained.
- The increase in addition of nano-Al₂O₃ decreases the QI result, contrary to this, the result of QI escalates by increasing the graphene.

3.3 The Effect Of Hot Isostatic Press On Mechanical Properties Of Aluminum Metal Matrix Composites

Composite material can be produced by different producing methods as given in Chapter 3.1. Stir casting method is generally used for synthesis of discontinuous aluminum matrix composites owing to its flexibility, budgetary and simplicity [37;64;84]. Although this method has positive properties, it has also negative aspects due to its nature. The most important negative aspect of this method is porosity because mechanical properties of final products are strongly connected with the microstructure and defects of castings [85]. There are two main reasons of porosity formation. One of them is shrinkage due to the lack of liquid metal to feed, the other one is gas evolution as a consequence of decreasing the solubility of hydrogen during solidification [86;87].

Hot isostatic press (HIP) method that involves both a high pressure gas application and an elevated temperature simultaneously can be used to eliminate porosity [88;89]. In literature, it can be seen in several studies of HIP application for producing composite materials.

Mostafavi Kashani et al. [90] investigated the effect of HIP on the mechanical properties of A356 cast alloy. They produced cast bar and applied heat treatment process (homogenized at 540°C for 2 hours and rapid cooling, then age hardened at 180°C for 4 hours). Later they addressed HIP process with a pressure of 104 MPa at 500°C for 2 hours. They obtained the results while comparing all samples as cast, age hardened and HIPed. They concluded that UTS and YS did not change significantly, but elongation was increased as 16% when applying HIP method. They clarified that the increase of elongation was due to the reducing of porosity from 2-8% to 0-4%. Ceschini et al. [91] studied on to determine the effect of HIP on the fatigue resistance of sand cast both with A356 and A204 aluminum alloys. They produced samples in two different conditions. One of them was that they generated samples in sand-cast method then T6 heat treatment was applied. On the other one, they produced samples in sand-cast method, later HIP process was applied before T6 heat treatment. They addressed the HIP method with pressure of 100 MPa at 520°C for 2 hours. They concluded that fatigue resistance could be increased by applying HIP method as 40% for A356 and 70% to A204 aluminum alloys. Ran et al. [92] researched the effect of

HIP method on the microstructure and mechanical properties of unmodified A356-T6 alloy which was produced by sand cast method. T6 heat treatment was applied to all samples, thereafter HIP method was addressed to half of samples at 520 °C, 100 MPa for 2 hours. They came into the conclusion that percentage of porosity was decreased by applying HIP. However, they declared that both Mg₂Si precipitate sizes were decreased and sub-grain boundaries were formed by using HIP method. Yet researchers in general have not given the cooling conditions of the HIPed samples. Aybarc et al. [93] investigated the effect of HIP on metallurgical and mechanical properties of A356 alloy. They applied HIP method with pressure of 100 MPa at 510°C for 2 hours and cooling condition as 50°C/minute. They addressed HIP to the samples taken from the determined steps of wheel production (as cast, before heat treatment, after heat treatment, between heat treatment and paint application) in order to determine the most appropriate step of HIP usage in wheel production. The maximum UTS and YS were obtained when applying HIP + heat treatment as 212 MPa and 74 MPa, respectively. Lee et al. [94] researched the effect of hot isostatic pressing on fatigue properties of A356 aluminum alloy. HIP method was practiced under a pressure of 103 MPa at 516°C for 2 hours. Later T6 heat treatment was applied. They generated the samples with and without degassing by applying tensile test and high-cycle fatigue test to samples and concluded that HIP process improved the YS, UTS, elongation and the fatigue strength at 10⁷ cycles. However, they declared that the volume fraction of pores considerably reduced, especially by degassing usage. Zulfia et al. [89] produced samples by practicing A357 aluminum alloy with and without 15 vol % SiC and by using stir casting; and applied HIP process with four different conditions which were named as HIP1 at 575°C/103 MPa/2 h, HIP2 at 575°C/103 MPa/2 h, HIP3 at 565°C/103 MPa/15 min followed by 535°C/103 MPa/2 h and HIP4 at 570°C/103MPa/40 min followed by 535°C/103 MPa/2 h. They concluded that the minimum porosity was attained while using the condition of HIP3. Thereupon, they also investigated the effect of heat treatment under T6 conditions. They produced samples as unreinforced and reinforced with 15 vol% SiC with different conditions as cast, cast + T6, HIPed1, HIPed1+ T6, HIPed 3 and HIPed3 + T6. They practiced four point bend tests on them and summarized that the test results improved the bending properties (yield strength, bending moment and the bend nominal strength) by around 10–30% [88, 89].

3.3.1 Experimental procedure

The composite samples were produced as detailedly given in previous chapter. Reinforcements were chosen as 0.1 wt% SiC, 0.5 wt.% nano- Al_2O_3 and 0.25 wt.% graphenes by virtue of giving the maximum mechanical properties than the others. After the samples were generated, HIP method was also applied to all of them. Thereafter HIP method was practiced, T6 heat treatment was applied to all samples, thereupon they were machined to obtain the mechanical tests as in standards given the previous chapter.

3.3.2 Results and discussions

The macrostructure images and grain size measurements are given in Figure 3.29 and Table 3.11, respectively.

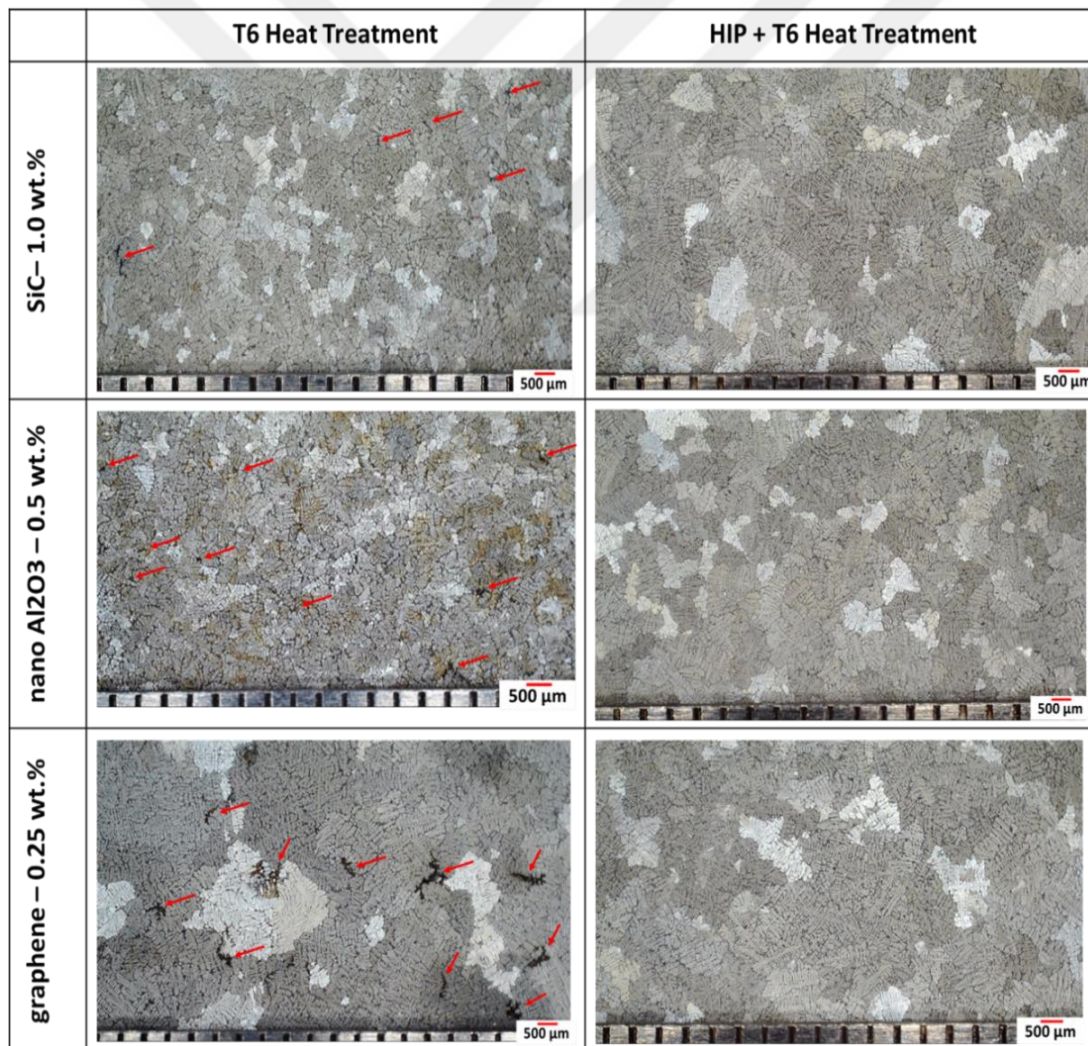


Figure 3.29 : Macrostructure of samples with and without HIP process.

Table 3.11 : Macro grain size measurements of samples applied and unapplied HIP process (μm).

Reinforcement	un-HIPed	HIPed
SiC – 1. wt. %	593 ± 52	95 ± 24
nano- Al_2O_3 – 0.5 wt. %	756 ± 53	95 ± 22
Graphene – 0.25 wt. %	1925.9 ± 429	142 ± 37

Some researchers declared in their papers that HIP method has an insignificant effect on grain size value [91]. The reason of this can be explained as researchers practiced HIP process, but after it was finished they did not apply any cooling process. They generally waited the temperature to go down to room temperature. But in this study, the cooling step was also applied as 50°C per minute and it can be clearly seen from Table 3.11 that after HIP method was practiced, microstructure of all samples were getting finer. The similar results were also obtained by Ammar et al. [86] who measured the average grain size of A356 before and after they were HIPed as $1182 \mu\text{m}$ and $316 \mu\text{m}$, respectively. Moreover, Dedyeva et al. [95] applied the cooling step in their research and they declared that the synthesis conditions lead to multinuclei crystallization.

The microstructure images and SDAS measurements are given in Figure 3.30 and Table 3.12, respectively.

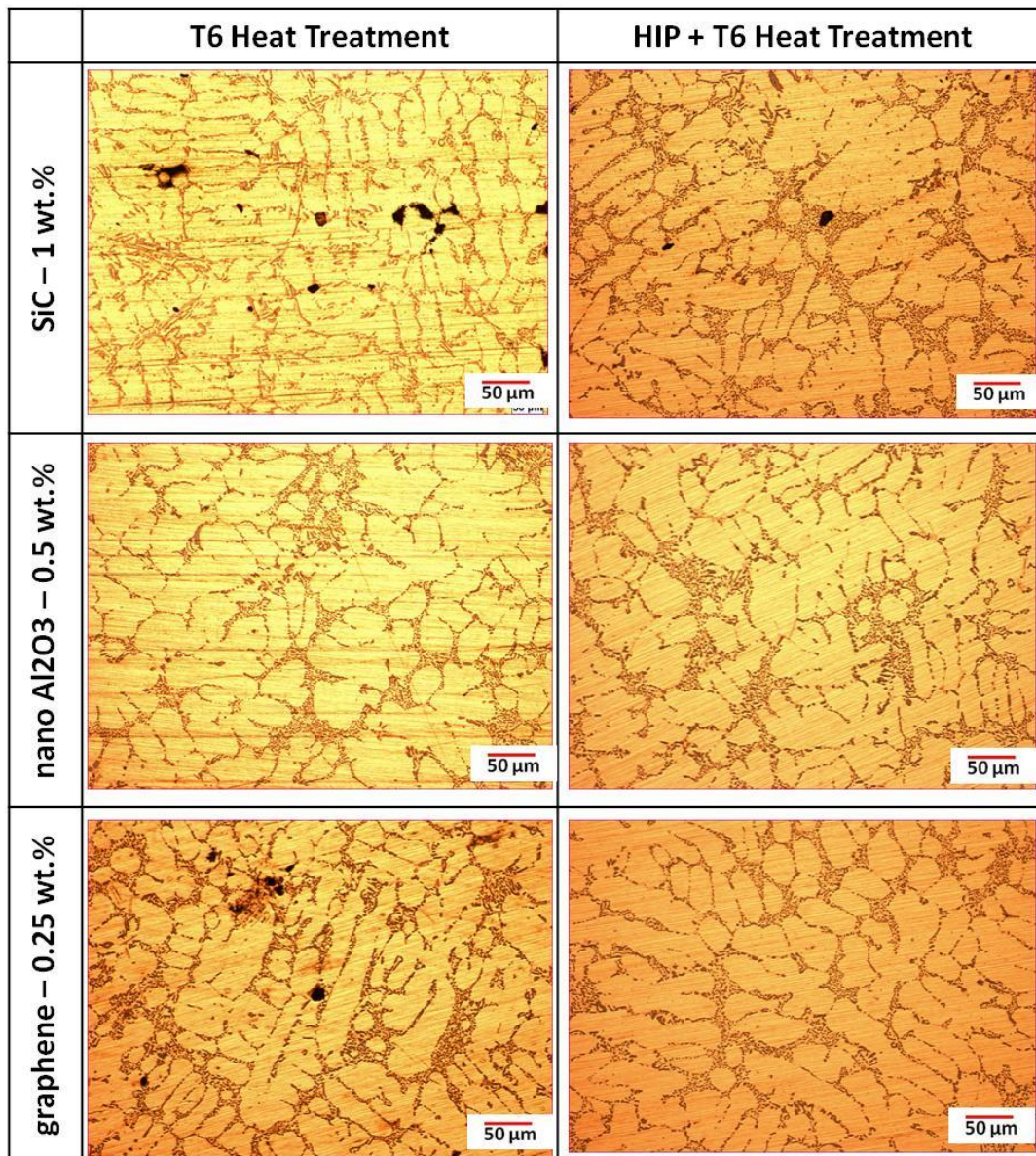


Figure 3.30 : Microstructure of samples with and without HIP process.

Table 3.12 : SDAS measurements of samples applied and unapplied HIP process (μm).

Reinforcement	un-HIPed	HIPed
SiC – 1. wt. %	38 ± 8	32 ± 6
nano- Al_2O_3 – 0.5 wt. %	32 ± 7	33 ± 7
Graphene – 0.25 wt. %	35 ± 6	35 ± 9

If SDAS measurements are taken into consideration, it can be seen that the measurements decrease after HIP process is practiced; yet this decrease is not at a

considerable extent. Ran et al. [92] also proved that SDAS is little affected by the HIP process.

The mechanical test results of samples with and without applied HIP are given in Figure 3.31. According to this figure, the mechanical properties of all samples increased when HIP process was practiced. If composite samples which were produced with the same reinforcement are taken into consideration, YS, UTS and elongation values of sample that was reinforced with SiC would increase as 7.1%, 7.5% and 1.6, respectively following HIP process practice. Similarly, with the addition of nano-Al₂O₃, YS, UTS and elongation values would increase as 11.3%, 16.2%, 80.9% after practicing HIP process, respectively. The results of YS, UTS and elongation values of samples, which were obtained with graphene reinforcements, increased as 11.5%, 17.8 and 104.3 after applying HIP process, respectively.

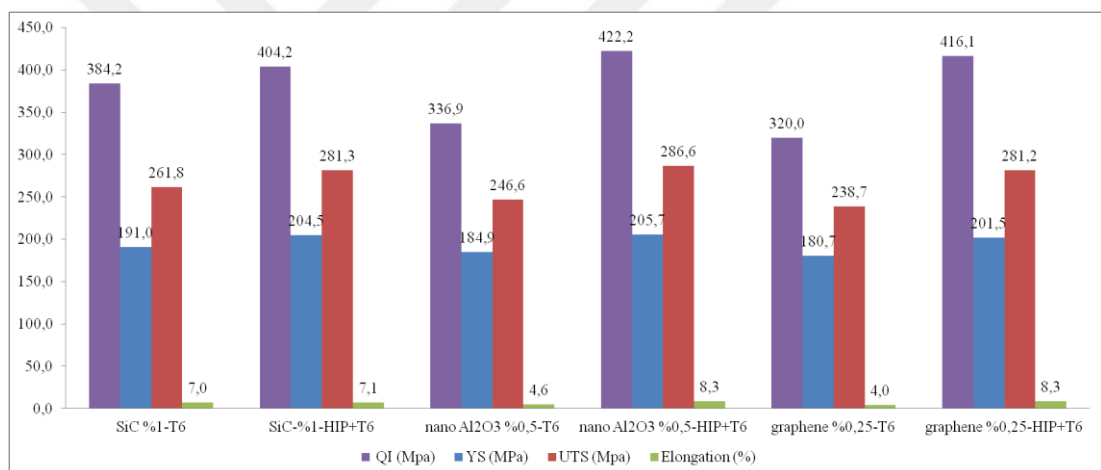


Figure 3.31 : Mechanical test results of samples with HIPed and un-HIPed.

If all sample groups were considered at the same time, the samples, which were reinforced with n- Al₂O₃, would have shown the maximum mechanical test results. Additionally, if the calculated QI, that explained in the previous chapter in detail, was taken into account, it could be seen that samples, that were reinforced with nano-Al₂O₃, showed the maximum result. It can be said that these results cause by the porosity percentages of the samples.

After HIP process was practiced, the surface of a sample is displayed in Figure 3.32. Many hollows can be seen on the surface that appeared due to the presence of porosity in the internal structure. Applying the condition of HIP at a high temperature and pressure creates a high press on the surface of samples leading

porosity to close while a hollow is occurring on the surface. Figure 3.29 and Figure 3.33 display the macrostructure of whole samples before and after HIP application. Porosity decreases after HIP application and this figure is the proof of the result.



Figure 3.32 : The surface of a sample after HIP process.

	T6 Heat Treatment	HIP + T6 Heat Treatment
SiC- 1.0 wt. %		
nano Al2O3 – 0.5 wt. %		
graphene – 0.25 wt. %		

Figure 3.33 : SEM images of samples before and after HIP process.

In these figures, it is easy to say that HIP process decreases the porosity content in the samples. The percentage of porosity was determined by using the formula given in the previous chapters. The alteration of mechanical test results of all samples with and without HIP processes are given in Figure 3.34, Figure 3.35 and Figure 3.36.

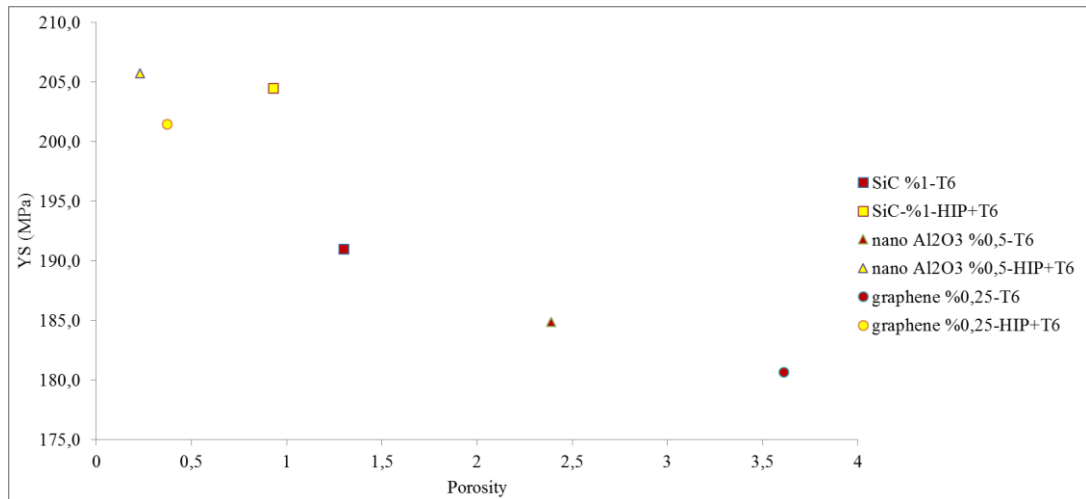


Figure 3.34 : The variation of YS versus porosity content.

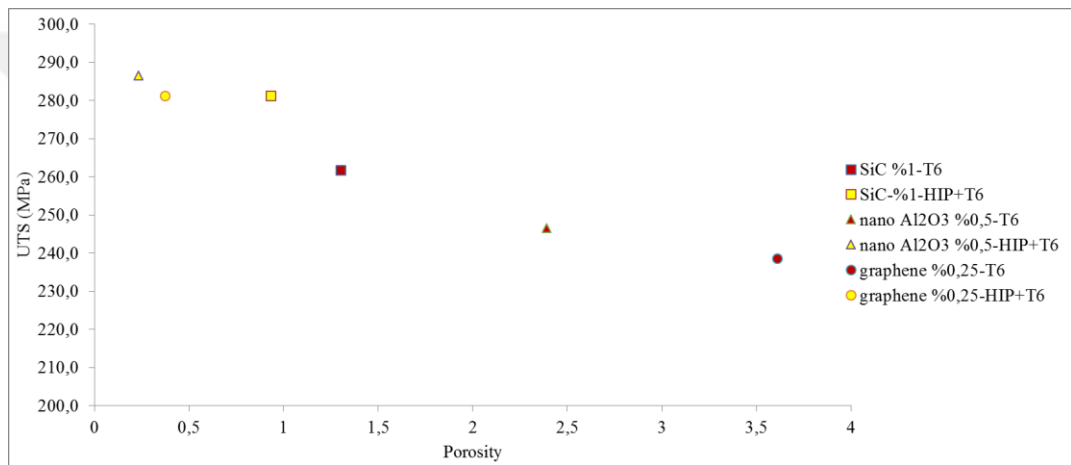


Figure 3.35 : The variation of UTS versus porosity content.

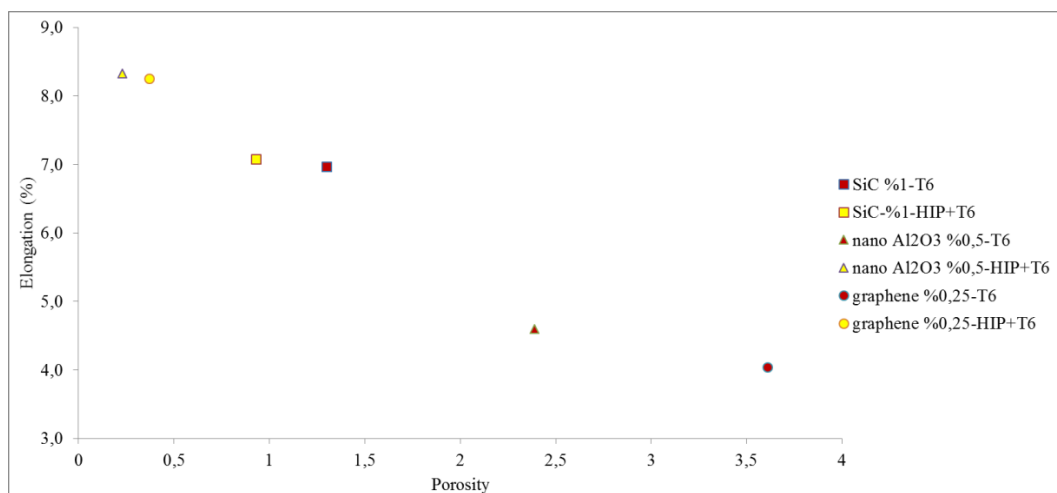


Figure 3.36 : The variation of elongation versus porosity content.

When YS, UTS and elongation values of porosity are examined, it is seen that mechanical properties increase by decreasing porosity during HIP process. These results were also explained in the literature, especially for elongation [90]; and

besides Li et al. [96] summarized that yield strength was improved up to 20% by applying HIP process.

When comparing the mechanical properties and porosity content obtained from the samples that are produced by using the same reinforcement before and after HIP process, YS values of the samples which are reinforced with SiC, nano- Al_2O_3 and graphene increase as 7.1%, 11.3% and 11.5%; UTS values escalates as 7.5%, 16.2% and 17.8% and elongation values expand as 1.6%, 80.9% and 104.3%, respectively. The samples which were reinforced with graphene showed the maximum improvement on mechanical properties. The reason of this was high porosity content before HIP process was applied. Hence, they showed the minimum mechanical test results. Posterior to the decrease in porosity content, the maximum variation of mechanical properties was obtained since porosity content was at vital importance on mechanical properties of a material, especially in service conditions. This phenomenon has been also clarified by many researchers in the previous investigations [87;97-99]. When taking all results into consideration, the maximum mechanical test results are attained with 0.5 wt% nano- Al_2O_3 addition by applying HIP process. Figure 3.37 illustrates the QI calculations.

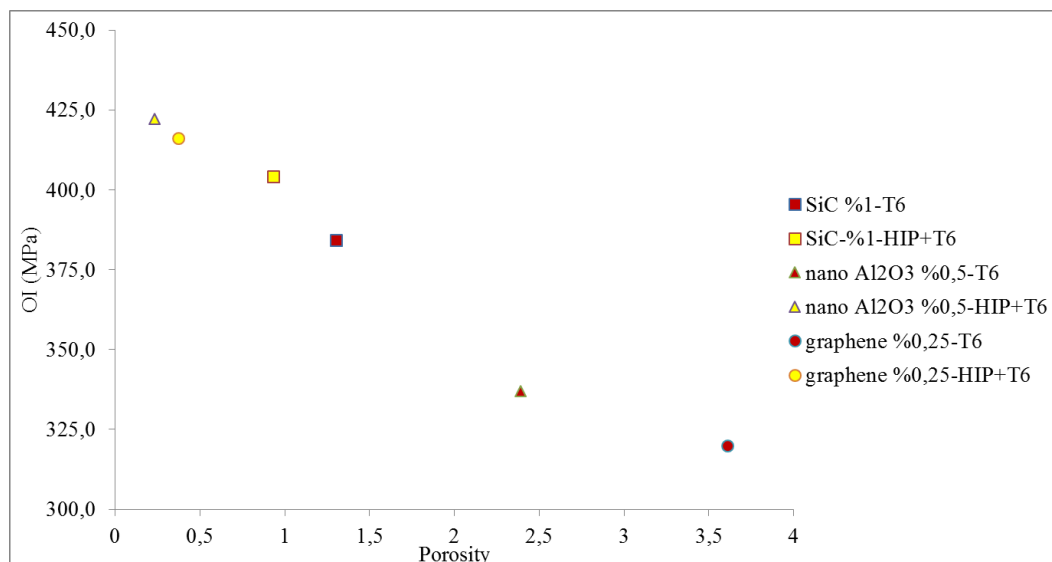


Figure 3.37 : The variation of QI versus porosity content.

In this figure it can be seen that the QI values of all samples have increased. The escalation in SiC reinforced samples was relatively low compared to the ones obtained from other additives. The maximum QI value is acquired with 0.5 wt% n- Al_2O_3 additions.

3.3.3 Conclusions

In this chapter A356 aluminum alloy was used as a matrix material and three different reinforcements were used as reinforcement materials with 1.0 wt% SiC, 0.5 wt% nano-Al₂O₃ and 0.25 wt% graphene. T6 heat treatment was applied to whole samples after HIP process. Tensile tests were addressed to all samples. The obtained results are summarized as follows;

- The porosity contents of all samples decreased by the help of using HIP process,
- The mechanical test results increased as a consequence of decreasing porosity contents,
- The samples reinforced with graphene showed the maximum alteration of mechanical increases.
- The maximum mechanical test results were obtained with the addition of nano-Al₂O₃.
- The maximum QI value was calculated with the addition of nano-Al₂O₃.

4. CONCLUSION AND FUTURE WORK

This thesis was investigated under three headings. One of them was the determination of the stirring type and mold design, the other one was using different reinforcement materials to improve the aluminum matrix composites and the latter one is the effect of hot isostatic press on mechanical and metallographical properties of aluminum metal matrix composites.

In the first part, investigations about aluminum metal matrix composites within literature are discussed in detail. Furthermore, reinforcement materials to be used are determined as SiC, micron size Al_2O_3 , nano size Al_2O_3 and graphene.

In the second part, three different stirring methods including mechanical, ultrasonic vibration and mechanical assisted ultrasonic vibration (named as hybrid stirring), are used to determine the appropriate stirring method with the help of both simulation and laboratory casting studies. The simulation results show that the distributions of reinforcement particles are, from higher to lower, as hybrid stirring, mechanical stirring and ultrasonic vibration. These simulation results proved with the laboratory casting studies. However, two different mold designs (bottom-fed and spoke mold) are used to determine the appropriate one. The simulation analysis illustrates that the spoke mold is more appropriate to produce aluminum metal matrix composite than the bottom-fed mold. According to our simulation analysis and laboratory test results, hybrid stirring method and spoke mold are determined to be the appropriate stirring type and mold design to produce aluminum metal matrix composite with particle reinforcement material.

In the third part, determined reinforcement materials are used in a different content. SiC and Al_2O_3 reinforcements are added as 0.5 wt%, 1.0 wt% and 1.5 wt%, graphene reinforcements are added as 0.075 wt%, 0.15 wt% and 0.25%. SiC and micro size Al_2O_3 reinforcements are used to ascertain the effect of different reinforcement materials with the same average particle size. Micron size Al_2O_3 and nano size Al_2O_3

are used to determine the affect of different particle size with the same reinforcement material. Nano size Al_2O_3 and graphene are applied to figure out the effect of under micron particle sizes of reinforcements with different reinforcement materials. In comparison with the reference sample, samples which are reinforced with SiC show the highest mechanical properties. There can be two factors. One of them is thermal conductivity and the other one is coefficient of thermal expansion. As a result, thermal conductivity of SiC is higher than the other reinforcements in which the solidification velocity of composite samples are improved. Thus, the metallographical examination illustrates a finer microstructure. However, on the grounds that higher coefficient of thermal expansion of SiC reinforcement, the mechanical properties of aluminum composite samples are improved. Additionally, porosity content has vital importance on mechanical behaviour of material; and in all laboratory casting studies it can be observed that SiC has minimum porosity content, especially with 1 wt%.

The fourth part includes three different reinforcements which show higher QI results, and that are produced one more time. In this part, hot isostatic press is used to determine the reinforcement effect on mechanical properties if porosity does not exist. On this wise, hot isostatic press process is applied to all samples before T6 heat treatment process. Porosity content decreases significantly, especially for nano size Al_2O_3 and graphene. Due to the decrease in porosity content, the mechanical properties (especially elongation value) of composite samples have increased. According to the QI calculated from mechanical test results, samples which have been reinforced with nano Al_2O_3 show the highest results as 422 MPa.

Finally, I note that the producing system, including hybrid stirring and spoke mold, is the most appropriate one to produce aluminum metal matrix composite with particle reinforcements. Additionally, when 1 wt% SiC reinforcement is used, the higher mechanical properties can be obtained. On the other hand, hot isostatic press method can be applied with 0.5 wt% nano size Al_2O_3 . For future work, a different coating material over the one on reinforcement may be also studied in order to determine the effect of coating on mechanical properties of aluminum composite materials.

REFERENCES

- [1] Dispinar, D., Akhtar, S., Nordmarka, A., Di Sabatinoa, M. & Arnberg, L. (2010). Degassing, hydrogen and porosity phenomena in A356. *Materials Science and Engineering A*, 527, 3719-3725. doi: <https://doi.org/10.1016/j.msea.2010.01.088>.
- [2] Tan, E., Tarakcilar, A.R. & Dispinar, D. (2012). Correlation between melt quality and fatigue properties of 2024, 6063 and 7075. *Supplemental Proceedings: Volume 2: Materials Properties, Characterization and Modeling TMS (The Minerals, Metals & Materials Society)*, 479-485. doi: <https://doi.org/10.1002/9781118357002.ch62>
- [3] Tsakiridis, P.E. (2012). Aluminum salt slag characterization and utilization - A review. *Journal of Hazardous Materials*, 217-218, 1-10. doi: [://doi.org/10.1016/j.jhazmat.2012.03.052](https://doi.org/10.1016/j.jhazmat.2012.03.052)
- [4] Hawari, A.A., Khader, M., Hasan, W. E., Alijla, M., Manawi A. & Benamour, A. (2014). A life cycle assessment (LCA) of aluminum production process. *World Academy of Science, Engineering and Technology International Journal of Mechanical, Industrial Science and Engineering*, 8(4), 679-685.
- [5] Kalpakjian, S. & Schmid, S.R. (2010). *Manufacturing Engineering and Technology: Seventh Edition*: Pearson.
- [6] Kandpal, B. C., Kumar, J. & Singh, H. (2014). Production technologies of metal matrix composite: a review. *International Journal of Research in Mechanical Engineering & Technology*, 4(2), 27-32.
- [7] Stojanovic, B. & Ivanovic, L. (2015). Application of aluminium hybrid composites in automotive industry. *Primjena Aluminijskih Hibridnih Kompozita U Automobilskoj Industrijii*, 22(1), 247-251. doi: 10.17559/TV-20130905094303
- [8] Ramnath, B. V., Elanchezhian, C., Annamalai, RM., Aravind, S., Atreya, T.S.A., Vignesh, V. & Subramanian, C. (2014). Aluminum Metal Matrix Composites - A review. *Reviews On Advanced Materials Science*, 38, 55-60.
- [9] Reddy, B.S.B., Das, K. & Das, S. (2007). A review on the synthesis of in situ aluminum based composites by thermal, mechanical and mechanical-thermal activation of chemical reactions. *Journal of Material Science*, 42(22), 9366-9378. doi: <https://doi.org/10.1007/s10853-007-1827-z>
- [10] Yousefian, R., Esmadoddin, E. & Baharnezhad, S. (2018). Manufacturing of the aluminum metal-matrix composite reinforced with micro-and nanoparticles of TiO₂ through accumulative roll bonding process (ARB). *Reviews On Advanced Materials Science*, 55(1/2), 1-11.
- [11] Stojanovic, B., Babic, M., Mitrovic, S., Vencl, A., Miloradovic, N. & Pantic, M. (2013). Tribological characteristics of aluminium hybrid composites

- reinforced with silicon carbide and graphite - a review. *Journal of the Balkan Tribological Association*, 19(1), 83-96.
- [12] Liu, Q., Qiu, F., Dong, B.X., Geng, R., Lv, M.m., Zhao, Q.L. & Jiang, Q.C. (2018). Fabrication, microstructure refinement and strengthening mechanisms of nanosized SiCp/Al composites assisted ultrasonic vibration. *Materials Science & Engineering A*, 753, 310-317. doi: <https://doi.org/10.1016/j.msea.2018.08.060>
- [13] Rahman, Md. H. & Mamun Al Rashed, H.M. (2014). Characterization of silicon carbide reinforced aluminum matrix composites. *Procedia Engineering*, 90, 103-109. doi: <https://doi.org/10.1016/j.proeng.2014.11.821>
- [14] Karvanis, K., Fasnakis, D., Maropoulos, A. & Papanikolaou, S. (2016). Production and mechanical properties of Al-SiC metal matrix composites. *IOP Conference Series: Materials Science and Engineering*, 161, 1-8. doi:10.1088/1757-899X/161/1/012070
- [15] Meena, K.L., Manna, A., Banwait, S.S. & Jaswanti, Dr. (2013). An analysis of mechanical properties of the developed Al/SiC-MMC's. *American Journal of Mechanical Engineering*, 1(1), 14-19. doi: doi:10.12691/ajme-1-1-3
- [16] Ozben, T., Kilickap, E. & Cakir, O. (2008). Investigation of mechanical and machinability properties of SiC particle reinforced Al-MMC, *Journal Of Materials Processing Technology*, 198(1-3), 220-225. doi: <https://doi.org/10.1016/j.jmatprotec.2007.06.082>
- [17] Singla, M., Dwivedi, D.D., Singh, L. & Chawla, V. (2009). Development of aluminum based silicon carbide particulate metal matrix composite. *Journal of Minerals & Materials Characterization & Engineering*, 8(6), 455-467. doi: DOI: 10.4236/jmmce.2009.86040
- [18] Johny James, S., Venkatesan, K. Kuppan, P. & Ramanujam, R. (2014). Hybrid aluminium metal matrix composite reinforced with SiC and TiB₂. *Procedia Engineering*, 97, 1018-1026. doi: 10.1016/j.proeng.2014.12.379
- [19] Prabu, S.B., Karunamoorthy, L., Kathiresan, S. & Mohan, B. (2006). Influence of stirring speed and stirring time on distribution of particles in cast metal matrix composite. *Journal of Materials Processing Technology*, 171(2), 268–273. doi: <https://doi.org/10.1016/j.jmatprotec.2005.06.071>
- [20] Sujan, D., Oo, Z., Rahman, M.E., Maleque, M.A. & Tan, C.K. (2012). Physio-mechanical properties of aluminum metal matrix composites reinforced with Al₂O₃ and SiC. *World Academy of Science, Engineering and Technology International Journal of Chemical, Molecular, Nuclear, Materials and Metallurgical Engineering*, 6(8), 678-681.
- [21] Singh, L., Ram, B. & Singh, A. (2013). Optimization of process parameter for stir casted aluminum metal matrix composite using taguchi method. *IJRET: International Journal of Research in Engineering and Technology*, 02(08), 375-383.
- [22] Alaneme, K.K. & Bodunrin, M.O. (2013). Mechanical behaviour of alumina reinforced aa 6063 metal matrix composites developed by two step – stir casting process. *Acta Technica Corviniensis Bulletin of Engineering*, 4(3), 105-110.
- [23] Mula, S., Padhi, P., Panigrahi, S.C., Pabi, S.K. & Ghosh, S. (2009). On structure and mechanical properties of ultrasonically cast Al-2%Al₂O₃ nanocomposite. *Materials Research Bulletin*, 44(5), 1154-1160. doi: <https://doi.org/10.1016/j.materresbull.2008.09.040>

- [24] Sajjadi, S.A., Ezatpur, H. R. & Beygi, H. (2011). Microstructure and mechanical properties of al-Al₂O₃ micro and nano composites fabricated by stir casting. *Materials Science and Engineering A*, 528 (29-30), 8765-8771. doi: <https://doi.org/10.1016/j.msea.2011.08.052>
- [25] Kok, M. (2001). Fabrication of 2024 aluminum alloy metal matrix composites reinforced with Al₂O₃ particles. *Fen ve Mühendislik Dergisi*, 4(2), 131-142.
- [26] Srivastava, N. & Chaudhari, G.P. (2018). Microstructure evolution and mechanical behaviour of ultrasonically synthesized Al6061-nano alumina composites, *Materials Science & Engineering A*, 724, 199-207. doi: <https://doi.org/10.1016/j.msea.2018.03.092>
- [27] Venkatesan, S. & Xavior, M.A. (2017). Mechanical behaviour of aluminum metal matrix composite reinforced with graphene particulate by stir casting method. *Journal of Chemical and Pharmaceutical Sciences*, 10(1), 55-59.
- [28] Bartolucci, S.F., Paras, J., Rafiee, M.A., Rafiee, J., Lee, S., Kapoor, D. & Koratkar, N. (2011). Graphene–aluminum nanocomposites, *Materials Science and Engineering A*, 528(27), 7933–7937. doi: <https://doi.org/10.1016/j.msea.2011.07.043>
- [29] Jagadish, B.S. (2015). Synthesis and characterisation of aluminum 2024 and graphene metal matrix composites by powder metallurgy means. *SSRG International Journal of Mechanical Engineering (SSRG-IJME)*, 2(7), 14-18.
- [30] Kumar, P., Aadithya, S., Dhilepan, K. & Nikhil, N. (2016). Influence of nano reinforced particles on the mechanical properties of aluminum hybrid metal matrix composite fabricated by ultrasonic assisted stir casting. *ARPN Journal of Engineering and Applied Sciences*, 11(2), 1204-1210.
- [31] Narwate, M.M. & Mohandas, K.N. (2016). A study on mechanical and tribological properties of aluminum metal matrix composite reinforced with tio₂ and graphene oxide. *International Journal of Advance Research and Innovation*, 4(4), 729-732.
- [32] Garg, H.K., Verma, K., Manna, A. & Kumar, R. (2012). Hybrid Metal Matrix Composites and further improvement in their machinability- A Review. *International Journal of Latest Research in Science and Technology*, 1(1), 36-44.
- [33] Umasankar, V. (2014). Experimental evaluation of the influence of processing parameters on the mechanical properties of SiC particle reinforced AA6061 aluminium alloy matrix composite by powder processing. *Journal Of Alloys And Compounds*, 582, 380-386. doi: <http://dx.doi.org/10.1016/j.jallcom.2013.07.129>
- [34] Magibalan, S., Kumar, P.S., Vignesh, P., Prabu, M., Balan, A.V. & Shivasankaran, N. (2017). Aluminium metal matrix composite - a review. *Transactions On Advancements In Science And Technology*, 1(2), 1-6.
- [35] Surappa, M. K. (2003). Aluminium matrix composites: challenges and opportunities. *Sadhana*, 28(1-2), 319-334. doi: 10.1007/BF02717141
- [36] Panwar, N. & Chauhan A. (2018). Fabrication methods of particulate reinforced aluminium metal matrix composites-a review. *Materials Today: Proceedings*, 5, 5933-5939. doi: <https://doi.org/10.1016/j.matpr.2017.12.194>
- [37] Balasivanandha Prabu, S., Karunamoorthy, L., Kathiresan, S. & Mohan, B. (2006). Influence of stirring speed and stirring time on distribution of particles in cast metal matrix composite. *Journal of Materials Processing Technology*, 171(2), 268-273. doi: <https://doi.org/10.1016/j.jmatprotec.2005.06.071>

- [38] Ulhas, K. A. & Kumar, G. B. V. (2017). Method of stir casting of aluminum metal matrix composites: a review. *Materials Today: Proceedings*, 4, 1140-1146. doi: <https://doi.org/10.1016/j.matpr.2017.01.130>
- [39] Mathur, S. & Barnawal, A. (2013). Effect of process parameter of stir casting on metal matrix composites, *Intenational Journal Of Science And Research*, 2(12), 395-398.
- [40] Jia, S. & Nastac, L. (2013). The influence of ultrasonic stirring on the solidification microstructure and mechanical properties of A356 alloy. *Chemical and Materials Engineering*, 1(3), 69-73. doi: DOI: 10.13189/cme.2013.010301
- [41] Jia, S., Zhang, D., Xuan, Y. & Nastac, L. (2016). An experimental and modeling investigation of aluminum-based alloys and nanocomposites processed by ultrasonic cavitation processing. *Applied Acoustics*, 103(B), 226-231. doi: <https://doi.org/10.1016/j.apacoust.2015.07.016>
- [42] Zhang, D. & Nastac, L. (2014). Numerical modeling of the dispersion of ceramic nanoparticles during ultrasonic processing of aluminum-based nanocomposites. *Journal of Materials Research and Technology*, 3(4), 296-302. doi: <http://dx.doi.org/10.1016/j.jmrt.2014.09.001>.
- [43] Nastac, L. (2014). Numerical modeling of fluid flow and solidification characteristics of ultrasonically processed A356 alloy. *ISIJ International*, 54(8), 1830-1835. doi: <http://dx.doi.org/10.2355/isijinternational.54.1830>
- [44] Sijo, M.T., Jayadevan, K. R. & Janardhanan, S. (2017). Numerical simulation of centrifugal casting for functionally graded metal-matrix cposites. *International Journal of Mechanical Engineering and Technology (IJMET)*, 8(4), 66-74.
- [45] Jia, S., Zhang, D. & Nastac, L. (2015). Experimental and numerical analysis of the 6061-based nanocomposites fabricated vis ultrasonic processing. *Journal Of Materials Engineering And Performance*, 24, 2225-2233. doi: 10.1007/s11665-015-1467-4
- [46] Shen, M.G., Ying, T., Chen, F.Y. & Hou, J. M. (2016). Effect of micro- and nano- SiC particulate reinforcements in magnesium-based metal matrix composites. *Journal Of Materials Engineering and Performance*, 25(6), 2222-2229. doi: <https://doi.org/10.1007/s11665-016-2068-6>
- [47] Loukus, A. & Loukus, J. (2011). Heat treatment effects on the mechanical properties ans microstructure of preform-based squeeese cast aluminium metal matrix composites. *International Journal of Metalcasting*, 5(1), 57-65. doi: <https://doi.org/10.1007/BF03355508>
- [48] Bindumadhavan, P.N., Chia, T.K., Chandrasekaran, M., Wah, H.K., Lam, L. N. & Parabhakar O. (2001). Effect of particle-porosity clusters on tribological behavior of cast aluminum alloy A356-SiCp metal matrix composites. *Materials Science and Engineering A*, 315(1-2), 217-226. doi: [https://doi.org/10.1016/S0921-5093\(00\)01989-4](https://doi.org/10.1016/S0921-5093(00)01989-4)
- [49] Sharma, P., Chauhan, G. & Sharma, N. (2005). Production of AMC by stir casting - an overview. *Journal Of Contemporary Practices*, 2(1), 23-46.
- [50] Aybarc, U., Yavuz, H., Dispinar, D. & Seydibeyoglu, M.O. (2019). The use of stirring methods for the production of SiC-reinforced aluminum matrix composite and validation via simulation studies. *International Journal of Metalcasting*, 13(1), 190-200. doi: <https://doi.org/10.1007/s40962-018-0250-3>

- [51] Naher, S. Brabazon, D. & Looney, L. (2007). Computational and experimental analysis of particulate distribution during Al–SiC MMC fabrication. *Composites Part A Applied Science and Manufacturing*, 38(3), 719-729.
- [52] Jia, S. Zhang, D. & Nastac, L. (2015). Experimental and numerical analysis of the 6061-based nanocomposites fabricated via ultrasonic processing. *Journal Of Materials Engineering And Performance*, 24(6), 2225-2233. doi: <https://doi.org/10.1007/s11665-015-1467-4>
- [53] Qian, M., Ramirez, A., Das, A. & StJhon, D. H. (2010). The effect of solute on ultrasonic grain refinement of magnesium alloys. *Journal Of Crystal Growth*, 312(15), 2267-2272. doi: <https://doi.org/10.1016/j.jcrysgro.2010.04.035>
- [54] Sozhamannan, G.G., Prabu, S.B. & Venkatagalapathy V.S.K. (2012). Effect of processing parameters on metal matrix composites: stir casting process. *Journal of Surface Engineered Materials and Advanced Technology (JSEMAT)*, 2, 11-15. doi: [doi:10.4236/jsemat.2012.21002](https://doi.org/10.4236/jsemat.2012.21002)
- [55] Lloyd, D. J., Lagace, H., Mcleod, A. & Morris, P. L. (1989). Microstructural aspects of aluminium-silicon carbide particulate composites produced by a casting method. *Material Science and Engineering A*, 107, 73-80. doi: [https://doi.org/10.1016/0921-5093\(89\)90376-6](https://doi.org/10.1016/0921-5093(89)90376-6).
- [56] Zakeri, M. & Rudi A.V.A. (2013). Effect of Shaping Methods on the Mechanical Properties of Al-SiC Composite. *Material Research*, 16(5), 1169-1174. doi: [10.1590/S1516-14392013005000109](https://doi.org/10.1590/S1516-14392013005000109)
- [57] Liu, X., Jia, S. & Nastac, L. (2014). Ultrasonic cavitation-assisted molten metal processing of cast A356-nanocomposites. *International Journal Of Metalcasting*, 8(3), 51-58. doi: <https://doi.org/10.1007/BF03355591>
- [58] Jia, S. (2015). Experimental and Theoretical Analyses on the Ultrasonic Cavitation Processing of Al-Based Alloys and Nanocomposites, The University of Alabama.
- [59] Khomamizadeh, F. & Ghasemi, G. (2004). Evolution of quality index of A-356 aluminum alloy by microstructural analysis. *Scientia Iranica*, 11(4), 386-391.
- [60] Czekaj, E., Zych, J., Kwak, Z. & Garbacz-Klempka, A. (2016). Quality index of the AlSi7Mg0.3 aluminium casting alloy depending on the heat treatment parameters. *Archives Of Foundry Engineering*, 16(3), 25–28.
- [61] Jian, X., Xu, H. Meek, T. T. & Han, Q. (2005). Effect of powr ultrasound on solidification of aluminum A356 alloy. *Materials Letter*, 59(2-3), 190-193. doi: <https://doi.org/10.1016/j.matlet.2004.09.027>
- [62] Das, A. & Kotadia, H. R. (2011). Effect of high-intensity ultrasonic irradiation on the modification of solidification microstructure in a Si-rich hypoeutectic Al–Si alloy. *Materials Chemistry And Physics*, 125, 853-859. doi: [10.1016/j.matchemphys.2010.09.035](https://doi.org/10.1016/j.matchemphys.2010.09.035)
- [63] Tsunekawa, Y., Suzuki, H. & Genma Y. (2001). Application of ultrasonic vibration to in situ MMC process by electromagnetic melt stirring. *Materials & Design*, 22(6), 467-472. doi: [https://doi.org/10.1016/S0261-3069\(00\)00079-0](https://doi.org/10.1016/S0261-3069(00)00079-0)
- [64] Hashim, J., Looney, L. & Hashmi, M.S.J. (1999). Metal matrix composites: production by the stir casting method. *Journal of Materials Processing Technology*, 92-93, 1–7. doi: [https://doi.org/10.1016/S0924-0136\(99\)00118-1](https://doi.org/10.1016/S0924-0136(99)00118-1)
- [65] Ramirez, A., Qian, M., Davis, B., Wilks, T. & StJohn, D.H. (2008). Potency of high-intensity ultrasonic treatment for grain refinement of magnesium alloys. *Scripta Materialia*, 59, 19-22. doi: [doi:10.1016/j.scriptamat.2008.02.017](https://doi.org/10.1016/j.scriptamat.2008.02.017)

- [66] Wang, G., Dargusch, M.S., Qian, M., Eskin, D.G. & StJohn, D.H. (2014). The role of ultrasonic treatment in refining the as-cast grain structure during the solidification of an Al-2Cu alloy. *Journal Of Crystal Growth*, 408, 119-124. doi: <https://doi.org/10.1016/j.jcrysgro.2014.09.018>
- [67] Atamanenkko, T.V., Eskin, D.G., Zhang, L. & katgerman, L. (2010). Criteria of grain refinement induced by ultrasonic melt treatment of aluminum alloys containing Zr and Ti. *Metallurgical and Materials Transactions A*, 41(8), 2056-2066. doi: 10.1007/s11661-010-0232-4
- [68] Bhandare, R.G. & Sonawane, P.M. (2014). Preperation of aluminium matrix composite by using stir casting method & it's characterization. *International Journal of Current Engineering and Technology, Special Issue 3*, 148-155.
- [69] Hernandez-Sandoval, J., Samuel, A. M. & Samuel, F. H. (2016). Effect of SiC and Al₂O₃ particulates on the microstructure and tensile properties of Al-Si-Cu-Mg cast alloys. *International Journal Of Metalcasting*, 10(3), 253-263. doi: <https://doi.org/10.1007/s40962-016-0035-5>
- [70] Chawla, N. & Shen, Y.L. (2001). Mechanical behaviour of particle reinforced metal matrix composites. *Advanced Engineering Materials*, 3(6), 357-370. doi: [https://doi.org/10.1002/1527-2648\(200106\)3:6<357::AID-ADEM357>3.0.CO;2-I](https://doi.org/10.1002/1527-2648(200106)3:6<357::AID-ADEM357>3.0.CO;2-I)
- [71] Kaba, M., Donmez, A., Cukur, A., Kurban, A.F., Cubuklusu, H.E. & Birol, Y. (2018). AlSi5Mg0.3 alloy for the manufacture of automotive wheels. *International Journal of Metalcasting*, 12(3), 614-624. doi: <https://doi.org/10.1007/s40962-017-0191-2>
- [72] Emamy, M., Razaghian, A., Lashgari, H.R. & Abbasi, R. (2009). The effect of Al-5Ti-1B on the microstructure, hardness and tensile properties of Al₂O₃ and SiC-containing metal-matrix composites. *Materials Science and Engineering A*, 485(1-2), 210-217. doi: <https://doi.org/10.1016/j.msea.2007.07.090>
- [73] Rajeswari, B., Amirthagadeswaran, K. S. & Ramya, K. (2014). Microstructural studies of aluminium 7075-silicon carbide-alumina metal matrix composite. *Advanced Materials Research*, 984-985, 194-199. doi: <http://www.scientific.net/AMR.984-985.194>
- [74] Bozic, D. & Dimcic, B. (2011). Synthesis and properties of discontinuously reinforced aluminum matrix composites. *Nanocomposites With Unique Properties And Applications In Medicine And Industry*, Edited by John Cuppoletti, 151-174. doi: 10.5772/19195
- [75] Emamy M., Razaghian A., Lashgari H.R. & Abbasi R. (2009). The effect of Al-5Ti-1B on the microstructure, hardness and tensile properties of Al₂O₃ and SiC-containing metal-matrix composites. *Materials Science and Engineering A*, 485(1-2), 210-217. doi: <https://doi.org/10.1016/j.msea.2007.07.090>
- [76] Oztop, B. & Gurbuz, M. (2017). Investigation of properties of composites produced by reinforcement graphene matrix obtained from waste aluminium. *International Journal of Multidisciplinary Studies and Innovative Technologies*, 1(1), 4-8.
- [77] Ghosh, P.K. & Ray, S. (1986). Effect of porosity and alumina content on the mechanical properties of compocast aluminium alloy-alumina particle composite. *Journal of Materials Science*, 21(5), 1667-1674. doi: <https://doi.org/10.1007/BF01114723>

- [78] Ray, S. (1993). Review synthesis of cast metal matrix particulate composites. *Journal Of Material Science*, 28(20), 5397-5413. doi: <https://doi.org/10.1007/BF00367809>
- [79] Bellos, E. & Tzivanidis, C. (2018). Thermal analysis of parabolic trough collector operating with mono and hybrid nanofluids. *Sustainable Energy Technologies and Assessments*, 26, 105-115. doi: <http://dx.doi.org/10.1016/j.seta.2017.10.005>
- [80] Ezatpour, H.R., Sajjadi, S.A., Sabzevar, M.H. & Huang, Y. (2014). Investigation of microstructure and mechanical properties of Al6061-nanocomposite fabricated by stir casting. *Materials & Design*, 55, 921-928. doi: <https://doi.org/10.1016/j.matdes.2013.10.060>
- [81] Babu, N.H., Fan, Z. & Eskin, D.G. (2013). Application of external fields to technology of metal-matrix composite materials. *TMS2013 Annual Meeting Supplemental Proceedings TMS*, 1037-1044. doi: <https://doi.org/10.1002/9781118663547.ch127>
- [82] Suthar, J. & Patel, K.M. (2018). Processing issues, machining and applications of aluminum metal matrix composites. *Materials and Manufacturing Processes*, 33(5), 499-527. doi: 10.1080/10426914.2017.1401713
- [83] Su, H., Gao, W., Feng, Z. & Lu, Z. (2012). Processing, microstructure and tensile properties of nano-sized Al₂O₃ particle reinforced aluminum matrix composites. *Materials and Design*, 36, 590-596. doi: 10.1016/j.matdes.2011.11.064.
- [84] Singh, L., Ram, B. & Singh, A. (2013). Optimization of process parameter for stir casted aluminum metal matrix composite using taguchi method. *IJRET: International Journal of Research in Engineering and Technology*, 02(08), 375-383.
- [85] Fiorese, E., Bonollo, F., Timelli, G., Arnberg, L. & Gariboldi, E. (2015). New classification of defects and imperfections for aluminum alloy castings. *International Journal of Metalcasting*, 9 (1), 55-66. doi: <https://doi.org/10.1007/BF03355602>
- [86] Ammar, H.R., Samuel, A.M. & Samuel, F.H. (2008). Effect of casting imperfections on the fatigue life of 319-F and A356-T6 Al-Si casting alloys. *Materials Science and Engineering A*, 473(1-2), 65-75. doi: <https://doi.org/10.1016/j.msea.2007.03.112>
- [87] Akhtar, S., Arnberg, L., Si Sabatino, M., Dispinar, D. & Syvertsen, M. (2009). Acomparative study of porosity and pore morphology in an directionally solidified A356 alloy. *International Journal of Metalcasting*, 3(1), 39-52. doi: <https://doi.org/10.1007/BF03355440>
- [88] Atkinson, H.V., Zulfia, A., Lima Filho, A., Jones, H. & King, S. (1997). Hot isostatic processing of metal matrix composites. *Materials & Design*, 18 (4), 243-245. doi: 10.1016/S0261-3069(97)00058-7
- [89] Zulfia, A., Atkinson, H.V. & Jones, H. (1999). Effect of hot isostatic pressing on cast A357 aluminium alloy with and without SiC particle reinforcement. *Journal of Materials Science*, 34(17), 4305-4310. doi: <https://doi.org/10.1023/A:1004675424845>
- [90] Kashani, S.M.M., Rhodin, H. & Boutorabi, S. M. A. (2013). Effects of hot isostatic pressing on he tensile properties of A356 cast alloy. *Iranian Journal of Materials Science & Engineering*, 10(3), 54-64.
- [91] Ceschini, L., Morri, A. & Sambogna, G. (2008). The effect of hot isostatic pressing on the fatigue behavior of sand-cast A356-T6 and A204-T6

- aluminum alloys. *Journal of Materials Processing Technology*, 204(1-3), 231-238. doi: <https://doi.org/10.1016/j.jmatprotec.2007.11.067>
- [92] Ran, G., Zhou, J. & Wang, Q. G. (2006). The effect of hot isostatic pressing on the microstructure and tensile properties of an unmodified A356-T6 cast aluminum alloy. *Journal of Alloys and Compounds*, 421(1-2), 80-86. doi: <https://doi.org/10.1016/j.jallcom.2005.11.019>
- [93] Aybarc, U., Kara, A., Cubuklusu, H. E. & Ce, O. B. (2017). Effect of hot isostatic pressing on metallurgical and mechanical properties of A356 alloy. *Journal Of The Faculty Of Engineering And Architecture Of Gazi University*, 32(4), 1327-1335. doi: 10.17341/gazimmfd.369853
- [94] Lee, M.H., Kim, J.J., Kim, K.H., Kim, N.J., Lee, S. & Lee, E.W. (2003). Effect of HIPping on high-cycle fatigue properties of investment cast A356 aluminum alloys. *Materials Science And Engineering A*, 340(1-2), 123-129. doi: [https://doi.org/10.1016/S0921-5093\(02\)00157-0](https://doi.org/10.1016/S0921-5093(02)00157-0)
- [95] Dedyaeva, E. V., Nikiforov, P. N., Padalko, A. G., Talanova, G. V. & Shvorneva, L. I. (2016). Effect of barothermal processing on the microstructure and properties of Al-10 at % Si hypoeutectic binary alloy. *Inorganic Materials*, 52(7), 721-728. doi: <https://doi.org/10.1134/S0020168516070049>
- [96] Li, Q. E., Loh, N. L., Hung & N. P. (1995). Casting and HIPping of Al-based metal matrix composites (MMCs), *Journal of Materials Processing Technology*, 48(1-4), 373-378. doi: [https://doi.org/10.1016/0924-0136\(94\)01671-M](https://doi.org/10.1016/0924-0136(94)01671-M)
- [97] Tekmen, C., Ozdemir, I., Cocen, U. & Onel K. (2003) The mechanical response of Al-Si-Mg/SiCp composite: influence of porosity. *Materials Science and Engineering A*, 360(1-2), 365-371. doi: [https://doi.org/10.1016/S0921-5093\(03\)00461-1](https://doi.org/10.1016/S0921-5093(03)00461-1)
- [98] Sigworth, G. (2011). Understanding quality in aluminum castings. *International Journal Of Metalcasting*, 5(1), 7-22. doi: <https://doi.org/10.1007/BF03355504>
- [99] Caceres, C. H. & Selling, B. I. (1996). Casting defects and the tensile properties of an-Al-Si-Mg alloy. *Materials Science And Engineering: A*, 220(1-2), 109-116. doi: [https://doi.org/10.1016/S0921-5093\(96\)10433-0](https://doi.org/10.1016/S0921-5093(96)10433-0)

CURRICULUM VITAE

Uğur AYBARÇ

Educational Background

Degree	Department	University	Year
Post graduate	Metallurgical and Materials Engineering	Dokuz Eylul University Institute of Science and Technology	2010 - 2013
Post graduate	Production Management and Industrial Business Administration	Dokuz Eylül University Graduate School of Social Sciences	2007 - 2005
Undergraduate	Metallurgical and Materials Engineering	Dokuz Eylul University	2001 - 2005

Work Experience

Company	Position	Year
CMS Jant ve Makina San. A.Ş.	R & D Engineer	2013 - ...
İNCİ Akü San. ve Tic. A. Ş.	R & D Engineer	2011 – 2013
Ege Çelik Endüstri A.Ş.	Chief of Continues Casting Machines	2009 – 2011
Ege Çelik Endüstri A.Ş.	Shift Supervisor	2008 – 2009
Tübitak Marmara Research Center	Intern	2004
Çebitaş Demir Çelik End.	Intern	2003

List of Publications:

1. U. Aybarç, H. Yavuz, D. Dışpınar, M.Ö. Seydibeyoğlu, "The Use of Stirring Methods for the Production of SiC Reinforced Aluminum Matrix Composite and Validation Via Simulation Studies", *International Journal of Metalcasting*, 2019; Vol: 13 (1), pp: 190-200. DOI: 10.1007/s40962-018-0250-3
2. U. Aybarç, D. Dışpınar, M.O. Seydibeyoğlu, "Aluminum Metal Matrix Composites with SiC, Al₂O₃ and Graphene – Review", *Archives of Foundry Engineering*, 2018; Vol: 18 (2), pp: 5-10. ISSN (1897-3310)
3. U. Aybarç, A. Kara, H. E. Cubuklusu, O. B. Ce, "Effect of Hot Isostatic Pressing on Metallurgical and Mechanical Properties of A356 Alloy", *Journal of the Faculty of Engineering and Architecture of Gazi University*, 2017; Vol: 32 (4), pp: 1327-1335. DOI: 10.17341/gazimmfd.369853

Conference Papers

1. U. Aybarç, D. Dışpınar, E. Dokumacı, O. Ertuğrul, M.Ö. Seydibeyoğlu, "Investigation of Mechanical Properties Of SiC And Al₂O₃ Reinforcement In Aluminum Metal Matrix Composite Produced By Mechanical Stirring Promoted With Ultrasonic Stirring Application", *19th International Metallurgy and Materials Congress*, 2018.
2. U. Aybarç, H. Yavuz, D. Dışpınar, M.Ö. Seydibeyoğlu, "Investigation of Effect of Different Stirring Methods for Production of Aluminum Metal Matrix Composite and Comparison with Simulation Studies", *10th International Foundry Congress*, 25-27 December 2018.
3. H. Yavuz, U. Aybarç, "The Effect of Mold and Casting Temperature on the Distribution of Reinforcement Material in Composite Material Production", *1st International University Industry Cooperation, R&D and Innovation Congress*, 18-19 December 2017.